2–3 Data Processing

2–3–1 Considerations on the Difference of Drainage Area

Consideration will be given how to reflect the factors of area on data processing when there are various areas of drainage represented by independent samples.

In the Projeto Geoquimica no Vale do Ribeira, each parameter of the drainage area (AD) such as AD < 5km², 5–10km², 10–20km² was calculated by geological unit.

Table II–3 shows MG (backgroud), DG (standard deviation) and MG x DG² taken out

Table II–3 Statistical Parameters by Element

Geology & Area \ Parameter \ Element	N	Cu MG	Cu DG	Cu MGx DG²	Pb MG	Pb DG	Pb MGx DG²	Zn MG	Zn DG	Zn MGx DG²
Açungui Setuva	197	26	1,904	92	12	1,773	32	58	1,693	154
AD < 5 Km²	80	26	1,876	93	11	1 620	29	55	1 743	167
= 5 10 Km²	53	26	1,773	81	12	1,576	31	61	1,576	153
= 10 20 Km²	30	24	2,116	109	13	1,885	46	57	1,570	141
Açungui Clastico	509	23	2,151	105	16	1,860	55	52	1,869	182
AD < 5 Km²	147	26	2,002	103	16	1,764	50	58	1,729	175
= 5 10 Km²	129	22	2,234	108	15	1,861	53	50	1,879	177
= 10 20 Km²	70	19	2,177	92	15	1,608	39	49	1 910	178
Açungui Quimico	176	18	2,395	104	19	2,561	125	46	2,115	204
AD < 5 Km²	61	19	2,056	120	20	2,564	144	43	2 061	183
= 5 10 Km²	48	20	2,327	110	19	2,751	145	52	2,363	292
= 10 20 Km²	30	16	2,434	93	16	2 235	79	44	1,852	152
Grupo Açungui	868	23	2,134	103	15	2,010	61	52	1,865	182
AD = 20 40 Km²	69	22	2,422	129	14	1,701	40	46	1,986	183
> 40 Km²	22	20	2,247	101	16	1,800	52	50	2,078	217
Granitos	345	11	1,976	43	17	1,636	45	40	1,521	92
AD < 5 Km²	47	11	2,029	46	16	1 618	41	39	1,622	103
= 5 10 Km²	95	12	2,213	60	17	1 758	51	41	1,505	92
= 10 20 Km²	65	11	1,965	41	18	1,620	48	39	1,597	99

MG Background DG Standard Deviation

from the tables of A–8–7 (Cu), 8–9 (Pb) and 8–11 (Zn) in appendices.

In general, when the drainage is large, the sediment would naturally come from wider area, so that it will be more homogegeneous, resulting in the approach of MG to the mean of the group with decrease of DG. Thus it is expected that threshold value will take principally low value. Such tendency can be read in the table with a few exceptions.

However, when comparing the values of AD < 5km² and AD = 5–10km², significant difference can not be recognized except the cases such as zinc in chemical sediments of the Açungui group and copper in granite. Therefore, it seems that the discrimination of these areas is unnecessary and that they might be able to be treated in a bundle.

In the case of AD = 10 ~ 20km², the differences are generally much greater compared with the former two. Therefore, it is questionable to treat them in a bundle.

However, as for 37 samples which represent areas of more than 10km², they were processed in a bundle because they were small in number, sharing only about 5% of the whole samples.

2–3–2 Interpretation Method

The area for interpretation is 7,600km², among which the area of drainage represented by the extracted samples is 3,993km², showing only 53% of the whole area. In addition, the 37 samples of more than 10km² are included, so that the detailed study is difficult because of considerable deviation of the data.

Here, a statistical processing by computor was attempted regardless of deviation of the data.

At first, histograms were made on the whole extracted data by element and lithology (4 units) (Fig. II–4–1 ~ 4–8), then mean ($\overline{X}$) and standard deviation (σ) were calculated, which are shown in Tables II–4 and II–5.

Table II–4 Distribution of Geochemical Data

Area(Km²) \ Lithology	1	2	3	4	5	6	7	8	9	10	Total
1–5	3	116	60	146	47	18	0	5	25	15	435
6–10	4	87	36	95	19	3	0	1	21	3	269
11–15	0	12	3	14	3	0	0	0	1	2	35
16–	0	2	0	0	0	0	0	0	0	0	2
Total	7	217	99	255	69	21	0	6	47	20	741

Total Area = 3,993 Km²

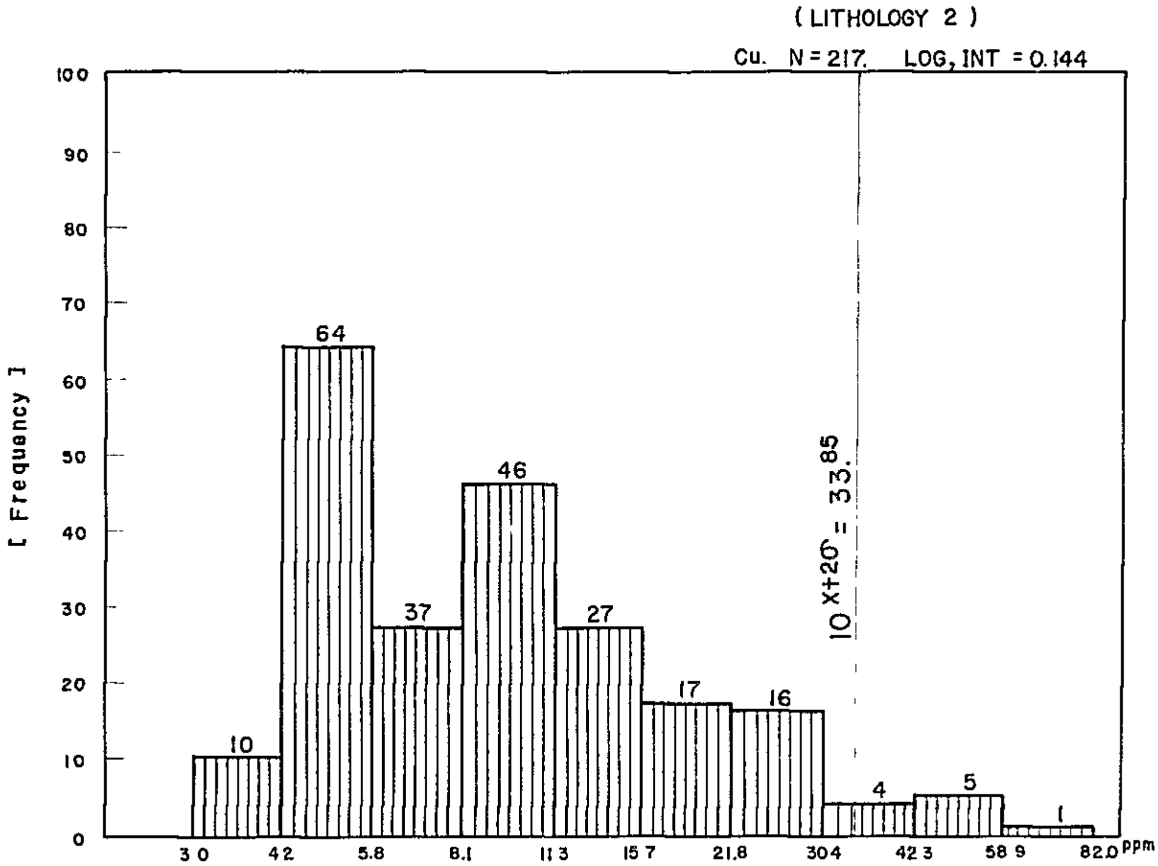

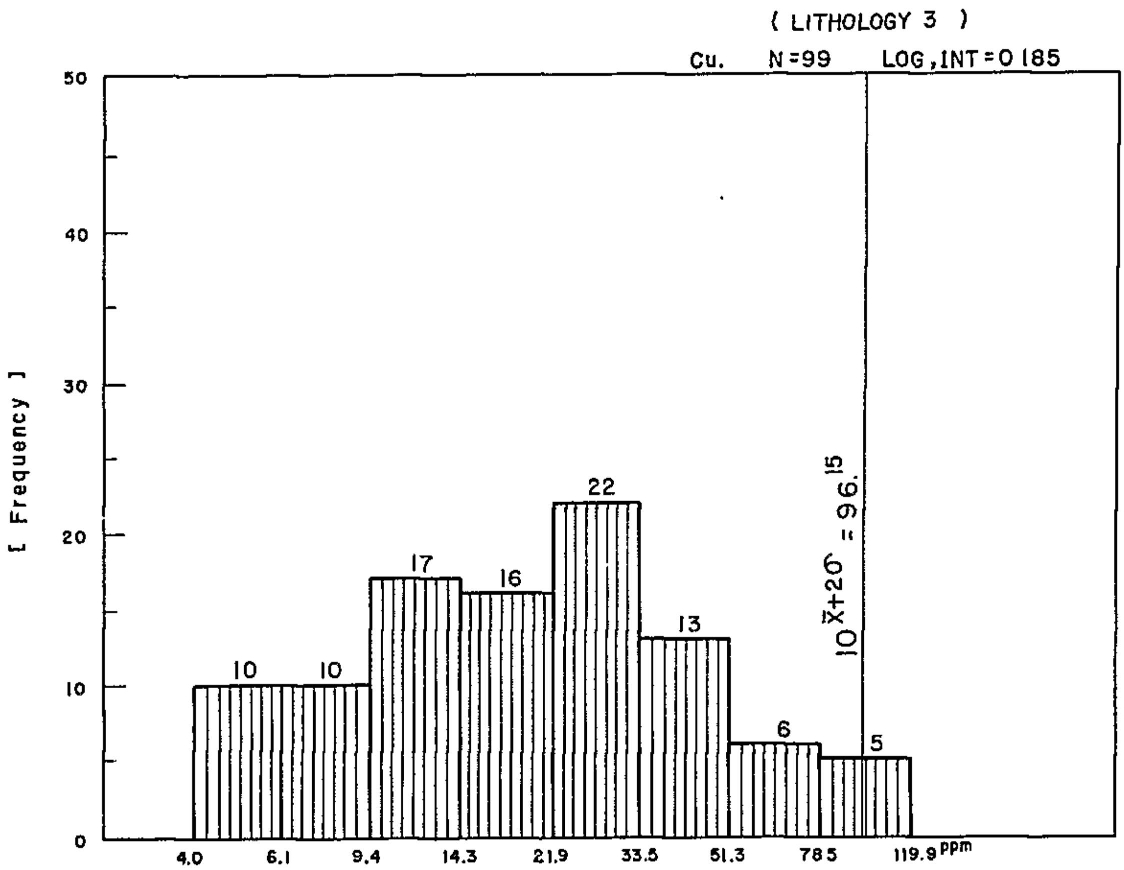

Fig. II–4–1 Histogram for Cu by Lithology

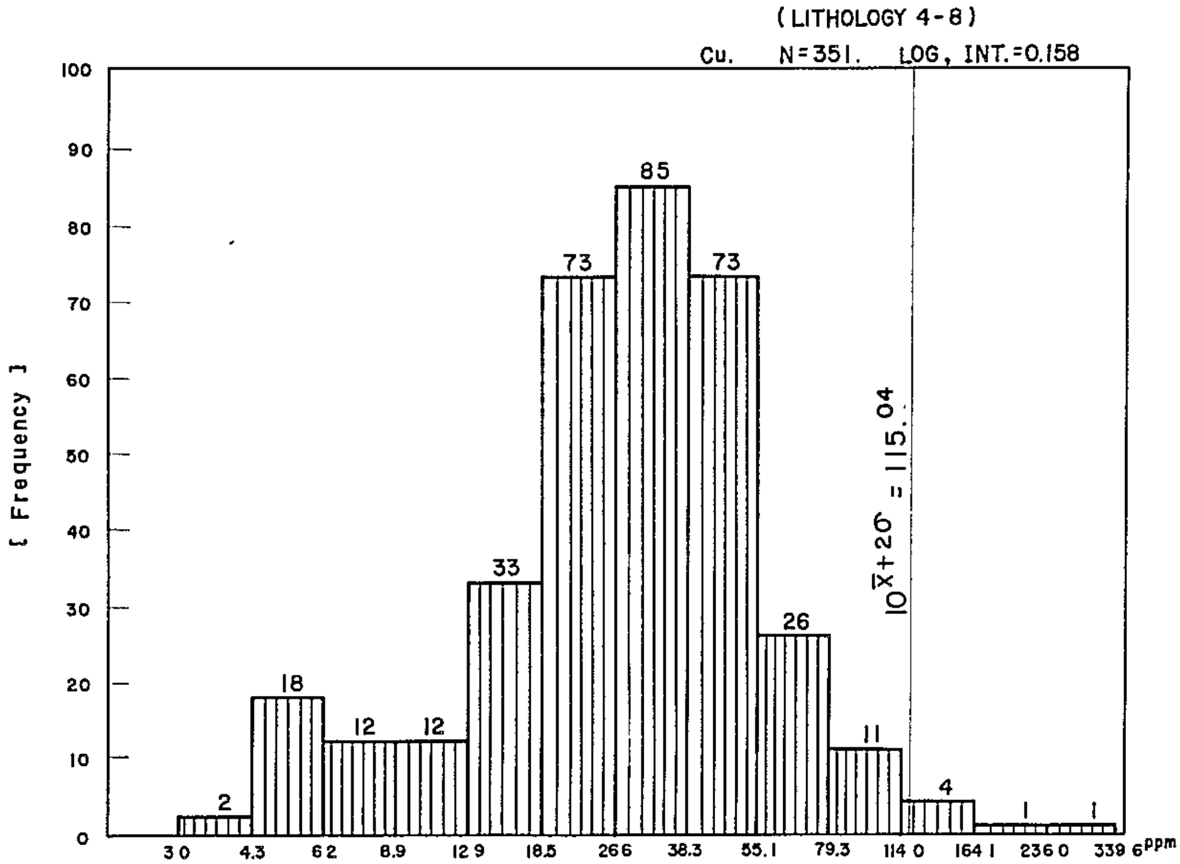

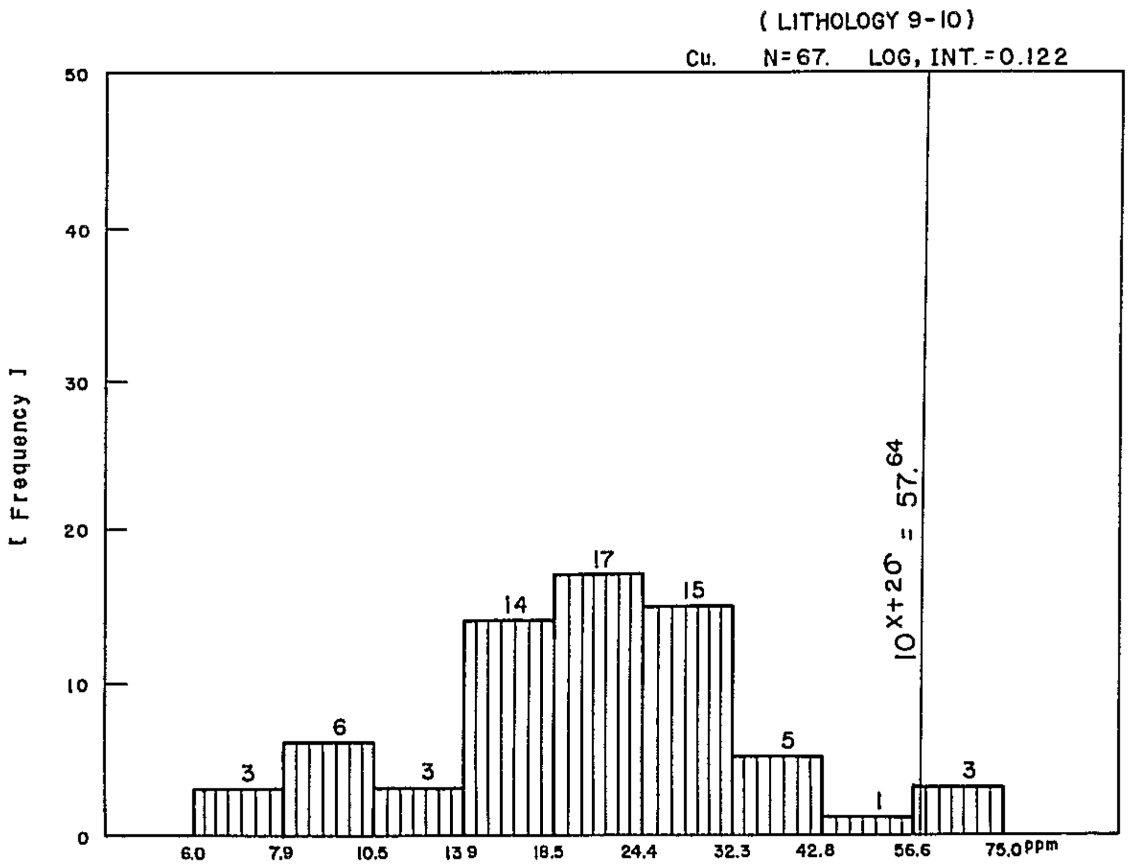

Fig. II–4–2 Histogram for Cu by Lithology

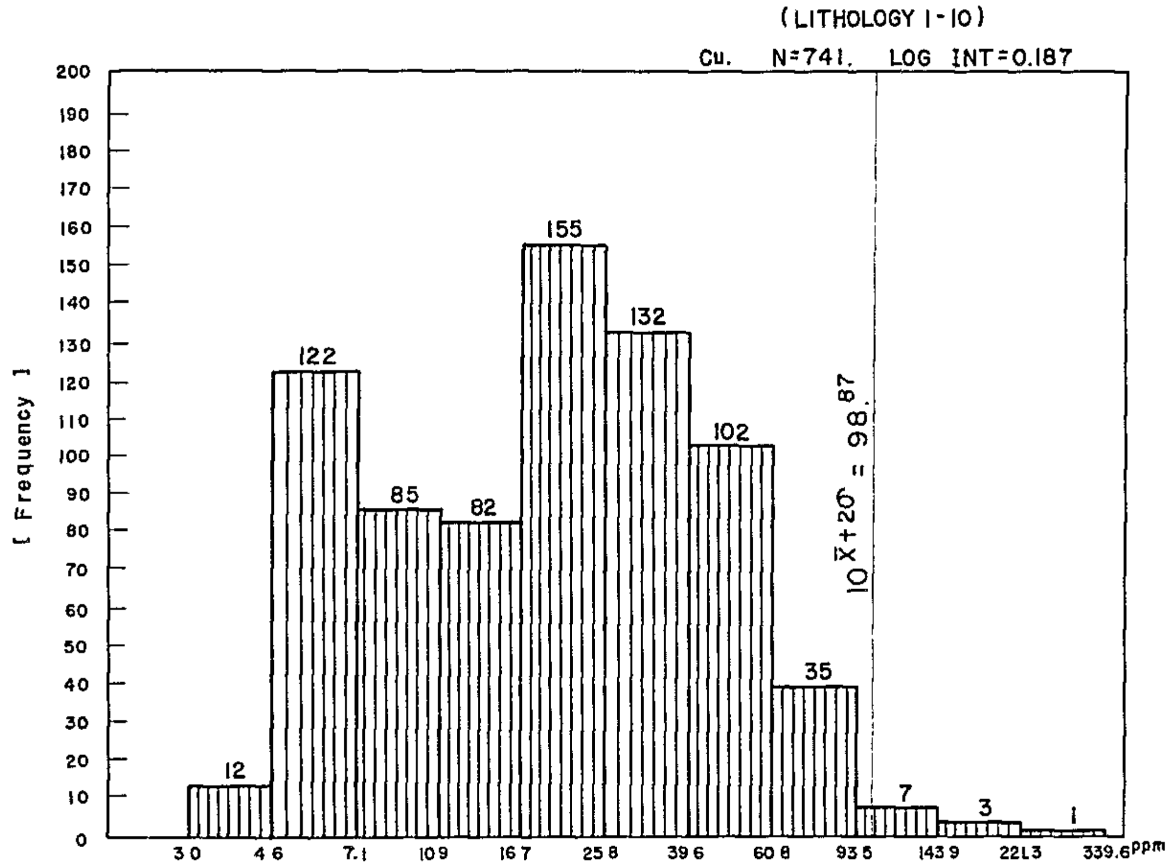

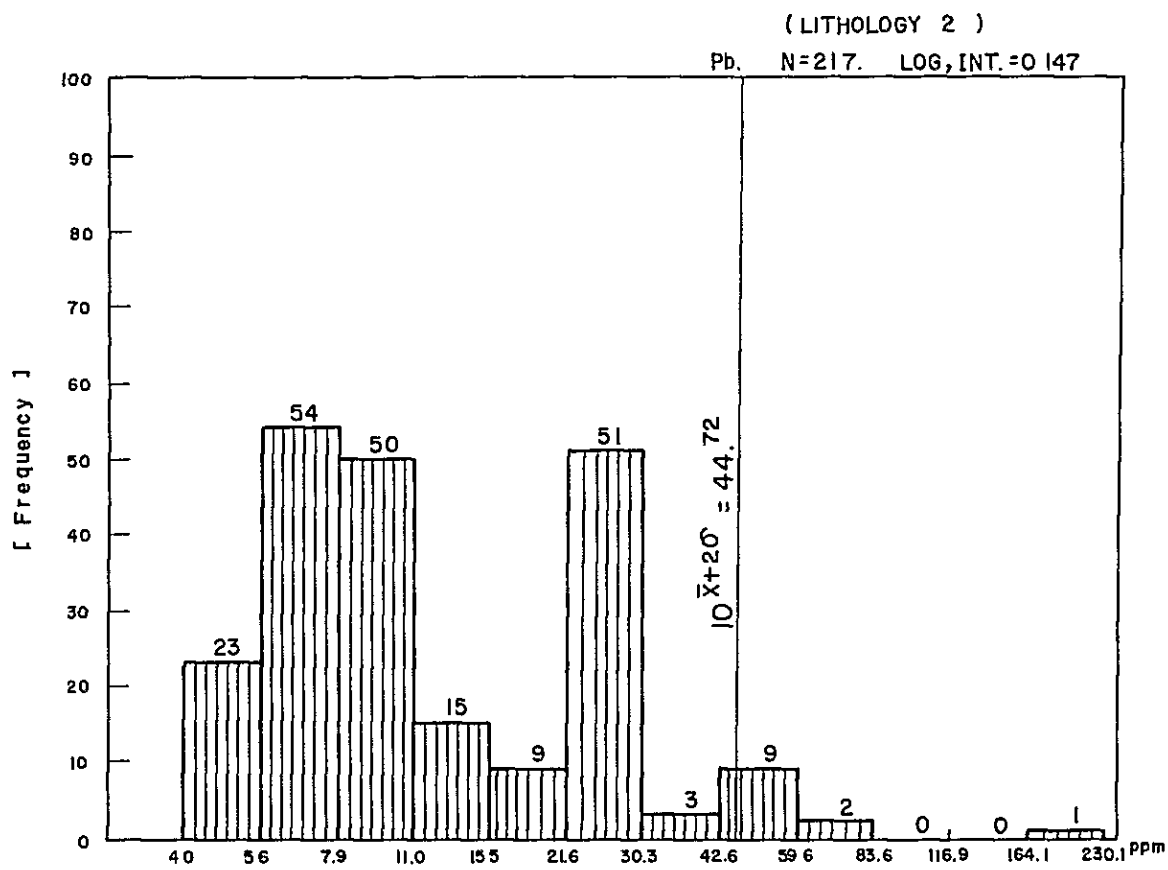

Fig. II–4–3 Histogram for Cu & Pb by Lithology

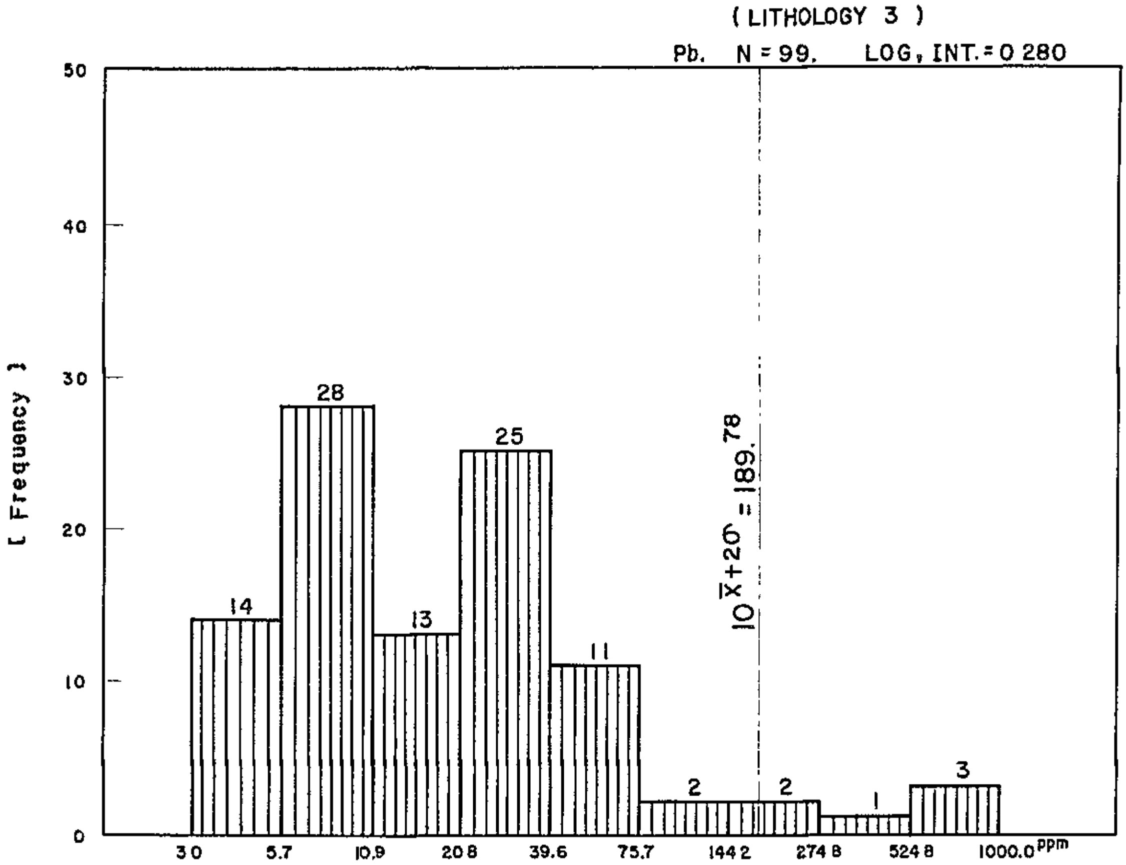

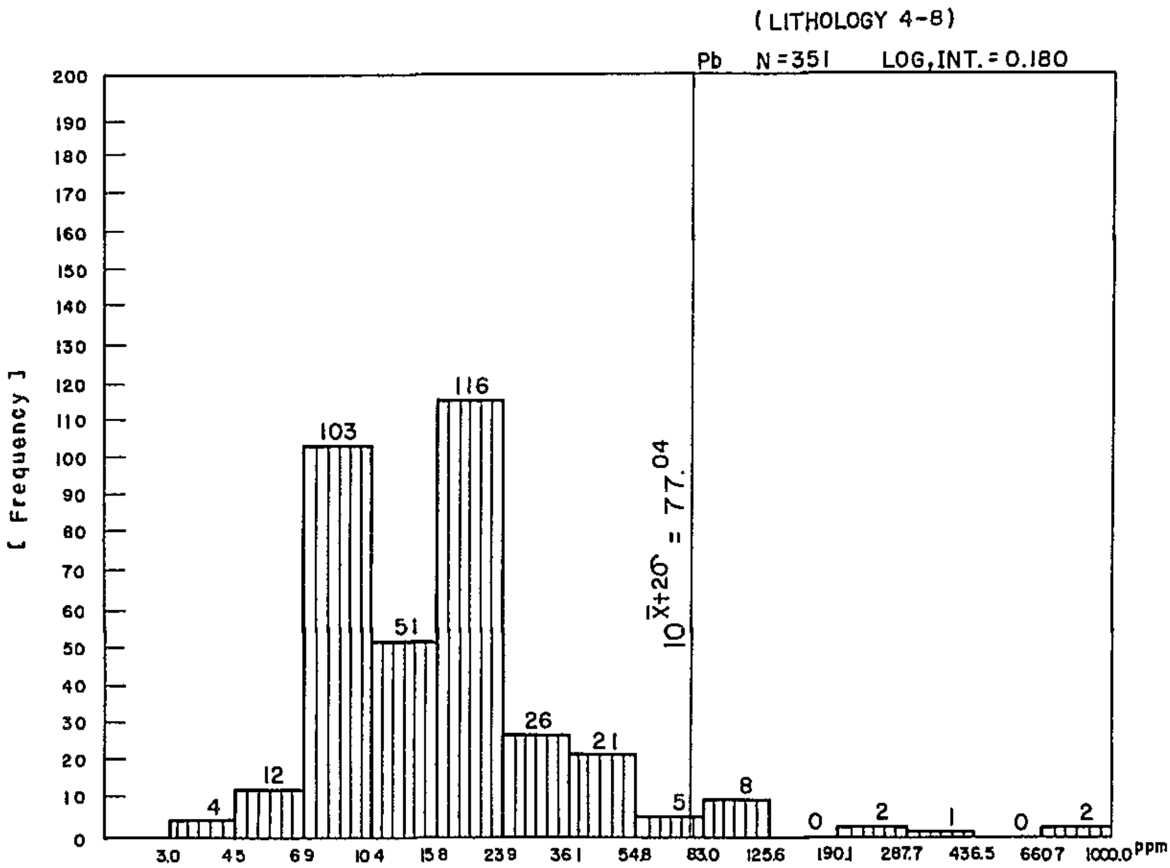

Fig. II-4-4 Histogram for Pb by Lithology

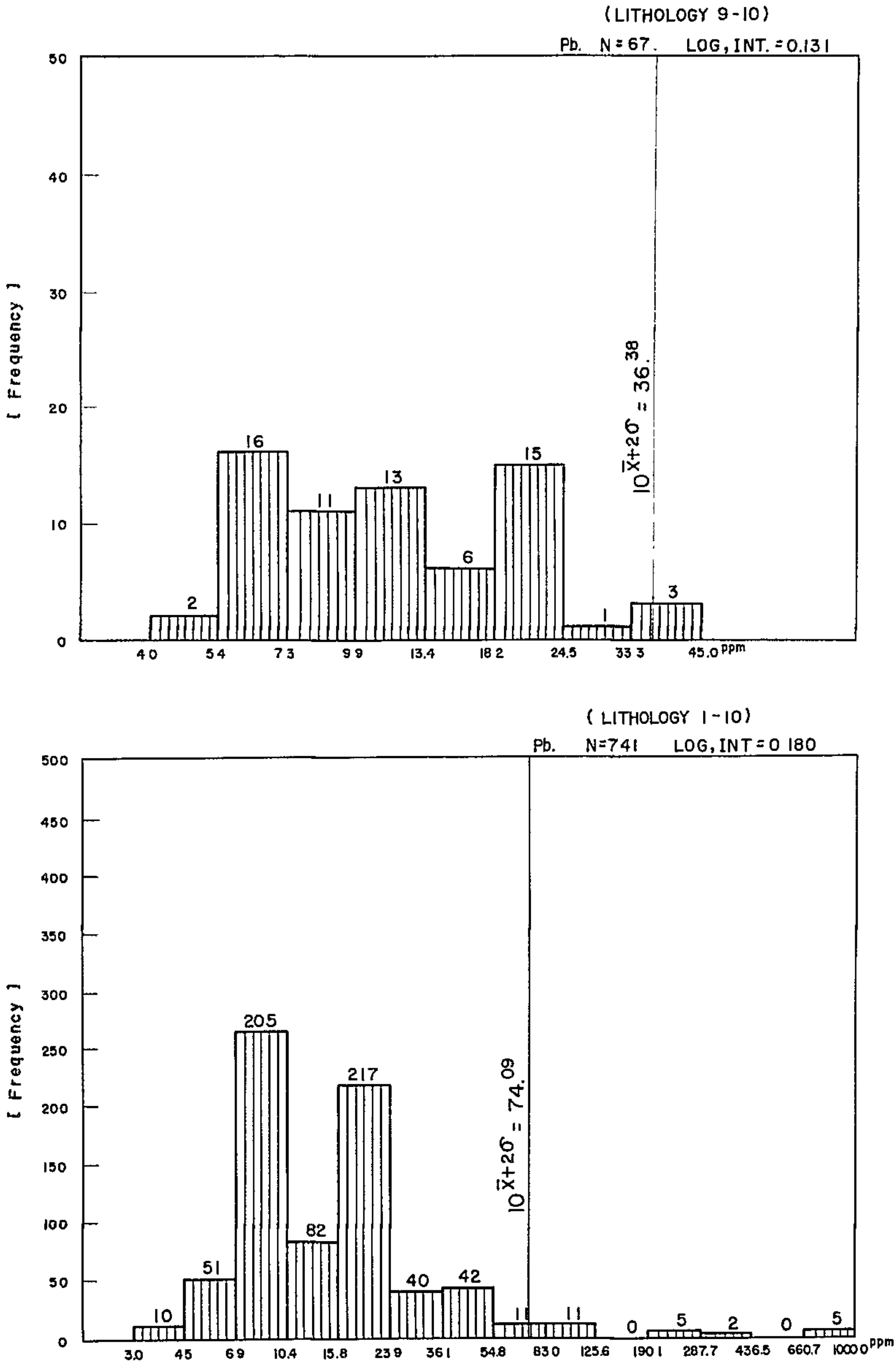

Fig. II-4-5 Histogram for Pb by Lithology

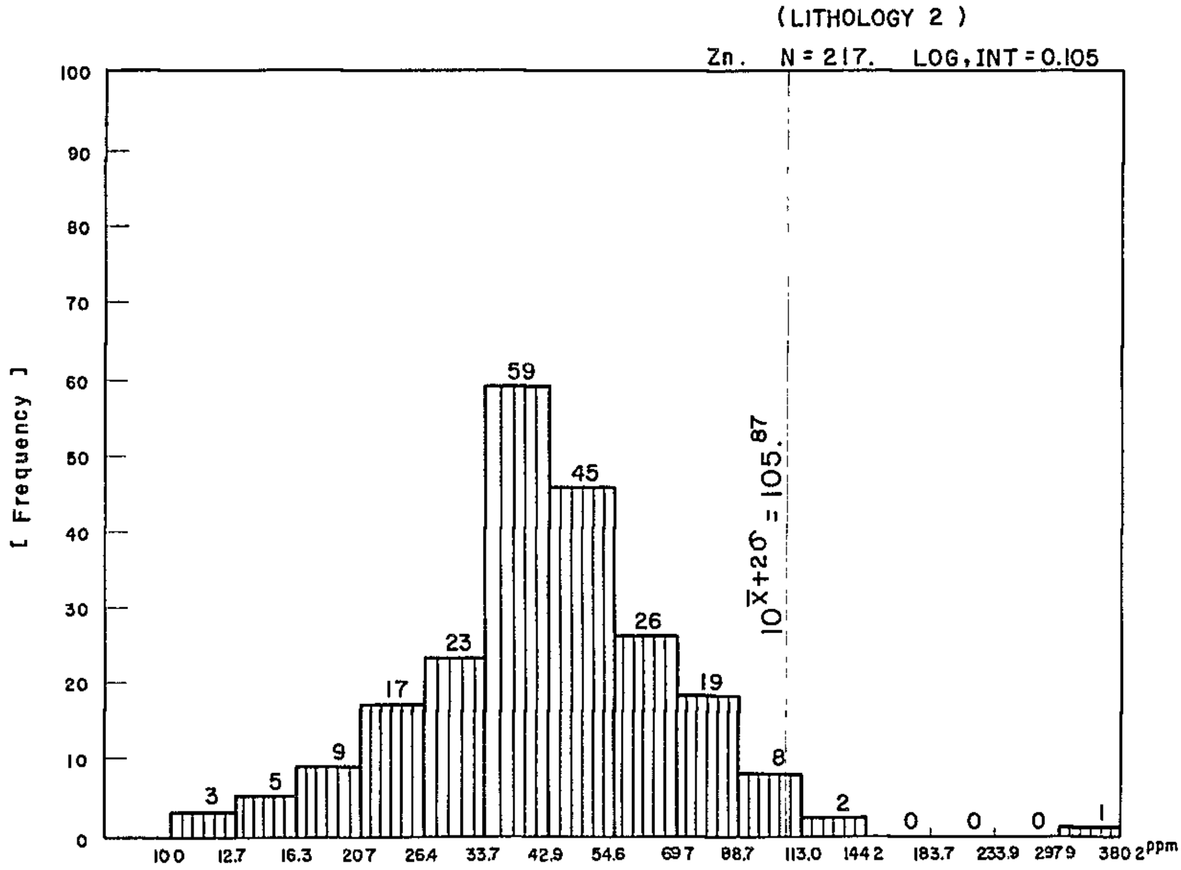

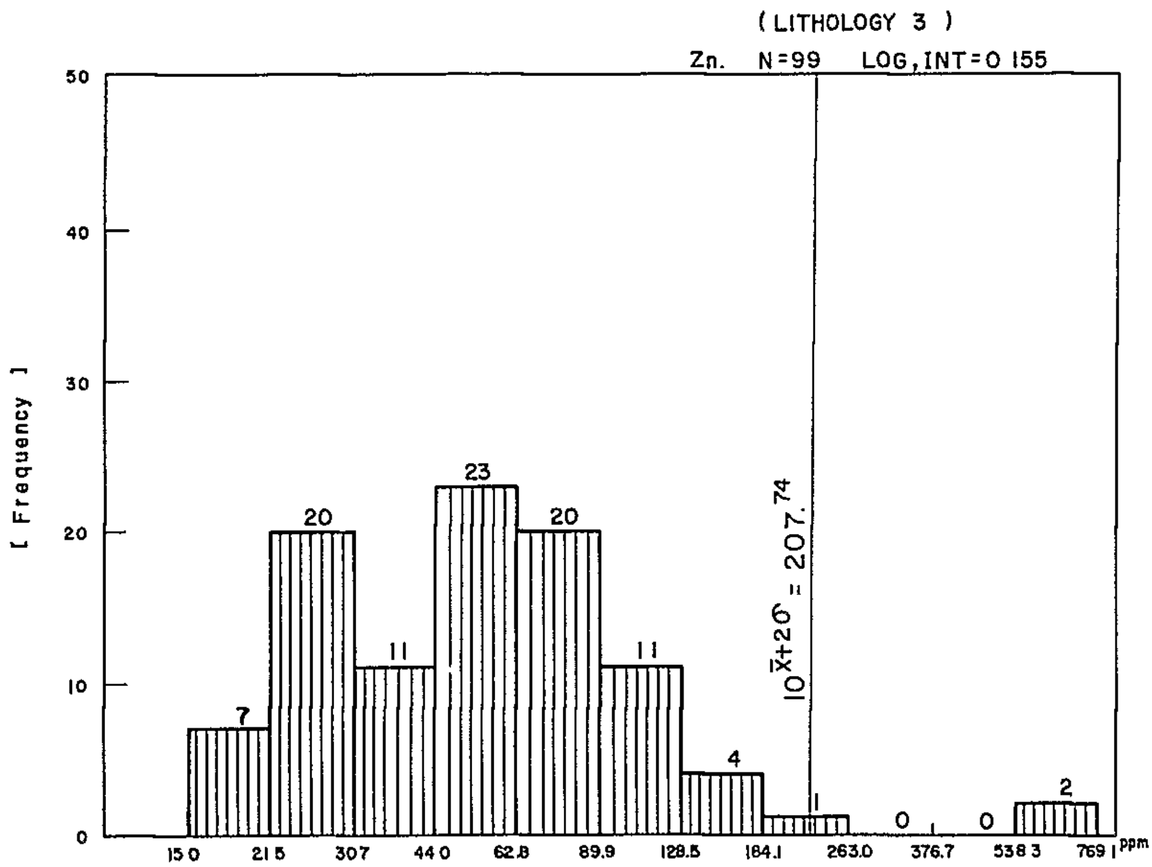

Fig. II–4–6 Histogram for Zn by Lithology

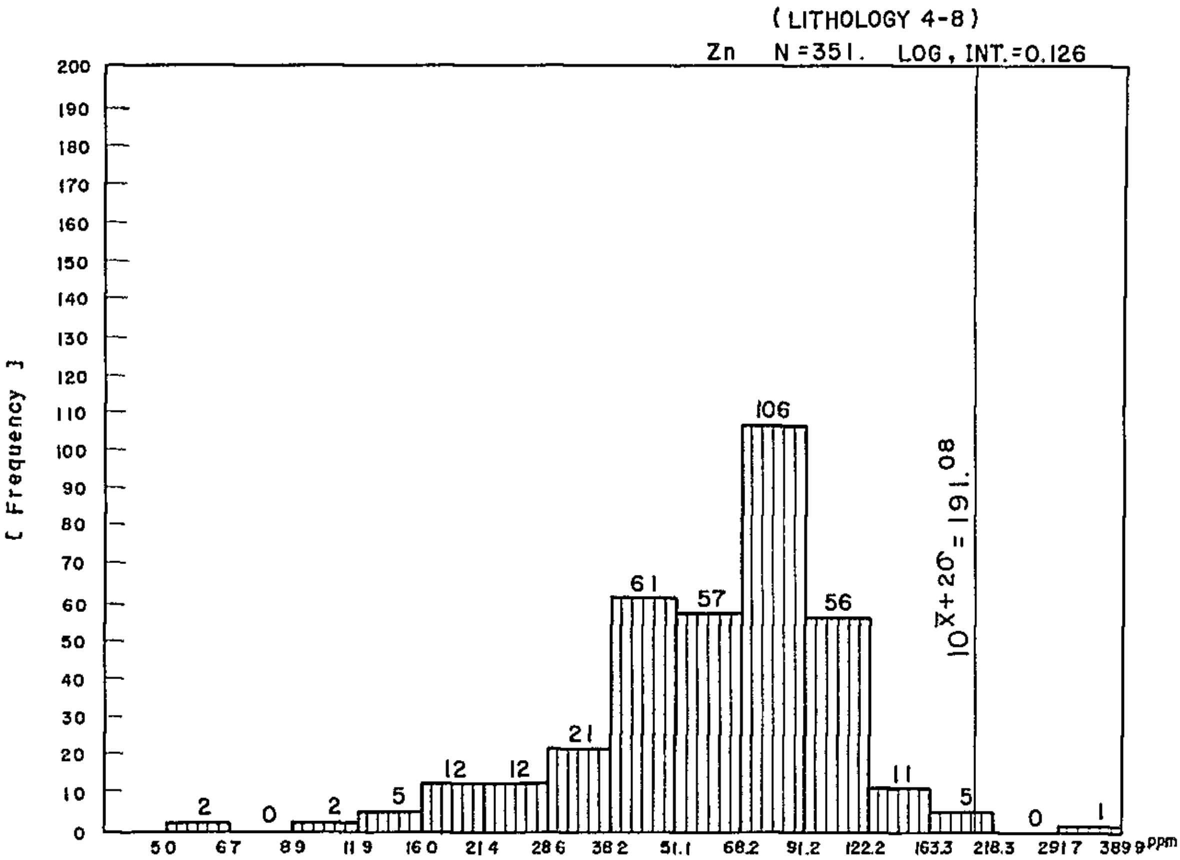

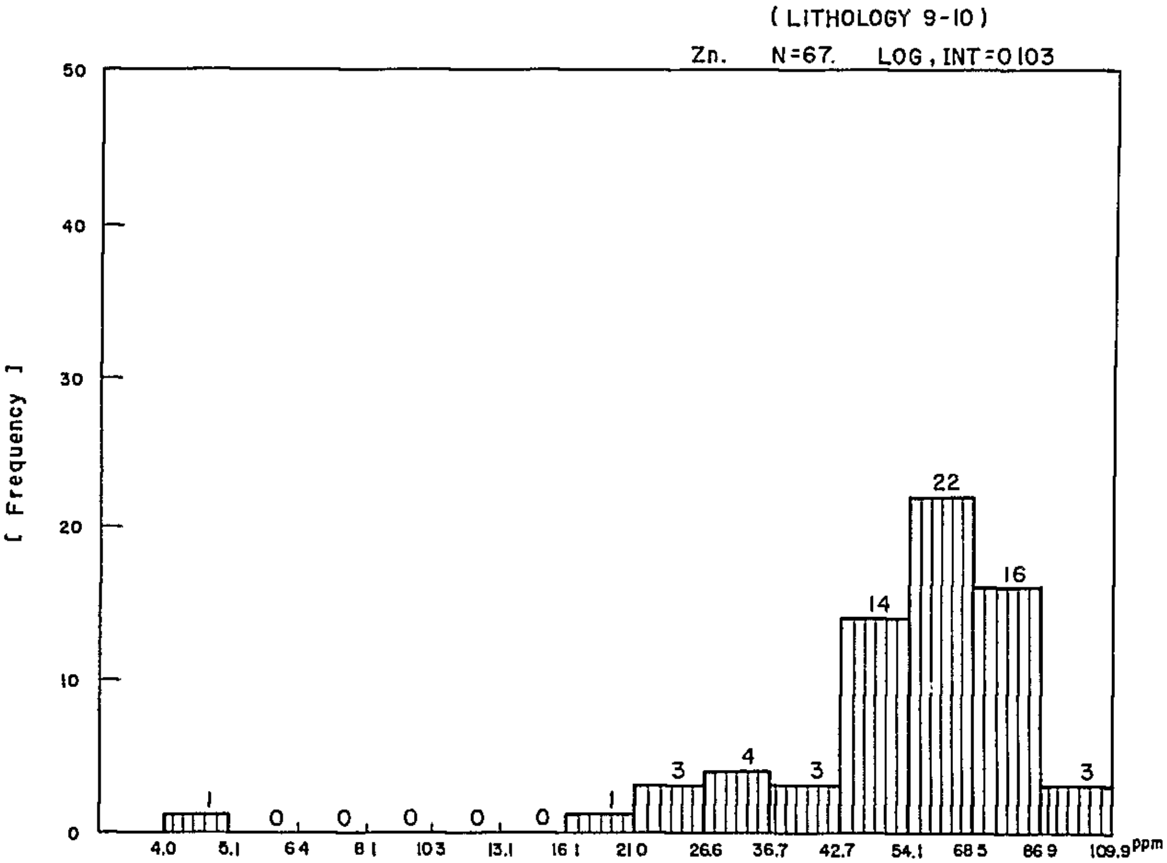

Fig. II-4-7 Histogram for Zn by Lithology

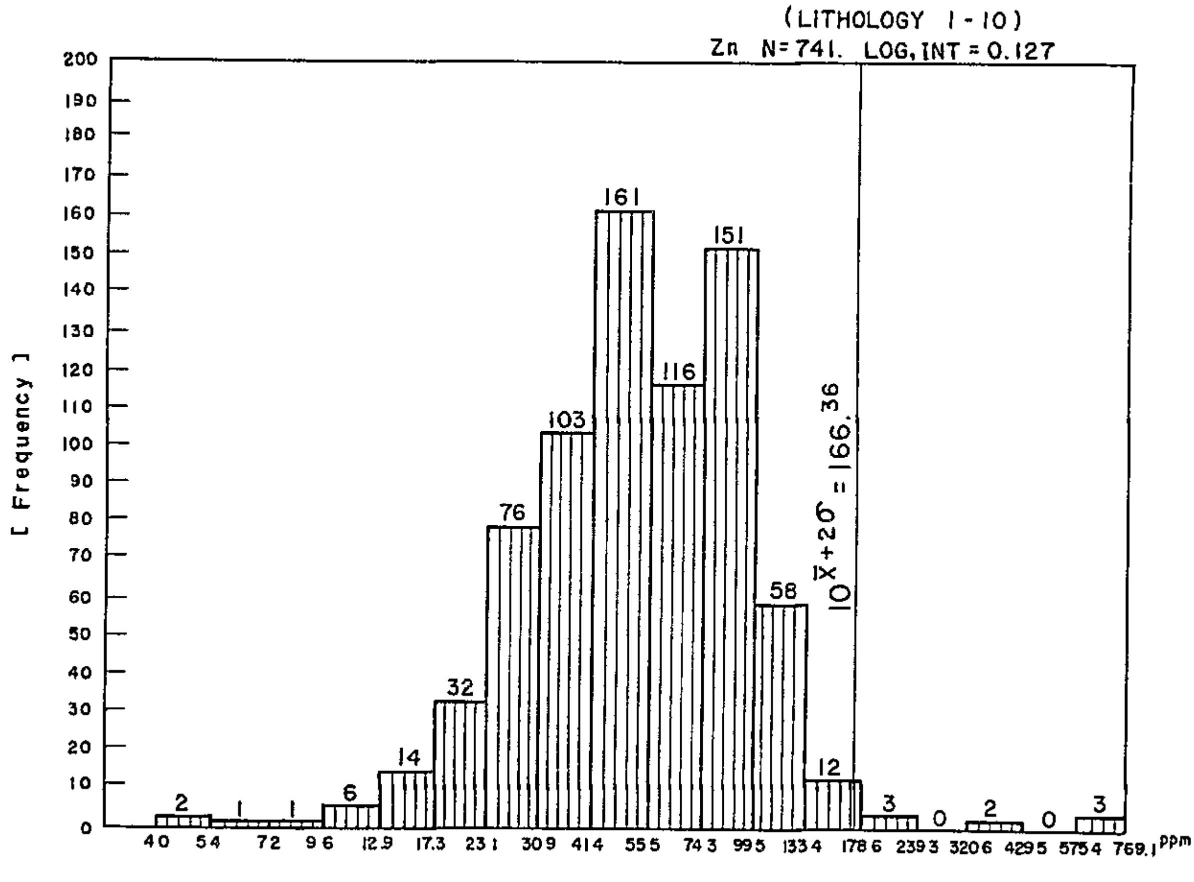

Fig. II–4–8 Histogram for Zn by Lithology

Table II–5 Mean and Standard Deviation of Stream Sediment Samples by Lithology

Element	Lithology	Number	Max (ppm)	Min. (ppm)	Mean $10^{\bar{x}}$	S.D. 10^{σ}	$10^{\bar{x}+\sigma}$	$10^{\bar{x}+2\sigma}$
Cu	2	217	82	3	9.27	1.91	17.71	33.85
	3	99	120	4	19.23	2.23	17.71	33.85
	4–8	351	340	3	27.23	2.06	43.00	96.15
	9–10	67	75	6	20.09	1.69	34.04	57.64
	1–10	741	340	3	18.49	2.31	42.74	98.78
Pb	2	217	230	4	11.97	1.93	23.14	44.72
	3	99	1,000	3	17.46	3.30	57.53	189.78
	4–8	351	1,000	3	16.11	2.19	35.24	77.04
	9–10	67	45	4	11.78	1.76	20.71	36.38
	1–10	741	1,000	3	14.52	2.26	32 80	74.09
Zn	2	217	380	10	41.30	1.60	66.09	105.87
	3	99	770	15	52.48	1.99	104.41	207.74
	4–8	351	390	5	61.38	1.76	108.36	191.08
	9–10	67	110	4	52.36	1.60	83.94	134.43
	1–10	741	770	4	52.84	1.77	93.72	166.36

Table II–6 Correlation Coefficient amang Three Elements

Element \ Lithology / N	2	3	4 – 8	9 – 10	1 – 10
N	217	99	351	67	741
Cu - Pb	0.35	0.61	0.28	–0.02	0.36
Pb - Zn	0.59	0.71	0.49	0.43	0.59
Zn – Cu	0.58	0.79	0.65	0.22	0.65

The correlation coefficient and correlation diagram between each element are shown in Table II–6 and Fig. II–5–1 ~ 5–5 respectively. According to these, it is clear that the correlation coefficients such as Pb–Zn and Zn–Cu are high.

On the contrary, correlation coefficients of Cu–Pb are low except in limestone zone (lithological unit 3).

There are many insufficient descriptions of lead content in the original list of data, which are noted as interferencia. Among those, some are marked by the rank in the Projeto Geoquimica no Vale do Ribeira (Anexo VI ~ X), of which the means were substituted.

Lead content

Marked rank	Mean (substitutes)
< 15 ppm	7 ppm
15 – 30	22
30 – 60	45
60 – 120	90

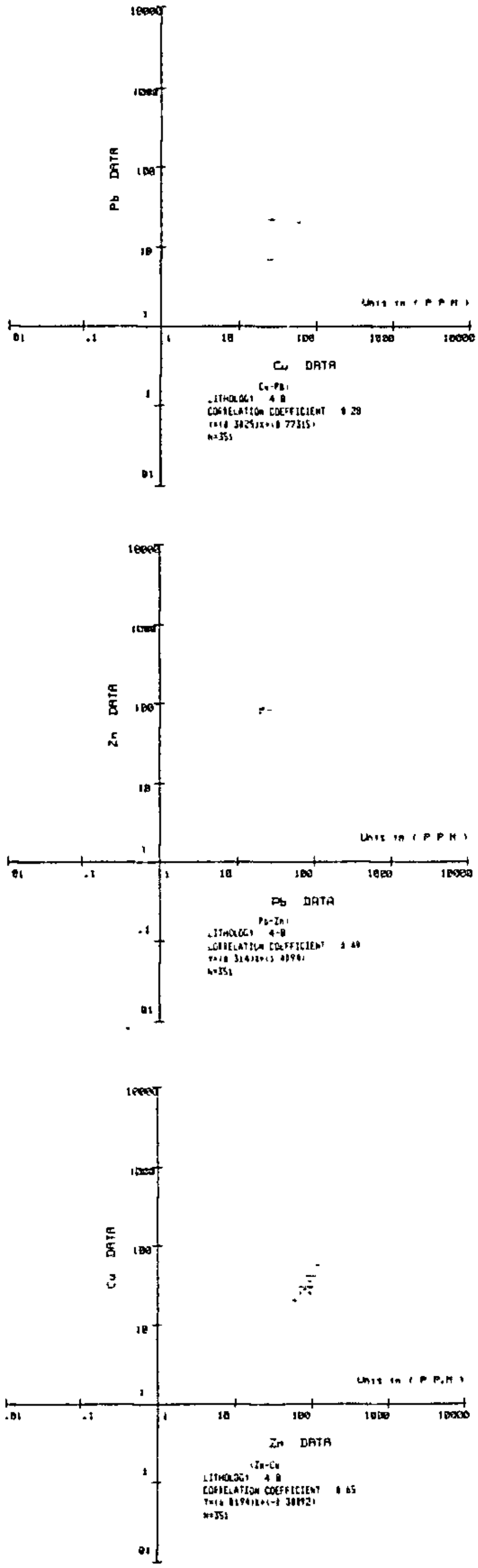

Fig. II–5–1 Correlation Diagrams (Lithology 2)

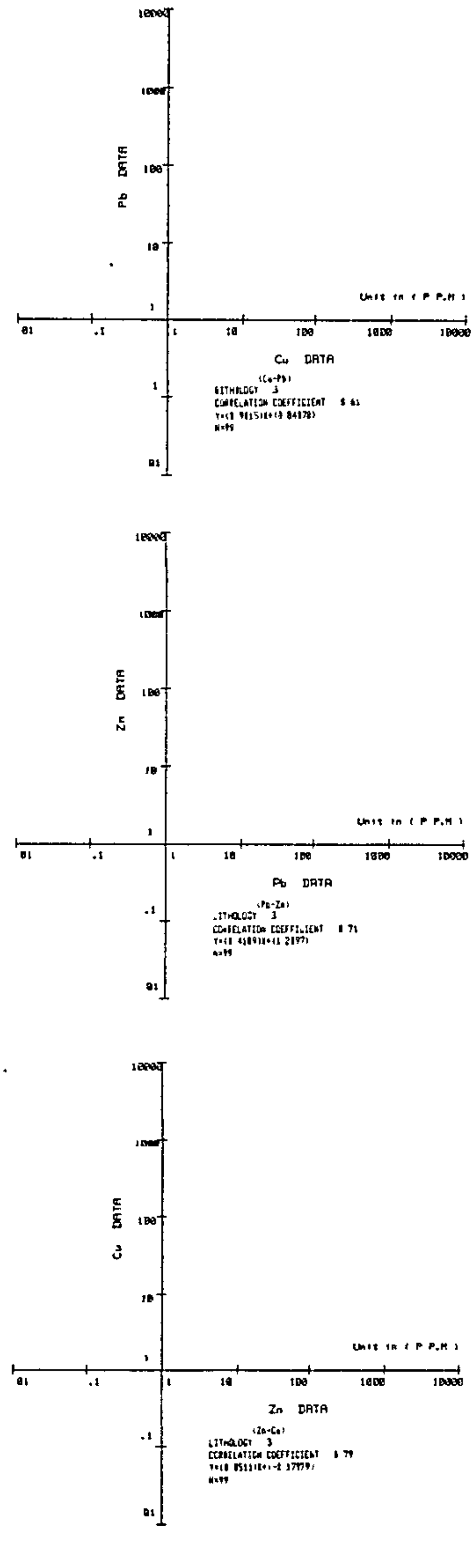

Fig. II–5–2 Correlation Diagrams (Lithology 3)

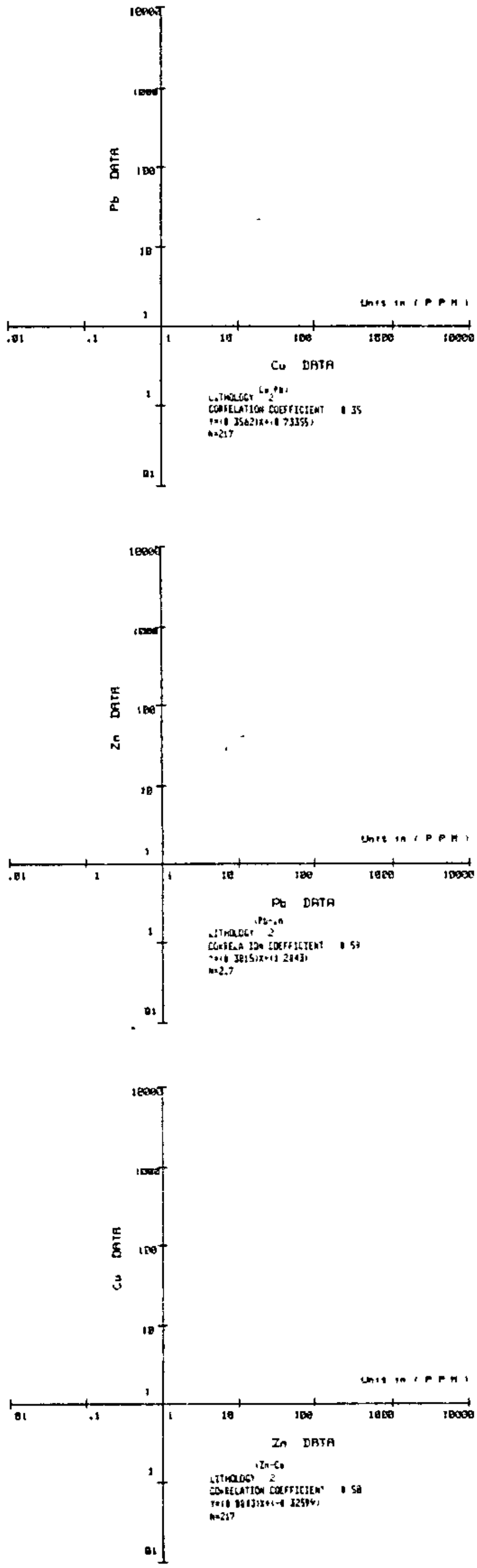

Fig. II–5–3 Correlation Diagrams (Lithology 4–8)

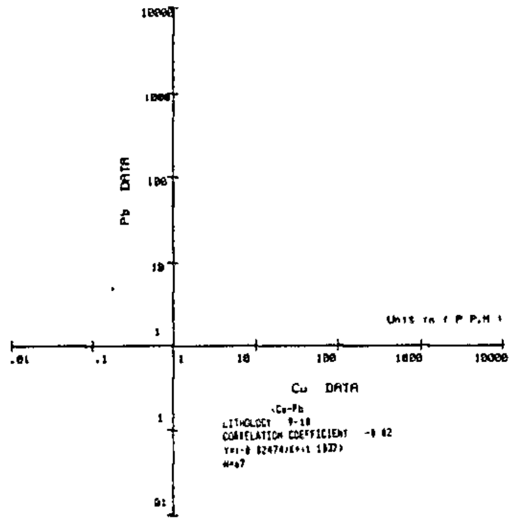

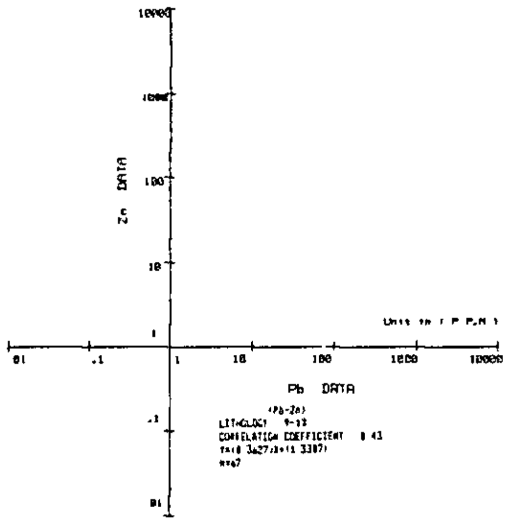

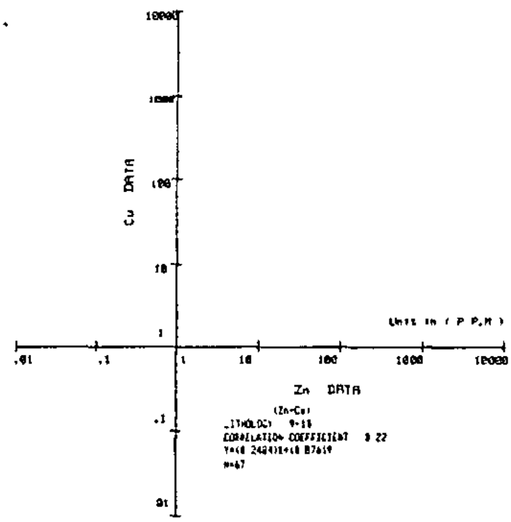

Fig. II–5–4 Correlation Diagrams (Lithology 9–10)

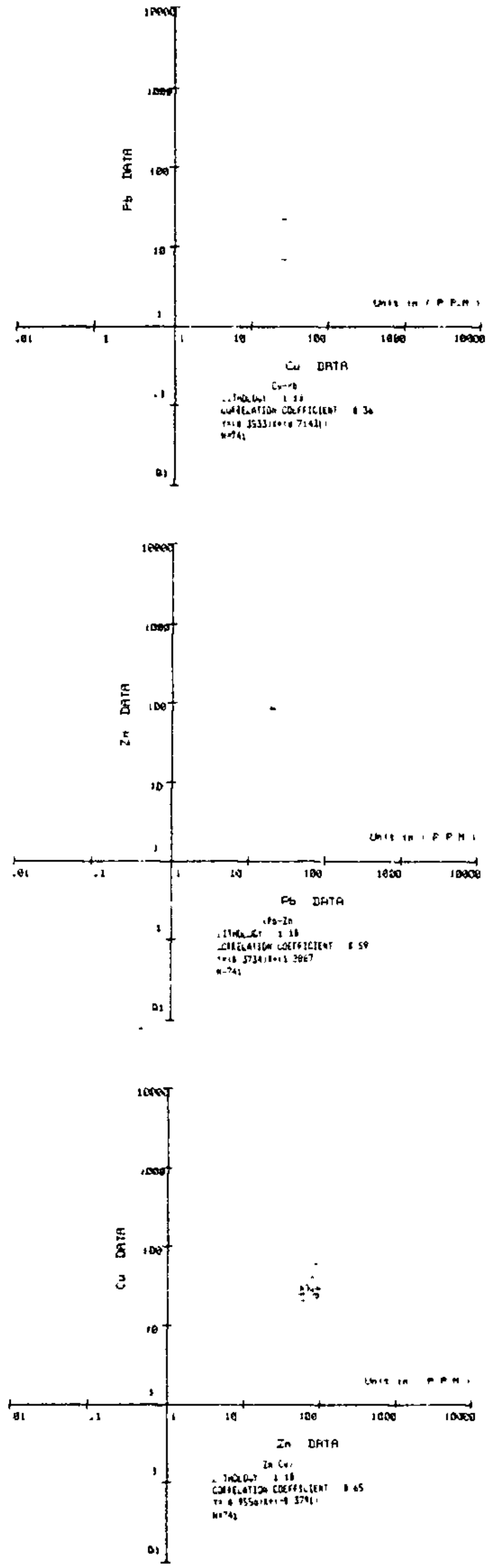

Fig. II–5–5 Correlation Diagrams (Lithology 1–10)

CHAPTER 3 INTERPRETATION OF THE ANOMALOUS AREA

3–1 Examination of the Anomalous Areas

Although $10^{x+2\sigma}$ value is adopted as anomalous value for each element, in order to observe the general tendency, $10^{x+\sigma}$ and $10^{x+2\sigma}$ areas are illustrated in the Plates (PL II–2–1, 2, 3) which show the anomalous areas for each element, and only $10^{x+2\sigma}$ areas are shown in the comprehensive map (PL II–3) in order to avoid complexity.

Copper :

The anomalous areas of copper which are above $10^{x+2\sigma}$ value are found in five places in granite; from east to west, one at Aguados Grande, one at Espirito Santo, one at Morro Agudo and two at Trés Córregos. Copper content ranges from 35 to 82 ppm and no extremely hgih values are obtained. In zone (3) where limestone is developed, the anomalous areas are found in the southwestern part of the drainage (IP–473) where the Furnas mine is located and in the north of the drainage (VA–17/172), showing 120 ppm in the former and 190 ppm and 340 ppm in the latter. It is probably due to the effect of copper in the barite bed of the Pretinhoe mine. Therefore, there is some possiblity of continuity of assay result). In zones (4)–(8) of the Açungui group, there are three anomalous areas, among which copper anomalies (AG–126, 129) with 140–150 ppm indicates the existence of copper mineralization in limestone. A weak anomaly with 62–90 ppm is shown on the west of the Perau mine, suggesting some relation with amphibolite.

In the surrounding area of gneiss zone of the Setuva formation (9), an anomalous area with 60–75 ppm are obtained, which is considered to be caused by chalcopyrite associated in the barite bed of the Pretinhoe mine. Therefore, there is a possibility of continuity of this horizon.

Lead :

There are five high lead anomalous areas (more than 1,000 ppm) in the whole area. All of them are known as the existing lead deposits or showings.

12 lead anomalies above 2σ are obtained, in which the contents are only in the range of 45–230 ppm, but they do not so rather concentrate. The drainage with the highest value of 230 ppm is located 15km north of Cerro Azul, where a small body of syenite is known.

Since limestone zone is the zone where lead ore deposits swarm the value of $10^{x+2\sigma}$ is as high as 190 ppm, which is two to three times those of granite and other Açungui group. When the anomalies which are above the value of 2σ are extracted, they agree well

with the existing typical deposits as shown in the following.

1 VA–167 (420 ppm) . . . . Espirito Santo

2 IP–473 (1,000 ppm) . . . . .Furnas mine

3 VA–130 (1,000 ppm) , IP–508 (235 ppm) . . . . . Lageado mine

4 AM–30 (1,000 ppm) . . . . Barrinha mine

5 TB–59 (1,000 ppm) . . . . Rocha mine

6 TB–126 (1,000 ppm) . . . . Quarenta Oitavos

However, low values such as 40 ~ 60 ppm obtained in the Panelas Mine area would indicate some problems on sampling.

In the Açungui group, lead anomalies of 100 and 210 ppm are obtained along the western periphery of the Agudos Grande granite body. In addition, an anomaly of 1,000 ppm is located in the drainage with the sampling density of $4km^2$/sample, 3km south of Iporanga, overlapping a copper anomaly. As the geological map of 1/100,000 made by Projeto Lesto do Parana (1977) has a thin bed of limestone and a symbol of the suspended iron mine, it is necessary to check.

The sample of VA–150, located 15km southwest of Iporanga, shows the lead content of 380 ppm. It would have been caused by limestone (lead bearing?) exposed at the divide.

As mentioned before, no lead anomalies do not appear in the vicinity of the Panelas deposit. Also in surrounding area of the Perau deposit occurring in the same group, no remarkable anomaly can be obtained, in spite of being under operation of mining and milling in the upstream.

In the Setuva formation and crystalline complex (9–10), $10^{x+2\sigma}$ is as low as 36 ppm and other anomalies obtained are insignificant.

Zinc.:

The anomalous areas of zinc are only nine places when the values of $10^{x+2\sigma}$ are taken, because the values are distributed more normally than those of copper and lead.

In granitic rocks (2), the anomalies are present 15km north of Cerro Azul overlapping the lead anomalies with the maximum value of 380 ppm.

In limestone (3), Zinc anomalies are present at the Furnas deposit area (IP–473, 770 ppm) and at the Lageado deposit area (VA–130, 710 ppm, IP–508, 230 ppm) overlapping the lead anomalies, but no anomaly is obtained in the areas such as Panelas and Rocha. This agrees with the existence of sphalerite in the both deposits of Furnas and Lageado, and on the contrary, with its absence in the Panelas and Rocha deposits.

In the Açungui group, the zinc anomaly obtained at the place 3km south of Iporanga coincides with the anomalies of copper and lead, showing 390 ppm.

In the Setuva formation and the crystalline complex, no notable anomaly is obtained.

3–2 Extraction of the Anomalous Areas and Comparison with the Data of CPRM

After selecting the areas with a homogeneous sampling density from the data of "Projet Geoquimica no Vale do Ribeira" conducted by DNPM–CPRM, and combining the ten existing lithological units into the four, such as granite, Açungui limestone (corresponds to the Açungui III formation of this time), Açungui schist (corresponds to Açungui I + II formations) and the Setuva formation, the extracted data was processed by computor.

The area represented by the samples which could be extracted is about a half of the whole area and the area of drainage represented by each sample was different, and a considerable number of estimated values were forced to be used, therefore there should be few difference between the anomalous areas worked out by the two method.

As a result, the highly anomalous zones are coincided with the CPRM report and the following anomalous zones have been newly obtained due to the change of mean and standard deviation by lithological unti.

1	AG–44	(Cu)
2	AG–156	(Cu)
3	AG–37	(Cu)
4	PP– 08	(Pb)
5	VA–60	(Cu)

As discussed in the previous chapter, AG–44, AG–157 and AG–37 occur as if they surrounded augen gneiss of the Setuva formation, which corresponds to the extension of the Pretinhoe deposit (Ba) which is the same horizon as the Perau deposit. Therefore, future investigation is recommended in this area.

The lead anomaly (PP–08, 45 ppm) in Morro Agudo granite 15km west-northwest of Tunas was shown as zinc anomalous area by the interpretation of CPRM. However, there is a zone of copper anomaly (TB–27, 55 ppm) on the east of the drainage, so that these anomalies may be caused not by the granite but by a weak mineralization.

In the same granite at the southwestern corner of the surveyed area, a copper anomaly (VA–60, 35 ppm) was newly obtained, but it is considered to be insignificant.

PART Ⅲ AEROMAGNETIC INTERPRETATION

CHAPTER 1 GENERAL REMARKS

An aeromagnetic survey analysis was performed for an area of approximately 10,000km^2 in the Antagorda area of Brazil. This study was a part of Phase I of a Mineral Resources Survey of that area and was intended to delineate the major underground structures.

This report describes the results of the interpretation of the Aeromagnetic data. Before analysis, the digitized data were obtained from the residual map for the south-western area (A-area, 6,750km^2), for the northeastern area (B-area, 3,250km^2), the residual map was made from a magnetic tape supplied by the Government of Brazil, using an electronic computer.

By using the geological information availbale for the A-area, this report discusses the major structures and lineament directions interpreted by this analysis.

CHAPTER 2 OUTLINE OF AIRBORNE MAGNETIC SURVEY

2–1 Survey Area

The analysis work described in this report was made from the aeromagnetic data in the area of 10,000km^2 is located near the boundary between the states of São Paulo and Parana, Brazil, and forms a polygon whose apexes are as listed below.

	Latitude S	Longititude W
A	24°27′	48°55.6′
B	24°27′	49°15′
C	24°30′	49°15′
D	24°30′	49°30′
E	24°45′	49°30′
F	24°45′	49°45′
G	25°05′	49°45′
H	25°05′	48°52.5′
I	24°52′	48°38.7′
J	24°48.7′	48°40.5′
K	24°45′	48°37.5′
L	24°45′	48°15′
M	24°15′	48°15′
N	24°15′	48°45′

In Phase I, the aeromagnetic map has been made only in the southwestern area (A-area ; A-B-C-D-E-F-G-H-I-J-A), the analytical work was conducted for A-area. And, for B-area (A-J-K-L-M-N-A), only the residual map was made.

2–2 Outline of Field Work

The airborne magnetic surveys covering this survey area were conducted by the D.N.P.M. (Departomento Nacional da Produção Mineral) of Ministério das Minas e Energia and CPRM (Companhia de Pesquisa de Recursos Minerais) as a part of the project of the integrated airborne geophysical survey, which also includes aeromagnetic and radiometric surveys. The project names, specifications for both A- and B-areas are as follows :

1) A-area

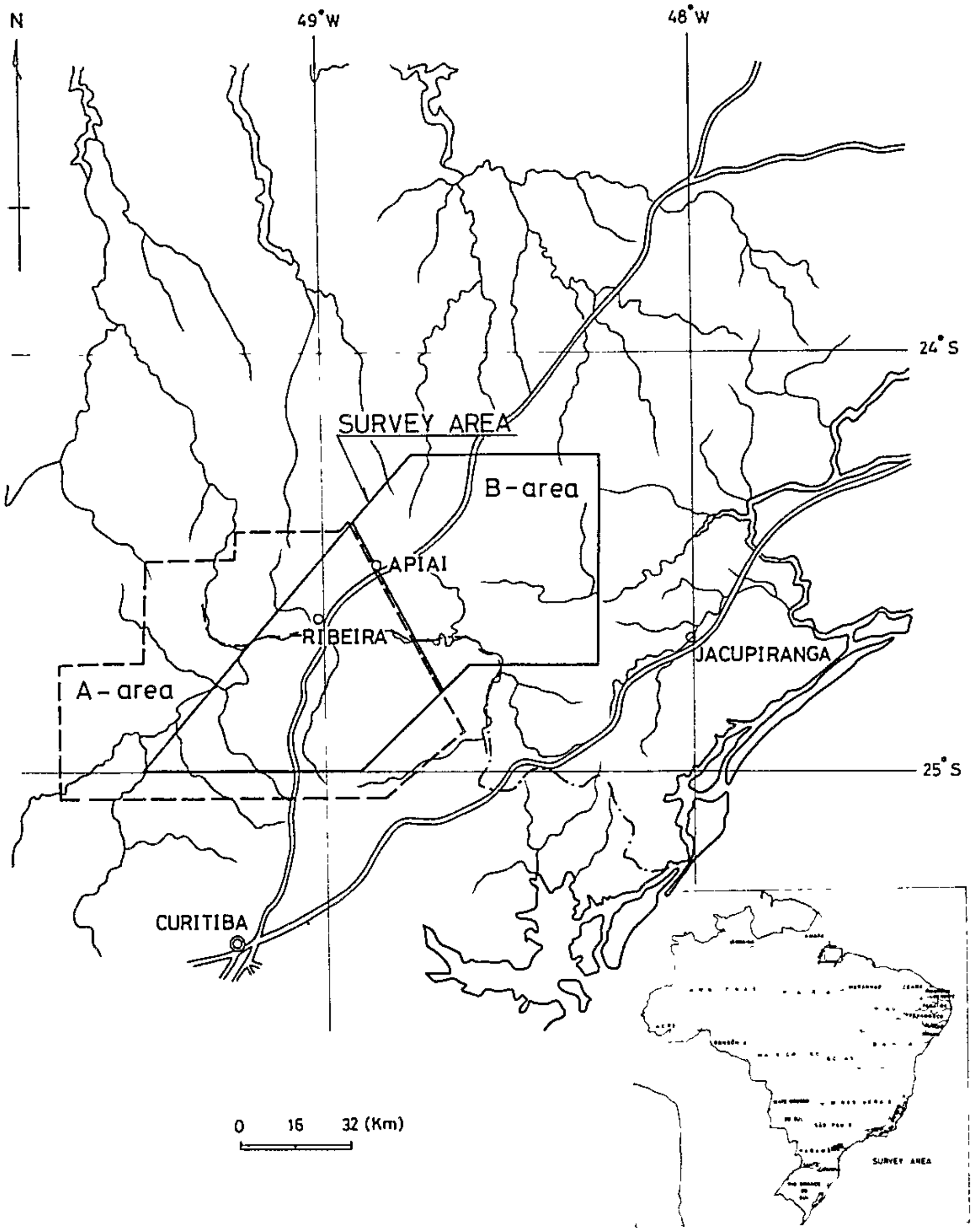

Fig. III-1 Location Map of Survey Area

Project Name : Serra do Mar Sul Project (Data Aquistion) – Airborne magnetic and radiometric survey at the Serra do Mar area, Santa Catarena and Parana.

Survey Period : August, 1975

Total Line Length : about 80,000km

Flight Altitude : 105 ~ 165m Above Ground Level (A.G.L.)

Separation of Flight Lines : 1km for the traverse lines and 20km for the tie lines.

Flight Directions : N30°W and N60°E

Geomagnetic Dip-Angle : 26°S

Geomagnetic declination : N14°W

Total Geomagnetic Intensity : 23,500 gammas

2) B-area

Project Name : Airborne geophysical survey at the São Paulo – Rio de Janeiro Area (airborn magnetic and radiometric surveys)

Survey Period : June to December, 1975

Total line length : about 32,000km

Flight Altitude : 150m A.G.L.

Separation of Flight Lines : 1km for the traverse lines and 20km for the tie lines.

Flight Directions : NS and EW

Geomagnetic Dip-Angle : 26°S

Geomagnetic Declination : N14°W

Total Geomagnetic Intensity : 23,500 gammas

2–3 Method of Analysis

The residual map has been drawn on the basis of the geomagnetic regional variation, which was calculated by subtracting the standard total intensity of the International Geomagnetic Reference Field (IGRF) from the aeromagnetic data. The analysis was made to the residual map.

There are two methods of analyzing aeromagnetic data. The first is a qualitative speculation of geological features selectively extracted from geomagnetic residual anomalies by means of some filtering procedures. The filters generally used are given as follows:

(1) Band-pass filter : which selectively extracts the magnetic anomalies with the optional region of wave length.

(2) Second vertical derivative filter : which emphasizes the short-wave length magnetic anomaly.

(3) Upward or downward continuation filter : which attennuates or emphasizes the short wavelength magnetic anomalies by means of calculating the magnetic value on the upper or lower level mathematically.

(4) Auto-correlation analysis : which delineate the geomagnetic characteristics by detecting similar magnetic anomalies.

(5) Spectrum analysis : This method is to understand the wave length characteristics of the geomagnetic anomalies in the survey area.

(6) Reduction-to-pole filter : which is used to infer the shapes of the magnetized body by means of calculating the magnetic anomaly at the magnetic pole mathematically.

The second analysis aims for estimating depths, shapes and magnetic properties of magnetized bodies. The corresponding methods are as follows :

(1) Specific Point Method
(2) Curve Matching Method
(3) Specific curve Method
(4) Analytical Method

This survey was conducted at the flight level of 105 ~ 165m A.G.L. in order to effectively detect the magnetic anomalies near the surface, it is assumed that the deep magnetic structure is masked by the shallow one.

In the present anomalies, the energy spectrum analysis by two-dimensional Fourier series was applied to the magnetic data obtained over 56km x 32km of the survey area including Rocha and Perau Mines. From the wavelength characteristics, two kinds of band-pass filter maps are obtained from the residual map. Thus three sheets of maps including the residual maps were obtained finally as the bases of qualitative analysis.

Quantitative curve matching analyisis, based on the residual map, were also made to the typical anomalies on the residual map.

The methods used in this analytical work are summarized in the following subsection. The flow chart of analyses is shown in Fig. III–2.

2–3–1 Spectrum Analysis

The wavelength characteristics of magnetic anomalies distributed over the survey area is usefully applied to a magnetic analysis through filtering as well as to an estimate of depth to

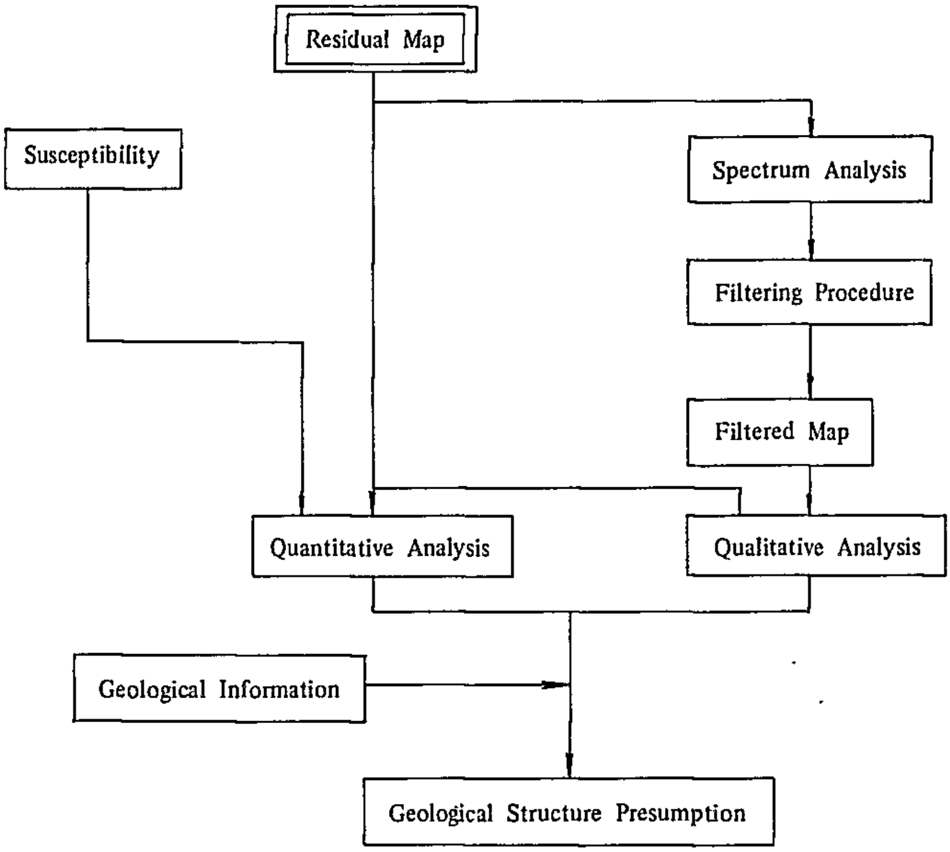

Fig. III-2 Flow Chart of Analysis

magnetic basement by using the potential theory.

1) Energy Spectrum

A value F(X, Y) in the rectangular coodinates is expressed in two-dimensional Fourier series as

$$F(x, y) = \sum_{m=0}^{\infty} \sum_{n=0}^{\infty} Amn \exp(-2\pi j (mx/L_1 + ny/L_2))\, dmdn$$

Hence, the Fourier coefficient Amn is given by

$$Amn = \frac{4}{L_1 L_2} \int_0^{L1} \int_0^{L2} F(x, y) \exp(2\pi j (mx/L_1 + ny/L_2))\, dxdy$$

The energy spectrum is then obtained as

$$Emn = / Amn /^2$$

2) Estimation of Mean Depth to Magnetic Basement

Assuming that an energy spectrum of magnetic anomalies due to a magnetic layer lying at a depth of H is white, the potential theory leads the following relation between energy spectrum Emn of wave numbers (m, n) and H. It is

$$Emn \propto \exp(-4\pi Hf),$$

Where f is a quantity called frequency :

$$f = \sqrt{(\frac{m}{L_1})^2 + (\frac{n}{L_2})^2}$$

The energy spectrum is plotted in an f vz. In Emn graph. A straight line is determined by the least square fitting to the plots. H is estimated from the tangent of the straight line.

2–3–2 Band-pass Filter

The band-pass filter is derived from the deviation two low pass filters whose cut-off frequencies are different from each other.

Assuming two cut off frequencies as ω_1, ω_2 $(\omega_1 > \omega_2)$, the coefficients of the band-pass filter is expressed as follows :

$$foo = (\omega_1 - \omega_2) / \pi^2$$

$$fno = fon = (\omega_1 \cdot \sin n\omega_1 s - \omega_2 \sin n\omega_2 s) / (n\pi^2 s)$$

$$fmn = (\sin m\omega_1 s \sin n\omega_1 s - \sin m\omega_2 \sin n\omega_2 s) / (m \cdot n\pi^2 \cdot s^2)$$

For actual computations, the band-pass filtered values are obtained by the convolution using the discrete magnetic data digitized at 1 km grid and the coefficient given by fmn.

2–4 Susceptivility Measurements of Rock Samples

A total of 56 rock samples were collected from outcrops at the location as shown in

PL. III–4. Magnetic susceptibility of all the samples were measured by means of a Bison Susceptibility Meter. The results are given in Table III–1.

The mean values of magnetic susceptibility amount to

2854×10^{-6}	cgs emu/cc	for	1	gabbro sample
1560	"	for	2	diabase samples
1400	"	for	2	syenite samples
467	"	for	6	granite samples
122	"	for	4	amphibolite samples
82	"	for	2	gneiss samples
52	"	for	16	pelitic rocks samples
51	"	for	6	psammitic rocks samples
48	"	for	10	limestone samples

Taking into account the susceptibility values, the rock samples were classified into four classes, class A (strongly magnetic rocks), class B (intermediately – magnetic rocks), class C (weakly magnetic rocks) and class D (slightly magnetic rocks). Gabbro, diabase and syenite belong to class A, granite to class B, amphibolite and gneiss to class C, pelitic rocks, psammitic rocks and limestone to class D.

According to the results of magnetic susceptibility measurements, it is expected that in the area where class A magnetic bodies are distributed, magnetic anomalies with a short wavelength and large amplitude are dominant, in the areas where the other classes magnetic bodies are distributed, there are many magnetic anomalies of small amplitude.

Table III–1 Susceptibility of Rock Samples (1)

	Sample No.	Rock Name	Density (gr/cm^3)		Susceptibility (x10^{-6} cgsemu)	
				Average		Average
Gneiss	F-66	Gneiss	2.61	2.76	65	82
	F-105	Gneiss	2.84		98	
	F-290	Gneiss	2.84		(503)	
Pelitic Rocks	F-2	Phyllite	2.62	2.55 (16)	42	52
	F-5	Mica-schist	(2.83)		(1,877)	
	F-28	Phyllite	2.60		74	
	F-76	Phyllite	2.45		28	
	F-293	Mica-schist	2.52		69	
	F-294	Phyllite	2.57		38	
	F-300	Sericite-schist	2.64		73	
	S-13	Sericite-schist	2.38		54	
	S-20	Sericite-schist	2.55		70	
	S-24	Calcareous-schist	2.73		62	
	T-10	Mica-schist	2.69		50	
	T-13	Mica-schist	2.67		51	
	T-16	Mica-schist	2.65		38	
	T-20	Sericite-schist	2.55		27	
	T-35	Phyllite	2.50		56	
	T-47	Phyllite	2.05		32	
	K-252	Sericite-schist	2.59		73	
Psammitic Rocks	F-1	Quartzite	2.64	2.63 (6)	61	51
	F-67	Quartzite	2.62		38	
	T-9	Psammitic-schist (metasandstone)	2.73		71	
	K-195	Psammitic-schist (metasandstone)	2.62		59	
	K-258	Psammitic-schist (metasandstone)	2.53		30	
	K-263	Psammitic-schist (metasandstone)	2.62		49	
Green-schist	T-30	Green-schist	2.92	2.87 (2)	88	85
	K-340	Green-schist	2.81		81	

Table III–1 Susceptibility of Rock Samples (2)

	Sample No.	Rock Name	Density (gr/cm^3)		Susceptibility (x10^{-6} cgsemu)	
				Average		Average
Limestone	F-72	Limestone	2.78	2.77 (10)	24	48
	S-15	Limestone	2.72		30	
	S-86	Limestone	2.77		47	
	S-89	Limestone	2.75		59	
	S-94	Limestone	2.73		61	
	S-128	Limestone	2.71		36	
	S-129	Limestone	2.75		43	
	T-58	Limestone	2.66		46	
	T-85	Limestone	2.72		54	
Amphibolite	F-7	Amphibolite	2.97	2.95	108	122
	F-272	Amphibole -schist	2.92		109	
	S-93	Amphibolite	2.99		117	
	K-176	Amphibole -schist	2.83		(4,115)	
	K-178	Amphibolite	2.99		(1,390)	
	K-182	Amphibolite	3.00		155	
Granite	F-39	Granite	2.61	2.64	225	467
	F-57	Granite	2.62		593	
	F-242	Granite	2.62		154	
	S-49	Granite	2.68		890	
	S-91	Granite	2.64		80	
	K-184	Granite	2.64		860	
Syenite	F-21	Syenite	2.59		1,272	1,400
	F-87	Syenite	2 65		1,528	
Gabbro	S-33	Gabbro	2.93		2,854	2,854
Diabase	S-17	Diabase	3.02	2.96	2,331	1,560
	S-95	Diabase	2.90		796	
	F-4	Magnetite	3.67		54,970	

CHAPTER 3 RESULTS OF ANOMALIES

In the residual map, the short wavelength magnetic anomalies reflecting shallower magnetic structure are dominant and the long wavelength which may correspond to deep magnetic structures ones are masked by those because of the flight of 105–165m A.G.L.

3–1 Residual Map

Judging from the magnetic anomalies shown in the residual map PL.III–1, the magnetic feature of the survey area are summarized as follows :

1) The southwestern part of A-area, is characterized by the groups of magnetic anomalies with the amplitude larger than 500 gammas and short wavelengths of 1–3km, of which the direction is almost NW–SE. This part is called as Zone A. In this zone, it is presumed that magnetic rocks belonging to class A such as gabbro, diabase and syenite, are extensively distributed.

2) In the area from central part to eastern part, there are small variation of magnetic value all over this area so magnetic bodies belonging to classes B, C and D may be distributed widely. At the northern and southeastern ends, there appear to be typical magnetic anomalies which may be caused by class A magnetic bodies.

The area from central to northeastern parts of this area, is called as Zone B, where relatively low magnetic values are detected. The southeastern part, called Zone C, is where relatively high magnetic values are detected.

3) In the northwestern part of the area, the northern part of Zones A and B, the trend of contour line with the direction of NE–SW is dominant and also there is a wide low magnetic anomaly with the direction of NE–SW. This part is called as Zone D.

From this point, the typical magnetic anomalies are classified with these zone signature.

3–2 Band Pass Maps

Fig. III–4 shows an energy spectrum analysis result of magnetic anomalies based on the residual map of an area 56km of N14°W–S14°E by 32km of N76°E–S76°W including Zones B and C (Fig. III–3). Judging from the energy spectrum distribution, the energy spectrum has a tendency to decrease with wavelength.

The wavelength domain is divided into three subdomains whose boundary wavelengths

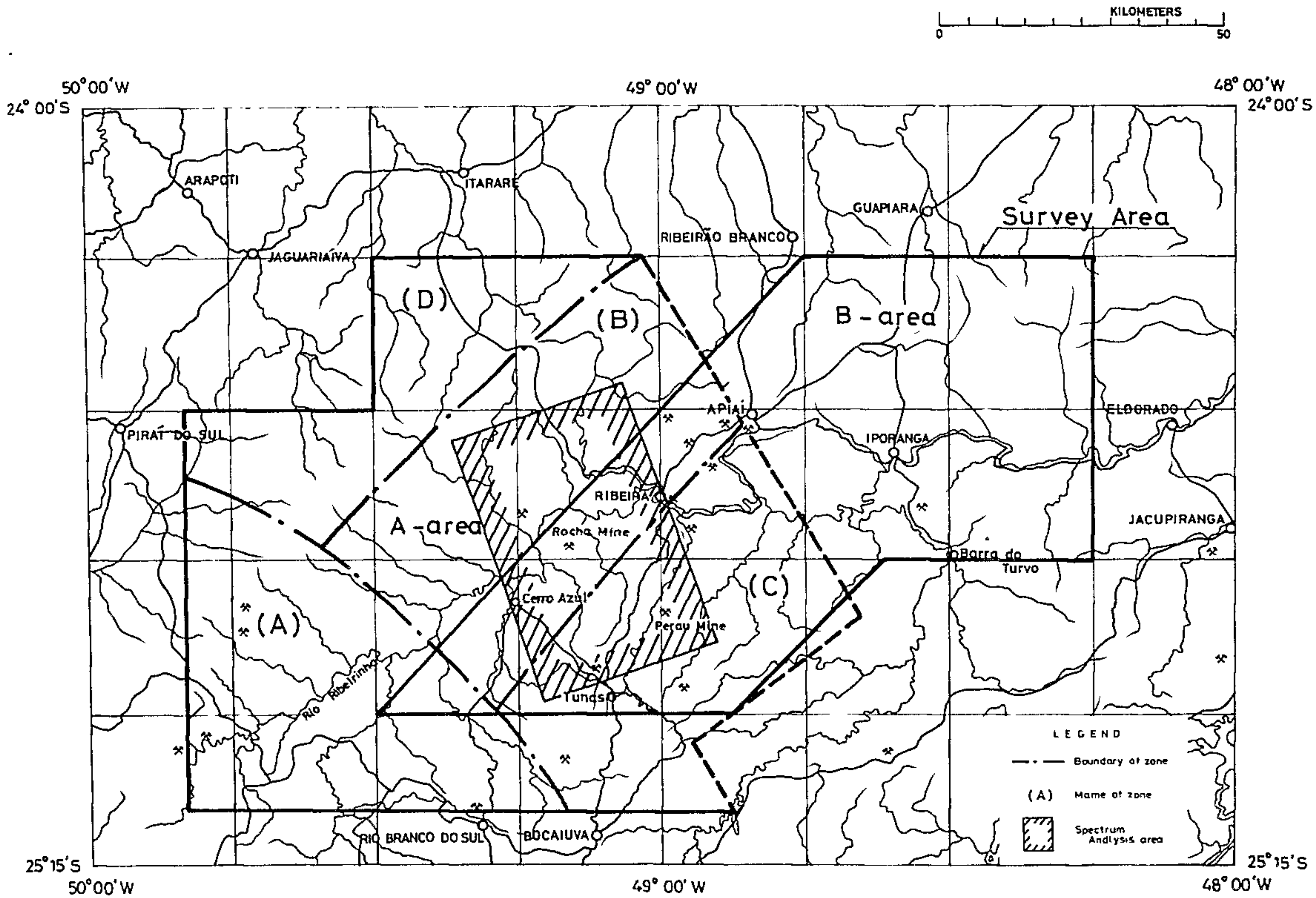

Fig. III–3 Index of Analyzed Area

(λ) are 2km, 4km and 16km. Straight lines are fitted by the least squares method in each of the subdomains, i.e. 2–4km and 4–16km. From the gradients of the straight lines, the depths to the magnetic basement are estimated as –2km and –6km from the flight level respectively. But as this survey flight path was not conducted by exactly horizontal flight, these values will be apparent depth for mathematical procedures.

In order to distinguish the distribution of the magnetic bodies from those sizes, the following two band-pass filters were designed.

1) BP–1 : Band-pass filter for a wavelength domain 2–4km.

2) BP–2 : Band-pass filter for a wavelength domain 4–16km.

These two filters were applied to the residual map to obtain two band-pass maps, BP–1 and BP–2.

Based on these band-pass maps, a qualitative discussion is given below.

3–2–1 Band Pass Map (BP–1)

This map has a similar distribution of the magnetic anomalies with the residual map, but the short wavelength anomalies became dominant. It can be seen that three are the continuities in the arrangement of magnetic anomalies detected in the residual map within each zones. In Zone A, the continuities of NW–SE direction are dominant. In Zone B, at the vicinity of the boundaries with Zone C and with Zone D, the trend of NE–SW direction is dominant, and partly there are continuities of the direction oblique or perpendicular with that direction. In Zone C and D, there are dominantly the continuities of NE–SW directions.

Magnetic anomalies with an amplitude larger than 500 gammas which exist within Zone A or which are classfied with the number of magnetic anomaly may be caused by the class A magnetic bodies.

In other part of Zones B and C excluding the intensive magnetic anomalies, where the amplitude of magnetic anomalies is relatively small, there may exist dominantly the class B, C and D magnetic bodies.

The magnetic discontinuity as judged from the magnetic anomaly features does not always coincide with geotectonic lines in a geological sense. Taking the above circumstances and the susceptibility measurement results of rock specimens into consideration, a qualitative interpretation is made to the BP–1 Maps follows.

1) Zone A : Plenty of small scale magnetic bodies of class A with the direction of the major geotectonic line (NW–SE) are distributed.

2) Zone B : The direction of the major geotectonic line is NE–SW, which is distributed almost parallel to the boundary with Zone D on north side and Zone C on south side. The south side geotectonic line is consisted of three sub-geotectonic lines ;

(i) one which runs from Cerro Azul to 5km east of Itapirapua and extends to the north (B–a),

(ii) one which starts Rocha mine to 5km north of Ribeira and extends to the northeast (B–b),

(iii) one with the NW–SE direction from 5km east of Itapirapua to 5km north of Ribeira (B– c)

It is thought that the magnetized body of class B (granite) is mainly distributed in Zone B and the magnetic discontinuities with the direction of NW–SE and the magnetic anomalies such as B-1, 2, 3, 4 and 5 are induced by the class A magnetized bodies (diabase, basaltic rocks).

3) Zone C : The direction of the major magnetic discontinuities, which disappear at the boundary with Zone A, is NE–SW. And also another geotectonic line may be existed from 10km east of Cerro Azul to Paneras mine. Like Zone B, in Zone C, as an amplitude of magnetic anomalies is very small, there exist widely the magnetic bodies of class B, C and D (granite, amphibolite, pelitic rocks, psammitic rocks and limestone). But class A magnetic bodies like gabbro, syenite and diabase, may induce the magnetic anomalies of C– 1, 2 and 4 with an amplitude of 500 γ.

4) Zone D : The direction of the major magnetic discontinuities is NE–SW, but, there are also small ones perpendicular to those direction. It is estimated that, in this zone, the magnetized bodies of class B, C and D (granite, amphibolite, pelitic rocks and limestone), causing magnetic anomalies less than 200 gammas, are dominantly distributed, excluding the northwestern edge where the magnetic bodies of class A may cause the magnetic anomalies with an amplitude larger than 500 gammas.

3–2–2 Band Pass Map (BP–2)

This map is characterized by the magnetic anomalies with an amplitude of 250 gammas and a half wavelength of about 10km.

At Zone A, the magnetic anomalies are arranged at the direction of NW–SE, which coincides with the direction of the major magnetic discontinuities as mentioned in 3–2–2. And

also, at Zone D, it can be seen that the trend of contour line is NE–SW and the low magnetic anomaly with long wavelength is distributed.

On the other hand, at Zones Band C, it is easily understandable that the magnetic anomaly features are derived from the smoothing effect for the magnetic anomalies like B–1 ~ 4 and C–1 ~ 5.

Therefore, it is thought that this map does not reflect the deep magnetic structure and expresses only the apparent magnetic anomalies as calculated mathematically.

3–3 Quantitative Analyses

Some profiles are drawn for typical magnetic anomalies on the residual map. Depths to the magnetic source and its apparent susceptibility were estimated from the data by means of the curve matching method using the standard curves of the prism, dyke and other models. In proportion to the obtained susceptibilities, the magnetic intensity of the source is classified into four classes A, B, C and D, as stated in 2–4.

P.L.III–4 shows the above results synthetically estimated from both the quantitative and the quantitative analyses.

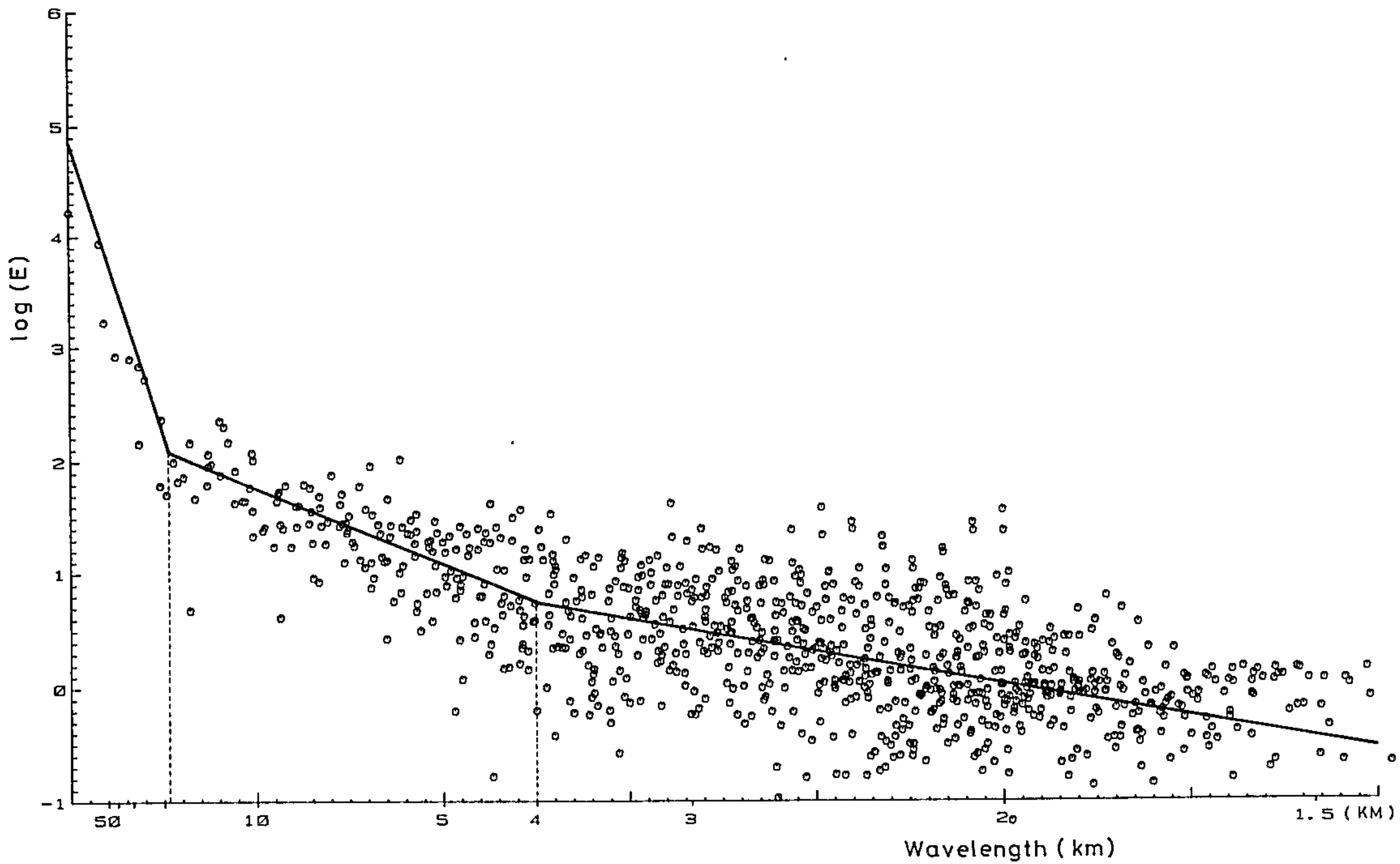

Fig. III—4 Energy Spectrum vs. Wavelength

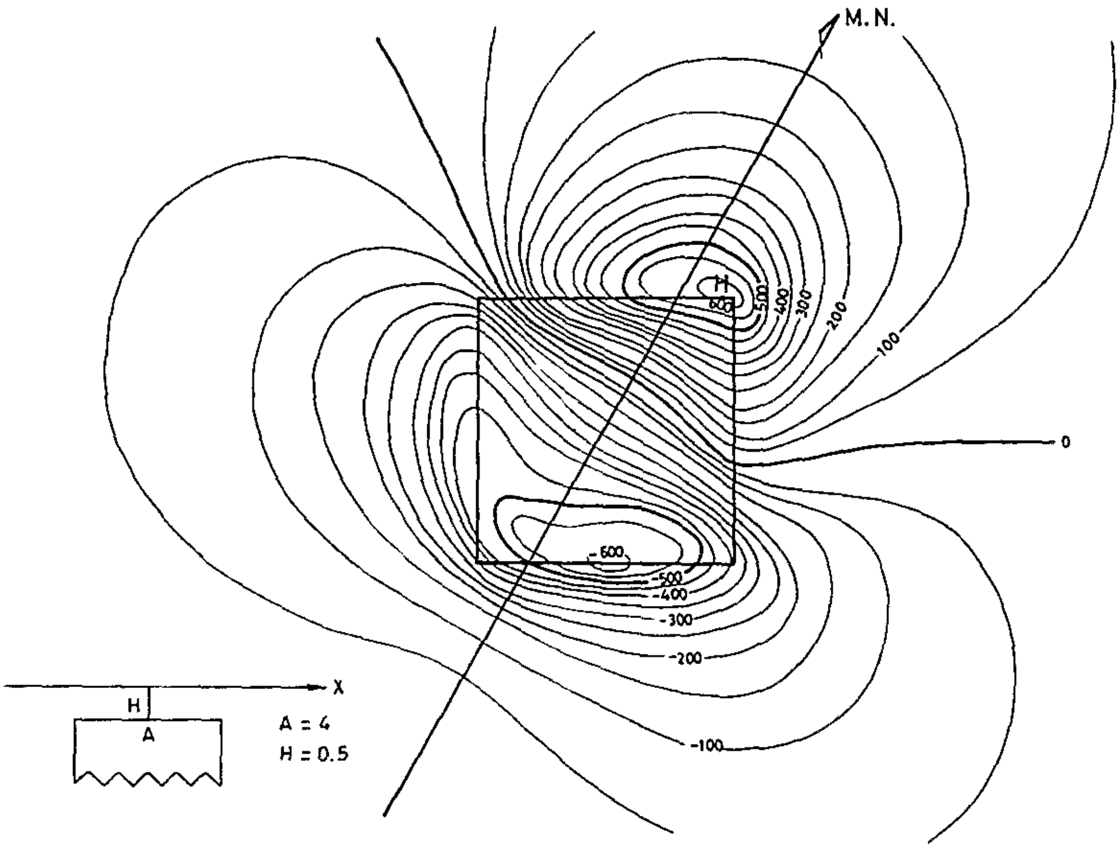

Fig. III–5 Magnetic Anomaly due to Prism Model
(Inclination 26°S)

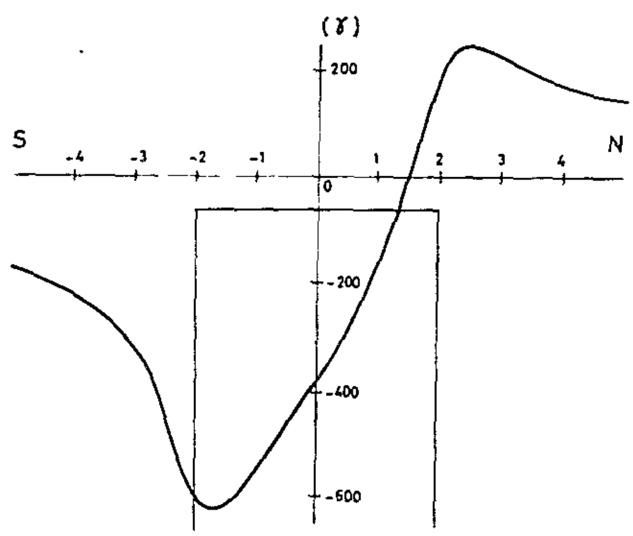

Fig. III–6 Magnetic Anomaly due to Dyke Model
(Inclination 26°S)

CHAPTER 4 CONCLUSIONS

Magnetic anomalies in the survey area are classified into four classes A, B, C and D, which are induced by the buried magnetic sources of class A (strongly magnetic), class B (intermediate magnetic), class C (weakly magnetic) and class D (slightly magnetic) respectively.

According to the magnetic susceptibility measurements of rock samples, gabbro, diabase and syenite belong to class A, granite to class B, amphibolite and gneiss to class C and pelitic rocks, psammitic rocks and limestone to class D.

The results of the survey can be summarized with geological implications as follows :

1) In the area from central to northeastern area (Zone B), class B magnetic body (granite) is prominantly distributed with a width of about 30km and trending the direction of NE–SW, and its both edges is limited by geotectonic lines. At the north end and central part in this body, magnetic bodies of class A (syenite, diabase) exist as intrusive rocks, in which B–1 and B–3 is outcropped but other B–2, B–4 and small magnetic bodies in the vicinity of B–3 are concealed. Also, narrow dykes of class A are expressed as the magnetic discontinuities of the NW–SE direction.

2) According to the geological information, there exists large amounts of granite (class B magnetic body) in the southwest of the area of Zone B . But, it is difficult to delineate its distribution because of the existence of many small class A magnetic bodies (diabase) with the NW–SE direction. It is possible to understand that the geotectonic lines detected in the southwestern part of the survey area correspond to narrow dykes of class A magnetic body.

3) In the southeastern part of the survey area, the magnetic bodies of class D is most widely distributed and the major geotectonic lines have the direction of NE–SW. The magnetized bodies of class A (gabbro and syenite) are detected near Rocha mine (B–5), south of Ribeira (C–1), near Tunas (C–4) and about 10km east of Perau mine. The relation between these intrusive rocks and mines is not clear now. The magnetized bodies of class C (gneiss, amphibolite) is distributed parallel to the above-stated geotectonic line from the south of Ribeira to about 20km southeast of Tunas.

Based on above-mentioned considerations, the following conclusions were derived:

The geological lineation runs in a NE–SW direction. This tendency is consistent with the magnetic lineament. The distributions of granite, sycnite, gabbro and diabase are almost

always recognized. Mines in the survey area locate within the magnetic body of class D. The relation these mines and the magnetic bodies of class A and B (gabbro, diabase, syenite and granite) is not clear.

It is suggested that, by means of re-analyzing aeromagnetic data of the B-area and considering both the results of Phase I and B-area, the distribution of class D magnetic body closely related with mines be recognized and the correlation between mine and class A and B magnetized bodies be also revealed.

APPENDICES

Photo. A–1 Microphotograph of Thin Section

Abbreviations

q	:	quartz
pl	:	plagioclase
kf	:	potash feldspar
bt	:	biotite
mus	:	muscovite
hb	:	hornblende
tr	:	tremolite
au	:	augite
ae	:	aegirine
ga	:	garnet
op	:	opaque mineral
tor	:	tourmaline
ser	:	sericite
chl	:	chlorite
srp	:	serpentine
ep	:	epidote
cal	:	calcite
dol	:	dolomite

Sample No. : F–105
Rock name : hornblende epidote biotite gneiss (Setuva F.)
Location : Cerra do Cadeado

0 1mm

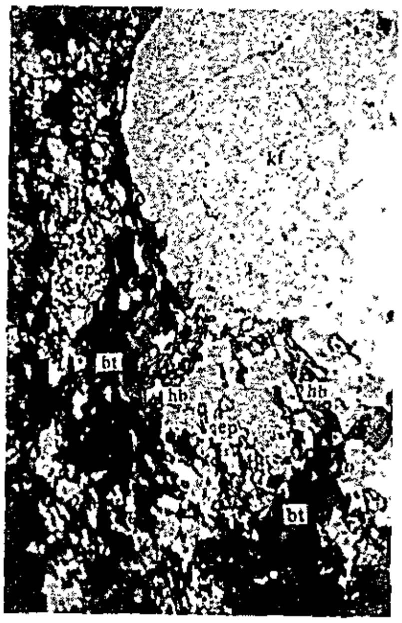

(only lower polar)

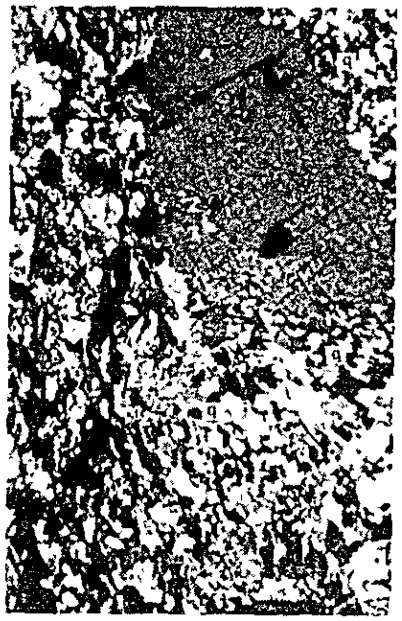
(crossed polars)

Sample No. : S–37
Rock name : biotite muscovite schist (Açungui I F.)
Location : Barrinha

0 0.5mm

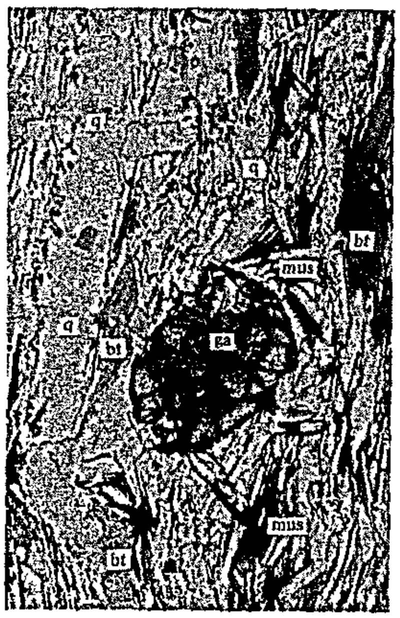

(only lower polar)


(crossed polars)

Sample No. : F–1
Rock name : quartzite (Açungui I F.)
Location : Perau Mine

(only lower polar)

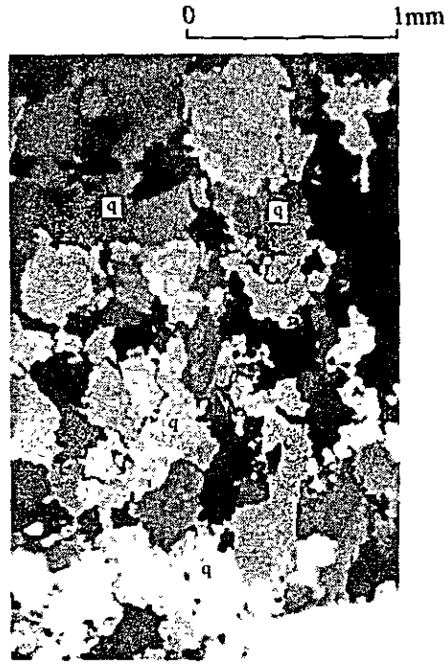

(crossed polars)

Sample No. : F–278
Rock name : calcareous muscovite tremolite schist (Açungui I F.)
Location : Perau Mine

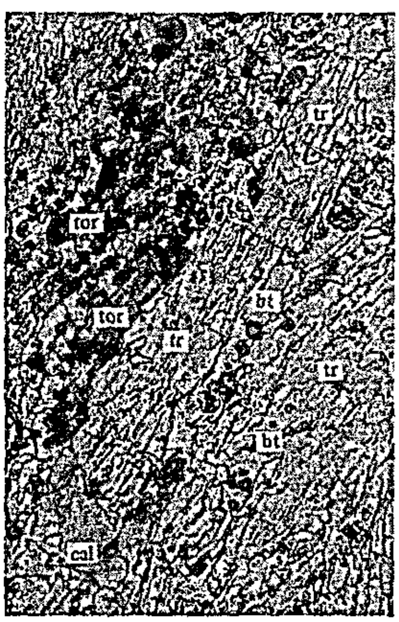

(only lower polar)

(crossed polars)

Sample No. : F–7
Rock name : amphibolite (Açungui I F.)
Location : Perau Mine

0 1mm

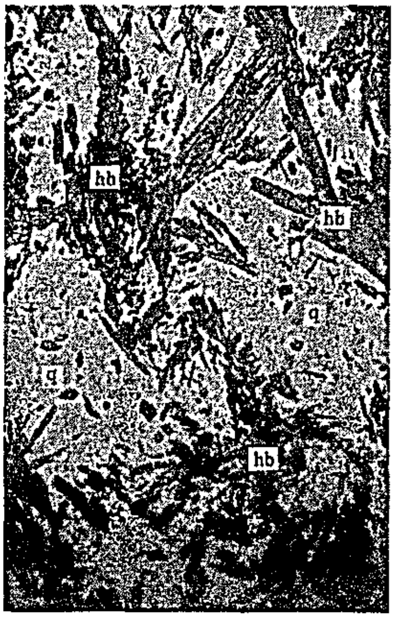

(only lower polar)

(crossed polars)

Sample No. : T–10
Rock name : chlorite sericite schist (Açungui II F.)
Location : Barra do Turvo

0 0.5mm

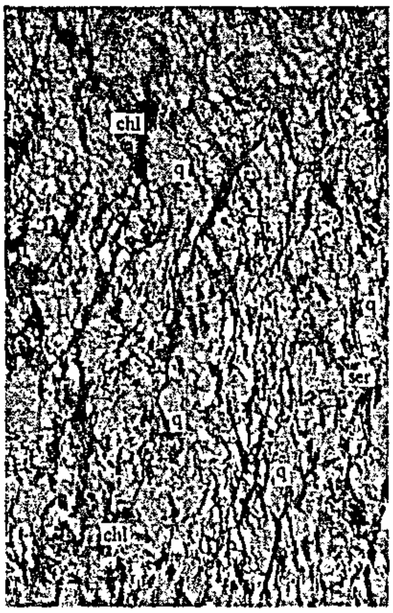

(only lower polar)

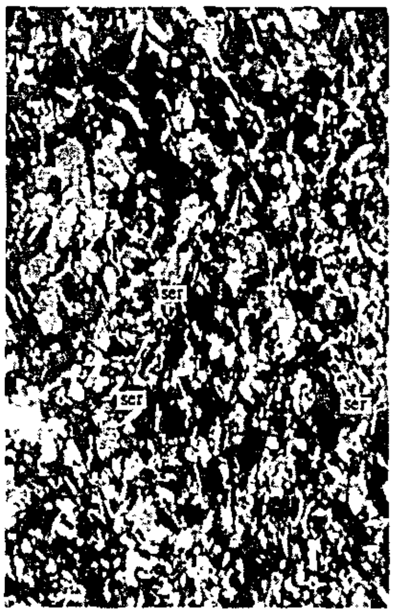

(crossed polars)

Sample No. : S–9
Rock name : sandstone (Açungui III F.)
Location : Adorianopolis

(only lower polar)

(crossed polars)

Sample No. : K–272
Rock name : sericite chlorite schist (Açungui III F.)
Location : Iporanga

(only lower polar)

(crossed polars)

Sample No. : S−126
Rock name : limestone (Açungui III F.)
Location : Rocha Mine

0 0.5mm

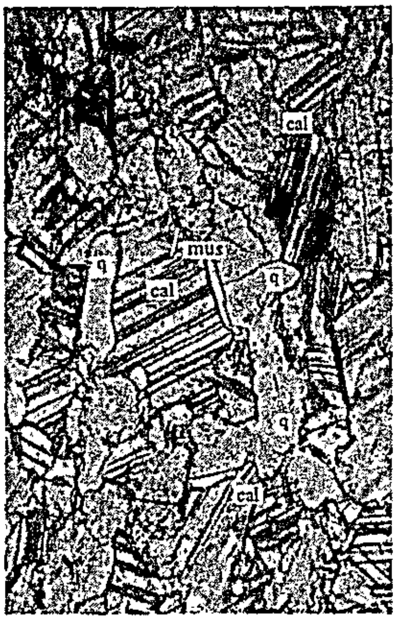

(only lower polar)

(crossed polars)

Sample No. : S−127
Rock name : dolomite (Açungui III F.)
Location : Rocha Mine

0 0.5mm

(only lower polar)

(crossed polars)

Sample No. : S–48
Rock name : amphibolite (Açungui III F.)
Location : Adrianopolis

0 1mm

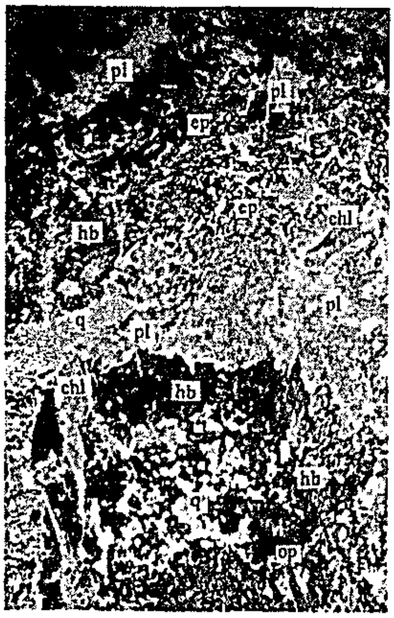

(only lower polar)

(crossed polars)

Sample No. : F–57
Rock name : granite
Location : Cerro Azul

0 1mm

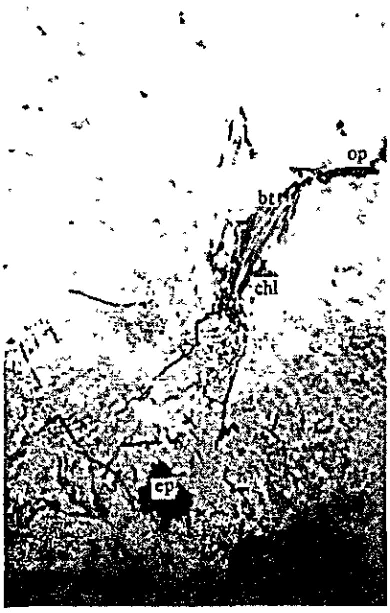

(only lower polar)

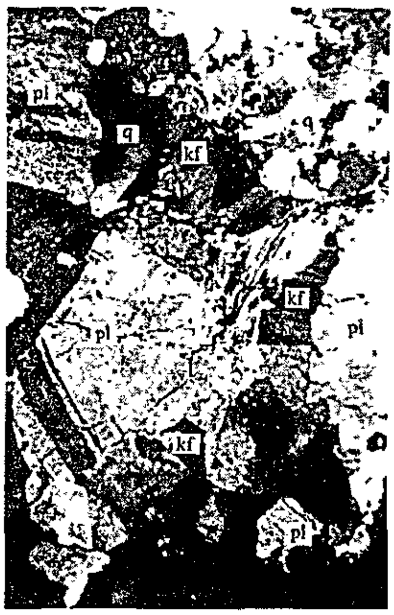

(crossed polars)

Sample No. : F–124
Rock name : granite
Location : Itaoca

0 1mm

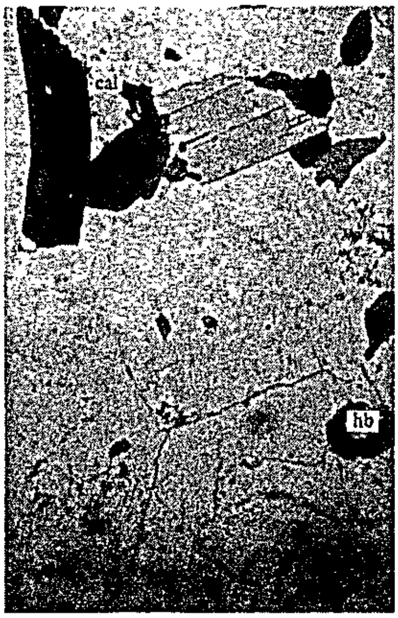

(only lower polar)

(crossed polars)

Sample No. : F–87
Rock name : aegirin syenite
Location : Tunas

0 1mm

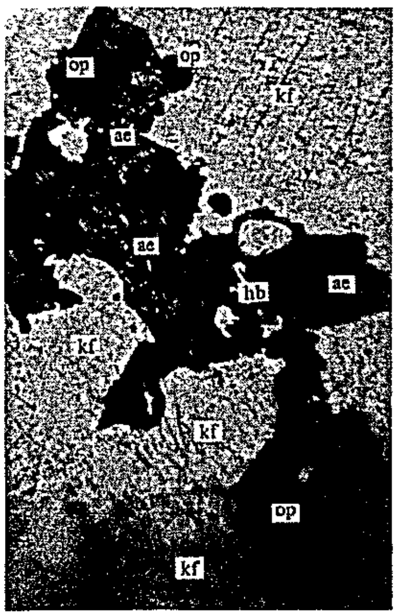

(only lower polar)

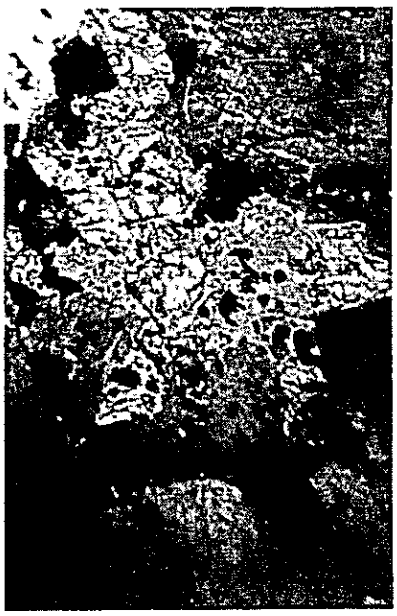

(crossed polars)

Sample No. : F–9
Rock name : diabase
Location : Perau

0 0.5mm

(only lower polar)

(crossed polars)

Sample No. : F–38
Rock name : gabbro
Location : Morro Agudo

0 1mm

(only lower polar)

(crossed polars)

Photo. A–2 Microphotograph of Polished Section

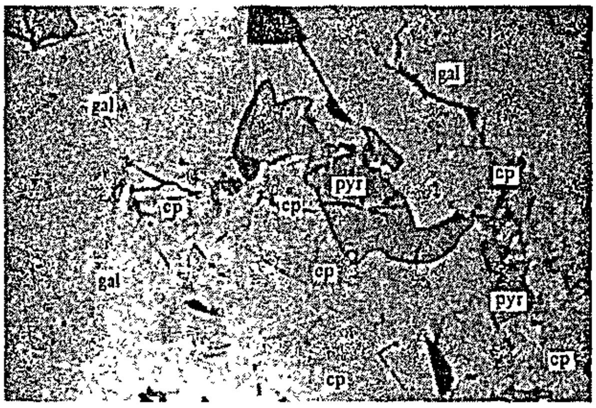

0 0.5mm

Sample No. : F–204
Rock name : lead ore
Location : Panelas Mine

Refrected light
Only lower polar

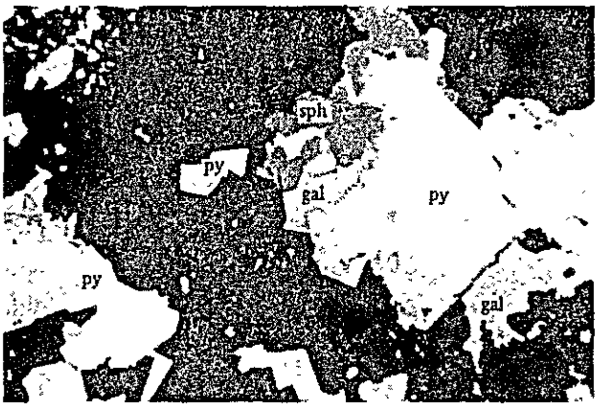

0 0.5mm

Sample No. : K–351A
Rock name : lead and zinc ore
Location : Lageado Mine

Refrected light
Only lower polar

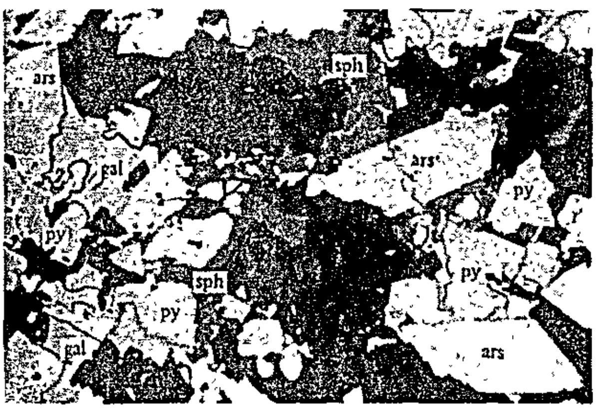

0 0.5mm

Sample No. : K–351C
Rock name : lead and zinc ore
Location : Lageado Mine

Refrected light
Only lower polar

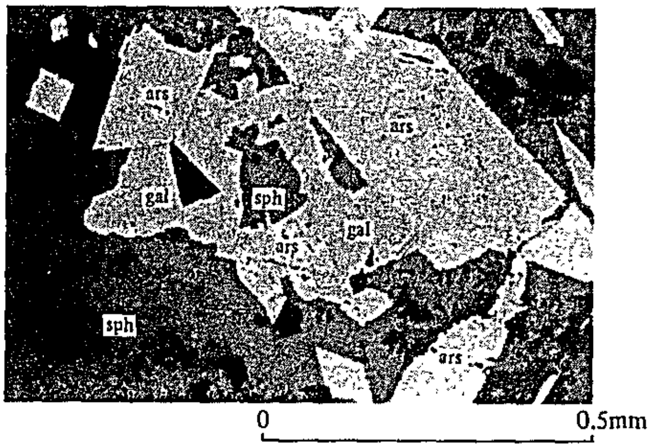

Sample No. : T–81
Rock name : lead and zinc ore
Location : Furnas Mine, 500mL

Refrected light
Only lower polar

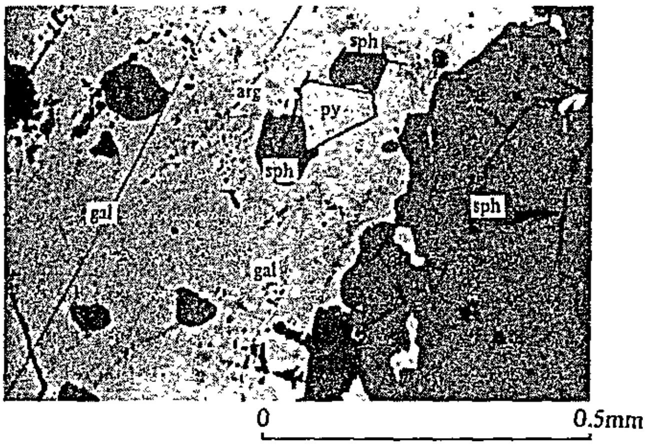

Sample No. : T–83
Rock name : lead and zinc ore
Location : Furnas Mine,
Santa Barbara II

Refrected light
Only lower polar

Abbreviations

py : pyrite
cp : chalcopyrite
ars : arsenopyrite
pyr : phyrrhotite
gal : galena
sph : sphalerite
arg : argentite

Table A-1 List of Mines and Showings

(1)

Ser. No.		Name of Mine	Kind of Ores	Type	Status Quo	Location	Host Rock	Ore Deposits: Strike & Dip	Ore Deposits: Lateral Extension	Ore Deposits: Longitudinal Extension	Ore Deposits: Average Width	Grade (%): Au	Grade (%): Ag	Grade (%): Cu	Grade (%): Pb	Grade (%): Zn	Ore-Mineral	Remarks
									m	m	m	g/T	g/T	%	%	%		
1.		Espirito Santo	Pb	vein	closed	Estado São Paulo Municipio Iporanga	Açungui III F limestone	N80W~N80E 65~80N	20	–	0.40	–	–	–	–	–	Ga, Sp, Py, Cp	
2.		Maximinioro	Pb, Ag	do	do	do	do	N40E 60S	100?	4	0.10	0	33	0.1	0.8	0.0	Ga, Q	
3.		Furnas	Pb, Ag	stratiform & vein	operating	do	do	N40–60W, 55N & E–W, 80S	100	300	0.20 0.20	0	200	0.1	12.0	8.0	Ga, Sp, Py, Cp, Cer, Lim	production (1981) 500T/M Pb:7% Ag:3,000g/T
4.	Lageado Group	Lourenço Velho	Pb	vein	closed	do	do	N50E 80S	20~30	–	0.30	–	–	–	–	–	Ga, Lim, Cer	
5.	Lageado Group	Santana Velha	Pb	do	do	do	do	N55E 75S	800	30	0.50	–	–	–	–	–	Ga, Lim	
6.	Lageado Group	Santana Nova	Pb	do	do	do	do	N60E 75S	600	200	0.20	1	1,050	0.0	30.3	0.0	Ga	ore pocket 50m x 5m x 0.2m
7.	Lageado Group	Mamangaba	Pb	do	do	do	do	N60E 60S	500	100	0.80	0	215	0.0	11.1	0.0	Ga, Sp, Py Cer, Lim	ore pocket 200m x 20m x 0.8m
8.	Lageado Group	Porco de Mato	Pb	do	do	do	do	N70E 70S	–	–	0.30	–	–	–	–	–	Ga, Sp, Py	
9.	Lageado Group	São Vicente	Pb	do	do	do	do	N40E 80S	–	–	0.30	0	1,210	0.3	30.2	0.2	Ga, Py, Sp, Lim	
10.	Lageado Group	S. Rafael	Pb	do	do	do	do	N40E 60S	–	–	2.00	1	1	0.0	0.9	0.0	Ga, Py, Po, Cp, Lim	
11.	Lageado Group	Jardim II	Pb	do	do	do	do	N40E 60S	200	5	–	0	1,130	0.3	29.8	0.1	Ga, Sp, Py	
12.	Lageado Group	Bugios	Pb	do	do	do	do	N40E 70S	?	–	–	–	–	–	–	–	Ga	
13.	Lageado Group	Coqueiro	Pb	do	do	do	do	N60E 80S	–	–	–	–	–	–	–	–	Ga	
14.		Rocha	Pb, Ag	do	operating	Estado Parana Municipio Adrianopolis	Açungui III F dolomite	N10~30W 60N,60S	180~400	150~300	0.10~2.00	1	130	0.5	18.0	0.4	Ga, Sp, Cp, Py	production (1981) 2,500T/M Pb:6.5% Ag:130g/T
15.		Barrinha	Pb, Ag	stratiform	under Exploration	do	Açungui III F limestone & calcareous shale	N50~70E 40~80N	50~70	70~200	0.50~14.00	1	150	0.1	30.6	0.0	Ga, Sp, Cp, Py Cer, Pyro	

Ser No.	Name of Mine	Kind of Ores	Type	Status Quo	Location	Host Rock	Ore Deposits: Strike & Dip	Ore Deposits: Lateral Extension	Ore Deposits: Longitudinal Extension	Ore Deposits: Average Width	Grade (%): Au	Grade (%): Ag	Grade (%): Cu	Grade (%): Pb	Grade (%): Zn	Ore-Mineral	Remarks
16.	Paqueiro	Pb, Ag	vein & stratiform	closed	do	Açungui IIIF limestone	N50~60E 80N~80S	1~70	40	0.20~1.20	1	214	0.5	9.6	0.0	Ga, Sp, Cp, Py	total production 16,300T Pb:9%
17.	Bueno	Pb, Ag	do	do	do	do	N35E 50S	15	20	1.50	1	70	0.2	23.1	0.0	Ga, Py	total production 66T Pb:10.6%
18.	Diogo Lopes	Pb, Ag	do	do	do	do	N75~85E 50–70S	10	50	0.80	1	221	0.1	16.1	0.4	Ga, Py	total production 144T Pb.9.72%
19.	Onça II	Pb	vein	do	do	do	N45E	–	–	–	–	–	–	–	–	Ga	
20.	Quarenta Qitava	Pb	do	do	do	do	N45E	–	–	–	–	–	–	–	–	Ga	
21.	Braz	F	do	do	do	do	–	–	–	–	–	–	–	–	–	F, Ga, Py, Cp	
22.	Carumbe	Pb, Cu	do	do	do	do	–	–	–	–	–	–	–	–	–	Ga, Py, Cp, F	
23.	Cecrisa	Pb	stratiform	do	do	Açungui III F calcareous shale	E–W 60N	–	–	0.10~0.50	0	187	0.1	7.9	0.0	Ga, Cer	
24.	Laranjal	Pb	do	do	do	do	N70E 60N	–	–	0.50	1	223	0.6	17.4	0.1	Ga	
25.	Onça I	Pb	vein	do	do	Açungui III F limestone	–	–	–	0.30	–	–	–	–	–	Ga	
26.	Panelas	Pb	stratiform & vein	operating	do	do	N40E 50N	900	200	0.30	0	130	0.3	24.0	0.0	Ga, Sp, Py, Po	total production 1,200,000T Pb:7.0% production (1981) 2,500T/M Pb:5.8% Ag.100g/T
27.	Fluorita de Sete Barras	F	vein	closed	do	do	N80E	50+	20	0.50	nd	(F) 24.6	nd	nd	nd	F	
28.	Mater Empresa de Mineração	Cu	stratiform	do	do	Açungui II F calc-silicate rock	N80W 35N	60	60	0.50	1	10	0.4	0.2	0.7	Cp, Py, (Ga)	
29.	Pretinhoe	Ba	do	operating	do	Açungui I F calc-silicate rock	N40E 35S	1,000	100+	1.50	($BaSO_4$) 85	(S) 0.5	ppm 800	ppm 50	ppm 60	Ba	production (1980) 140T/Y
30.	Perau	Pb	do	do	do	do	N10E 30W	300+	200	0.50	0	120	0.2	18.7	2.0	Ga, Sp, Cp, Py	production (1981) 1,500T/M Pb.8.5% Ag:100g/T
31.	Agua Clara	Cu	do	closed	do	Açungui I F dolomite	E–W 40S	10	50	0.20	0	8	0.8	0.0	0.0	Ga, Cp	

– no data

Ga : Galena Sp : Sphalerite Cp : Chalcopyrite
Cer : Cerussite Pyro : Pyromorphite Po : Pyrrhotite
Py : Pyrite Lim : Limonite F : Fluorite
Ba : Barite

Table A–2 Microscopic Observations (Thin Section)

Abbreviations

Rock forming minerals

q	:	quartz
pl	:	plagioclase
kf	:	potash feldspar
bt	:	biotite
mus	:	muscovite
hb	:	hornblende
tr	:	tremolite
au	:	augite
ae	:	aegirine
cpx	:	clinopyroxene
ga	:	garnet
op	:	opaque mineral
tor	:	tourmaline
ap	:	apatite
zi	:	zircon
sph	:	sphene
ser	:	sericite
chl	:	chlorite
srp	:	serpentine
ep	:	epidote
cal	:	calcite
dol	:	dolomite

Rock name

gn	:	gneiss
sch	:	schist

Metamorphic Rocks

(1)

Formation	Sample No.	Location	Rock name	Texture	q	pl	kf	bt	mus	hb	tr	ga	op	tor	ap	zi	sph	ser	chl	ep	cal	dol	Remarks
Setuva Formation	F– 66	Tunas	bt - ep - gn	porphyroblastic	◎	•	○	•	•			·			•			•	•	•			
	F–105	Cerra do Cadeado	hb - ep - bt - gn	porphyroblastic	◎		○	◎		•										○	•		see photograph.
	F–106	Cerra do Cadeado	bt - gn	porphyroblastic	◎	○		◎					•		•			○					
	F–290	Barra do Turvo	ep - hb - gn	nematoblastic	○	◎	○			◎		•	•					•		•	•		
Açungui Group, I Formation	F– 1	Perau Mine	quartzite	granoblastic	◎		•						•					•					see photograph.
	F– 7	Perau Mine	amphibolite	lepidoblastic	◎	•				◎			•		•								see photograph.
	F– 67	Tunas	quartzite	lepidoblastic	◎								•					•	•				
	F–115	Barrinha	bt - mus - sch	nematoblastic	◎			○	◎		•	•	•	•						•			
	F–278	Perau Mine	calcareous mus - tr - sch	lepidoblastic				○	•		◎		•	○							○		see photograph.
	K–331	Lageado Mine	phyllite	fibroblastic	◎				•				•					○					
	K–332	Lageado Mine	sandstone	blastopsammitic	◎								•	•									
	K–357	Lageado Mine	chl - ser - sch	fibroblastic	○								•	•				◎	◎				
	K–359	Lageado Mine	ser - chl - sch	porphyroblastic	◎									•				○	○				
	K–401	Rio des Pilões	chl - mus - sch	lepidoblastic	◎			•	◎					•					◎				
	S– 37	Barrinha	bt - mus - sch	nematoblastic	◎			○	◎			○											showing microfolding, see photograph.
	S– 41	Barrinha	bt - mus - sch	nematoblastic	◎			○	◎			•	•						•				
	S– 93	Barrinha	amphibolite	nematoblastic	○					◎			•				•						
	T– 30	Iporanga	calcareous green sch	lepidoblastic	○	•							•	•					◎		○		
	T– 31	Iporanga	phyllite	fibroblastic	◎								•					◎					fine grained.
	T–170	Rio Pescaria	phyllite	fibroblastic	◎								•					◎					
	T–173	Rio Pescaria	green sch	granoblastic							○		•						◎				
II Formation	T– 9	Barra do Turvo	ser - sch	lepidoblastic	◎								○					◎			•		
	T– 10	Barra do Turvo	chl - ser - sch	nematoblastic	◎									•				◎	○				see photograph.
	F–251	Adrianopolis	calcareous amphibolite	granoblastic							◎										◎		
	K–151	Araçaiba	chl - ser - sch	porphyroblastic	◎	•	•		•				•					◎	○				
	K–161	Apiai	sandstone	blastopsammitic	◎								•										
	K–192	Furnas	ser - chl - sch	lepidoblastic	◎										•		○	◎	◎				

(2)

Formation	Sample No.	Location	Rock Name	Texture	q	pl	kf	bt	mus	hb	tr	ga	op	tor	ap	zi	sph	ser	chl	ep	cal	dol	Remarks
III Formation	K–215	Furnas	calcareous sch	lepidoblastic	◎								•					•			◎		
	K–259	Iporanga	ser - chl - sch	porphyroblastic	◎								○	•		•		◎	◎		•		
	K–272	Iporanga	ser - chl - sch	porphyroblastic	◎								•	•				◎					see photograph.
	S– 9	Adrianopolis	sandstone	blastopsammitic	◎								○		•			○	•				see photograph.
	S– 13	Adrianopolis	chl - ser - sch	lepidoblastic	◎								◎	•				◎	○				
	S– 18	Rocha	ser - sch	lepidoblastic	◎								○	•		•		◎	•				
	S– 45	Adrianopolis	calcareous chl - sch	porphyroblastic	◎								○						◎		◎		
	S– 48	Adrianopolis	amphibolite	poikiloblastic	○	◎				◎			◎	•					◎	○			see photograph.
	S– 83	Barrinha Mine	calcareous chl - sch	lepidoblastic	◎								◎						○		◎		
	S–126	Rocha Mine.	limestone	granoblastic	•				•				•								◎		see photograph.
	S–127	Rocha Mine	dolomite	lepidoblastic	○				•				•									◎	see photograph.
	S–132	Espirito Santo	sandstone	blastopsammitic	◎								•		•	•		○	•				
	S–135	Espirito Santo	sandstone	blastopsammitic	◎								○	•		•		○	•				
	T– 87	Furnas Mine	limestone	granoblastic	•				•				○								◎		
	T–117	Furnas Mine	ser - sch	fibroblastic	◎								•					◎	○				showing microfolding.

Igneous Rocks

(3)

Sample No.	Location	Rock name	Texture	Phenocryst										Groundmass							Secondary mineral									Remarks
				q	kf	pl	bt	mus	hb	au	ae	ap	op	q	kf	pl	bt	hb	cpx	mus	q	cal	ser	chl	ep	op	sph	srp	bt	
F- 33	Morro Agudo	granite	equigranular	○	•	◎	○		•													•	•	•		•				
F- 57	Cerro Azul	granite	equigranular	◎	◎	◎	•																•	•	•		•			kf is composed mainly of microcline. see photograph.
F-124	Itaoca	granite	equigranular	◎	◎	○	○		○													•					•			kf shows microcline and perthite structure. see photograph.
F-242	Itaoca	granite	equigranular	◎	◎	○	•															•	•	•	•	•	•			kf is composed mainly of microcline.
K-101	Ribeirão Branco	granite porphyry	porphyritic	○	○	○	•							◎	○	○	○			○			•			•				ep forms veinlets.
K-102	Ribeirão Branco	granite porphyry	porphyritic	○	○	○	•						•	◎	○	○	•			•			•		•	•				
K-106	Ribeirão Branco	granite porphyry	porphyritic	○	○	○								◎	○	○				•			•	•		•				mafic min. altered to chl, containing garnet.
S- 28	Rocha	granite	equigranular	○	◎	◎		○														○	○	○		•				mafic min. altered to chl, kf shows perthite structure.
S- 36	Varginha	granite	mosaic	◎	◎	○	•																○	•	•					kf is composed mainly of microcline.
S- 50	Adorianopolis	granite	equigranular	◎	◎	◎	◎		•				•									•	•		•	•	•			containing garnet.
S-134	Espirito Santo	granite	equigranular	◎	◎	◎	○		○														•	•	•		•			kf shows perthite structure.
F- 87	Tunas	aegirin syenite	equigranular		◎	•			•		○		•										•			•	•			kf shows perthite structure. see photograph.
S- 90	Vinte e Sete	monzo-diorite	equigranular	•	◎	◎	○			○		•											•	•	•	•				
F- 9	Perau	diabase	doleritic			◎				○						◎			◎			•	•	•				•		see photograph.
F- 38	Morro Agudo	gabbro	equigranular			◎	•		•	◎														•		○				see photograph.
K-157	Apiai	altered gabbro	equigranular	•		◎				○											•				○		•			epidotized, silicified.
K-168	Apiai	diabase	doleritic			◎				○						◎			◎					◎		•			•	strongly chloritized.
K-169	Apiai	gabbro	ophitic			◎				◎											•			•		•				
S- 17	Rocha	gabbro	equigranular			◎				◎			•									•		•		•			•	

A–3 Microscopic Observations (Polished Section)

(1)

No	Sample No	Location	Names of Ore and Formation	Microscopic Observation	Remarks
1.	F 4	Perau Mine outcrop	Magnetite (Açungui IF)	Magnetite-gangue (quartz). Hematite replaces magnetite in regular directions	
2	F 11	Perau Mine G 1 sublevel	Galena-Pyrite (Açungui IF)	It is mainly composed of pyrite and galena. Galena fills fractures in pyrite A small amount of sphalerite and chalcopyrite can be seen Order of crystallization is pyrite, galena, spharelite and chalcopyrite from an earlier stage.	
3	F 18	Perau Mine G 4	Galena-Sphalerite-Pyrite (Açungui IF)	Main components minerals are pyrite and sphalerite. Pyrite has an euhedral or subhedral form and has replaced by sphalerite. Galena is accompanied with sphalerite.	
4	F 121	Mater Empresa de Mineração Mine	Pyrite (-Sphalerite) (Açungui IIF)	Pyrite crystals are crushed in various size (maximum 2mm ~ 0 1mm, average size : 0.8mm). A few sphalerite with galena fill the fractures Chalcopyrite grains are rarely observed in pyrite.	
5	F 204	Panelas Mine	Galena-Chalcopyrite-pyrrhotite (Açungui IIIF)	It is mainly composed of galena and pyrrhotite. Pyrrhotite after pyrite is in a xenomorphic granular form and enclosed by galena. Chalcopyrite and sphalerite are commonly accompanied with pyrrhotite.	see photograph
6	F 207	Panelas Mine	Galena-Pyrrhotite (Açungui IIIF)	Main components are xenomorphic granular pyrrhotite after pyrite and galena A few chalcopyrite replace pyrrhotite and are accompanied with sphalerite.	
7	F 221	Panelas Mine	Galena-Pyrite (Açungui IIIF)	Granular pyrite crystals are in gangue. Very fine grained galena is scattered in pyrite and gangue. A few chalcopyrite with an irregular form and covelline are also found in them.	
8	F 233	Panelas Mine	Galena-Pyrrhotite (Açungui IIIF)	Pyrrhotite after pyrite is enclosed by galena Both of them are penetrated by gangue veins.	

(2)

No.	Sample No.	Location	Names of Ore and Formation	Microscopic Observation	Remarks
9.	F–253	Panelas Mine	Galena-Pyrrhotite (Açungui IIIF)	Main components are pyrrhotite and galena. Both crystals are large in size. Chalcopyrite and sphalerite replace pyrrhotite along fractures and cleavages.	
10.	F–255	Panelas Mine	Galena-Pyrrhotite (Açungui IIIF)	It is mainly composed of pyrrhotite. Galena replace pyrrhotite irregularly. Euhedral pyrite grains partly replaced by galena and lath-shaped chalcopyrite are observed in pyrrhotite.	
11.	F–257	Perau Mine G–3	Galena-Sphalerite (Açungui IF)	Galena and sphalerite are main components Sphalerite is granular in form (0.3 ~0.5mm) and embeded in galena. There are tiny dots of chalcopyrite with an oriatation in sphalerite.	
12.	F–269	Galeria da Azurita	Oxidized Chalcopyrite (Açungui IF)	Chalcopyrite and gangue mineral. Chalcopyrite is oxidized into azurite along the fractures which are parallel to the bedding of dolomite.	
13.	F–276	Perau Mine G–1 Raise	Galena-Sphalerite (Açungui IF)	Galena streaks (0.2mm in width) are in host rock (calc--silicate rock). Galena replaces sphalerite and pyrite. No chalcopyrite can be seen.	
14.	F 280	Perau Mine G–3	Galena-Pyrite (Açungui IF)	It is mainly composed of pyrite and galena. Pyrite is granular in form (average size · 1mm) and enclosed in galena. There are a small amount of sphalerite in which exsolution dots of chalcopyrite exist.	
15.	F-307	Perau Mine	Galena-Chalcopyrite-Sphalerite (Açungui IF)	Granular pyrite and irregular chalcopyrite are in galena. Sphalerite has many oriented dots of chalcopyrite. A few pyrrhotite can be observed along the rims of spharerite and chalcopyrite.	
16.	S–54	Bueno Mine 550mL	Galena-Chalcopyrite-Pyrite (Açungui IIIF)	Large crystals of pyrite (2mm in size) are penetrated by chalcopyrite-sphalerite-galena vein. Chalcopyrite is partialy altered into covelline. Chalcopyrite dots are scattered in sphalerite.	

(3)

No.	Sample No.	Location	Names of Ore and Formation		Microscopic Observation	Remarks
17.	S–57	Paqueiro Mine Stockpile	Galena-Pyrite	(Açungui IIIF)	Cubic or granular pyrite grains are enclosed in galena. A few granular sphalerite are also accompanied. Chalcopyrite and galena dots are included in pyrite.	
18.	S–59	Paqueiro Mine 620mL	Galena	(Açungui IIIF)	Galena crystals with a few sphalerite. No chalcopyrite occurs.	
19.	S–76	Barrinha Mine	Galena		Galena with irregular form scatters in gangue and includes some dots of chalcopyrite	chemical analysis No. S–75
20.	S–77	Barrinha Mine	Galena	(Açungui IIIF)	Galena is penetrated by gangue minerals. Pyrite grains partly replaced by sphalerite are in galena. No chalco-pyrite.	
21.	S–79	Barrinha Mine Quatro	Galena-Pyrite	(Açungui IIIF)	Cubic or triangular pyrite and anhedral galena are main component minerals. In the pyrite a little amount of chalcopyrite and galena occur in the form of dot.	
22.	S–81	Barrinha Mine G2	Galena-Pyrite	(Açungui IIIF)	Euhedral pyrite grains (partly crushed) are enclosed by galena. A few dots of chalcopyrite, galena and sphalerite are found in pyrite. Many gangue veinlets penetrate all of the ore minerals.	
23.	S–109	Rocha Mine 600mL	Galena	(Açungui IIIF)	Much galena with very few pyrite. Narrow gangue veins penetrate regularly.	
24.	S 114	Rocha Mine 308mL	Galena	(Açungui IIIF)	Galena occupies the most part of the field. Chalcopyrite occurs in an irregular form No other minerals can been seen.	
25.	S–119	Rocha Mine 308mL	Galena-Pyrite	(Açungui IIIF)	Subhedral pyrite (1mm in size) are embeded in galena. Some pyrite crystals are crushed and penetrated by gangue or galena. A few granular sphalerite with chalcopyrite dots and chalcopyrite are observed in galena.	

(4)

No.	Sample No.	Location	Names of Ore and Formation	Microscopic Observation	Remarks
26.	S–122	Rocha Mine 403mL	Galena-Pyrite (Açungui IIIF)	Fine grained anhedral pyrite crystals are replaced by galena. A few sphalerite and chalcopyrite are in galena.	
27.	S–124	do	Galena-Pyrite (Açungui IIIF)	Same as S–122	
28.	S–125	Rocha Mine 308mL	Galena-Pyrite (Açungui IIIF)	Granular pyrite and irregular galena are main components. There are a few chalcopyrite and sphalerite in which oriented chalcopyrite dots can be seen.	
29.	S–136	do	Galena-Chalcopyrite-Pyrite (Açungui IIIF)	A few granular pyrite (0.1~1mm in size), irregular sphalerite (max 2mm, average 0.3mm) and chalcopyrite (average 0.1mm in size) occur in galena. Dots of sphalerite and chalcopyrite are also included in pyrite.	
30.	K–188		Chalcopyrite-Pyrite (Açungui IIIF)	Some amount of chalcopyrite in an irregular form, a few pyrite, few sphalerite and galena occur in gange minerals. The maximum width of vein is 2mm.	
31.	K–238	Lageado Mine	Galena (Açungui IIIF)	Galena irregularly fills cracks of host rock.	
32.	K–309	Lageado Mine Santa Nava	Galena-Pyrite	Granular pyrite is in galena, both of which are penetrated by gangue minerals. Pyrite includes some prismatic chalcopyrite.	
33.	K–316	Lageado Mine Santa Nava	Galena-Pyrite (Açungui IIIF)	Subhedral pyrite (some have intergrowth texture) are enclosed by galena. Very tinny dots of chalcopyrite are in pyrite.	
34.	K–322	Lageado Mine Mamangaba	Galena vein (Açungui IIIF)	Galena partly altered into cerussite? vein. Some corroded pyrite are replaced by enclosing galena.	
35.	K–329	Lageado Mine Copper Mine	Pyrite-impregnation (Açungui IIIF)	Pyrite-quartz veinlets and pyrite impregnation.	
36.	K–334	Lageado Mine São Vicente	Galena-Cerussite (Açungui IIIF)	Galena is partially replaced by cerussite. Some cubic pyrite are altered to limonite.	

(5)

No.	Sample No	Location	Names of Ore and Formation	Microscopic Observation	Remarks
37.	K–336	Lageado Mine	Galena (Açungui IIIF)	Massive galena is penetrated by irregular veins of gangue minerals. Galena is partially altered to cerussite and limonite	
38.	K–338	Lageado Mine Jardim II	Galena vein (Açungui IIIF)	Same as K–336	
39.	K -351A	Lageado Mine	Galena-Sphalerite-Pyrite (Açungui IIIF)	Main components are pyrite, galena and sphalerite. *Pyrite shows not only a framboidal texture but a* dissemination in a cubic form. There is a faint zoning in the field viz. 1) host rock 2) larger crystals of pyrite (0.1mm±), 3) fine grained framboidal pyrite (0.01mm±) 4) larger cubic pyrite (0 5~0.7mm) 5) anhedral galena and sphalerite.	see photograph
40	K 351B	Lageado Mine	Galena-Sphalerite-Pyrite (Açungui IIIF)	Galena-sphalerite veinlets (0.3mm± in width) are in host rock Pyrite with a cubic form is disseminated, and *partially replaced by sphalerite.*	
41	K 351C	Lageado Mine	Pyrite-Arsenopyrite (Açungui IIIF)	Some prismatic or rhombic arsenopyrite crystals coexist with framboidal pyrite. A few sphalerite and galena can be seen around arsenopyrite.	see photograph
42.	K -351D	Lageado Mine	Pyrite (Açungui IIIF)	Aggregation of fine grained cubic pyrite. No replacement occur A very few amount of galena with euhedral form exist	
43.	T -71	Furnas Mine 571mL	Galena-Pyrite (Açungui IIIF)	Pyrite is replaced by galena. A few sphalerite can be seen. The order of crystalization is pyrite, sphalerite, chalcopyrite and galena from an earlier stage.	
44.	T 81	Furnas Mine 500mL	Sphalerite-Galena-Pyrite (Açungui IIIF)	Cubic pyrite partially corroded by sphalerite, chalcopyrite with an irregular form and large subhedral galena (2mm in size) are enclosed in sphalerite. There are a few rhombic arsenopyrite.	see photograph

No.	Sample No.	Location	Names of Ore and Formation	Microscopic Observation	Remarks
45	T–82	Furnas Mine Santa Barbara II	Sphalerite-Galena-Pyrite (Açungui IIIF)	Same as T–81. The order of crystalization is pyrite, sphalerite, arsenopyrite and galena from an earlier stage.	
46.	T–83	do Santa Barbara II	Galena-Sphalerite-Pyrite (Açungui IIIF)	Galena and sphalerite are main components. Some cubic pyrite partially corroded are enclosed in galena and sphalerite. A very few argentite occur with or near sphalerite.	see photograph
47.	T–84	do	Galena-Pyrite (Açungui IIIF)	Cubic or granular pyrite (0.1mm in size) and massive galena. Pyrite is partially replaced by enclosing galena. Few chalcopyrite and sphalerite are present.	
48.	T–86	do	Galena-Sphalerite (Açungui IIIF)	Mineral assemblage is same as T–82. A few chalcopyrite dots occur in pyrite. There are also triangular arsenopyrite.	
49.	T–103	Furnas Mine	Galena vein (Açungui IIIF)	Galena veinlets (1~2mm in width) in host rock. Corroded pyrite is partially replaced by enclosing galena.	
50.	T–104	do	Galena-Pyrite (Açungui IIIF)	Galena veinlet (1cm in width) contains pyrite Cubic or subhedral pyrite grains are scattered in galena. A few rhombic arsenopyrite crystals are present.	
51.	T–113		Galena-Sphalerite (Açungui IIIF)	Granular pyrite crystals and granular ~ irregular formed sphalerite are enclosed galena vein (5mm in width). Very fine grained chalcopyrite dots are recognized in pyrite.	

Table A–4 X-ray Diffractive Analysis

Smec	:	Smectite
Ch	:	Chlorite
Ver	:	Vermiculite
K	:	Kaolinite
Tc	:	Talc
Sp	:	Serpentine
M	:	Mica
		t : trioctahedral – Phlogopite ~ Biotite
		d : dioctahedral – Muscovite
Tr	:	Tremolite
Q	:	Quartz
Cc	:	Calcite
D	:	Dolomite
Pl (ab)	:	Plagioclase (Albite)
Goe	:	Goethite
Ch/M	:	Chlolite – illite
Dra	:	Dravite $(Na, Ca)_{0.9} (Mg, Fe)_{2.9} (Al, Fe, Ti)_6 B_3Si_6O_{27}(OH, F)_4$
Hem	:	Hematite
Gas	:	Gaspeite $(Ni_{0.49} Mg_{0.43} Fe_{0.08}) CO_3$
Pyro	:	Pyromorphite $Pb_5 (PO_4, AsO_4)_3 Cl$

No.	Sample No	Rock Name	Location	Smec	Ch	Ver	K	Tc	Sp	M	Tr	Q	Cc	D	Pl(ab)	Goe	Others
1.	F-82	dolomite	Agua Clara									○		◎			
2.	F-216	fine, black limestone	Panelas Mine							t •	○		○				
3.	F-218	fine, grey limestone	do							t◎	○			•			
4.	F-225	coarse, grey limestone	do		:					• ?		•	◎				
5.	I-228	fine, black limestone	do							t△	•		◎				
6.	I-230	coarse, black limestone	do									•	○				
7	I 231	fine, black limestone	do								•	•	◎				
8	I 232	coarse, white limestone	do							t△	△	△	○				
9.	I 234	coarse, white limestone	do							t○	△?		○				
10	I 256A	banded limestone black part	do							t •		◎	◎				
11	I 256B	banded limestone white part	do							t •		•	◎				
12	I 270	dolomite	do							t • ?		◎		◎			
13	S 60	clay (altered)	Paqueiro Mine									•	○			△	
14	S 61	clay (do)	do	△	• ?		• ?			t,d • ?						•	
15	S-64	clay (do)	do							△		○				△	
16.	S-69	ore	do		• ?		• ?					•	◎			△	
17.	S-74	clay (altered)	Barrinha Mine		• ?			•	•	○		◎					
18	S-80	oxide ore	do							•							pyro ◎
19.	S-120	clay (altered)	Rocha Mine			◎				t△		○		○			
20.	S-126	dolomite	do							△		○	○	○			
21.	S-127	limestone	do							•		○		◎			
22.	T-54	clay (altered)	Furnas Mine							•		○	◎				
23.	T-62	clay (do)	do				△			○		○				•	
24.	T 63	clay (do)	do	△	• ?		• ?			◎		◎				•	
25	T-65	clay (do)	do							◎		◎					
26.	T 66	clay (do)	do							○		◎	◎				
27	T-67	clay (do)	do									•				△	
28	T-69	clay (do)	do		△					○		○	◎				ch/M •
29	T-70	clay (do)	do		△					○		○	◎				ch/M •
30	T-77	clay (do)	do			○						•	◎				
31	T-88	clay (do)	do				•			○		◎					
32	T-91	clay (do)	do							◎		◎	○				
33	T-105	clay (do)	do		•					○						•	
34	T 111	clay (do)	do							○						○	
35.	T-113	clay (do)	do		△					◎		◎					
36	K-101	granite	Ribeirão Branco							t△		◎			◎		
37	K 121	green rock	do							t •	◎	△					
38	K 122	green rock	do				△			•		◎			•		
39	K 123	green rock	do				•			•		◎			△		
40	K-133	green rock	Araçaíba		○					◎		◎					
41	K-140	psammitic schist	do					◎	○			◎					
42	K-147	pelitic schist	do						△			◎					
43	K-186	green rock	Apiai						△	△		◎					
44.	K-188	limestone	Apiai		• ?					•		○	◎				
45	K-192	calcareous schist	Apiai ~ Furnas		○					◎		◎	• ?		·		
46	K-197	altered sandstone	Apiai ~ Furnas									◎					Dra ○
47.	K-291	trachyte?	Iporanga		• ?				• ?	◎		◎					Hem △
48	K-308	clay (altered)	Lageado Mine									○	•				
49	K-314	dolomite	do		○					○		◎		◎			
50.	K-326	trachyte?	do							○		◎					
51.	K-350	ore	do							•							Gas ◎
52.	K-359	green rock	do		○					○		◎					
53.	K-401	green rock	Rio Pilões		◎							◎	△?	△?	○(ab)		
54.	K-403	green rock	do		◎							△			◎(ab)		

Table A–5 Results of Chemical Analysis

Ore

(1)

No.	Sample No.	Location	Occurrence		Au g/T	Ag g/T	Cu %	Pb %	Zn %
1	F–10	Perau Mine	galena impregnation	w.70	0.0	69.6	0.08	9.60	0.01
2	11	do	stratiform massive galena	w:60	0.4	92.9	0.00	25.35	0.14
3	12	do	do	w:35	0.1	79.6	0.44	7.42	0.70
4	14A	do	do	w:30	0.3	148.6	0.05	18.12	0.01
5	14B	do	galena impregration	w:30	0.3	22.3	0.76	0.41	0.07
6	15	do	massive galena	w.10	0.1	131.0	0.15	30.06	0.11
7	17	do	azulite (stockpile)		0.4	62.1	2.53	0.03	0 12
8	18	do	galena-pyrite-quartz vein	w:20	0.0	4.5	0.04	6.68	9.21
9	81	Agua Clara Mine	chalcopyrite-quartz vein	w:20	0.0	8.4	0.81	0.01	0.01
10	121	Mater Empresa de Mineracao	stockpile		0.5	10.5	0.39	0.18	0.65
11	204	Panelas Mine	massive galena-pyrite	w:30	0.1	287.0	0 36	30 45	0.01
12	207	do	galena-pyrrhotite	w:10	0.0	0 9	0.20	24.46	0 04
13	211	do	galena-pyrrhotite	w:10	0 3	134.3	0 26	15.36	0 00
14	221	do	stratiform galena-chalcopyrite	w 10	0 4	270 0	0.80	28.85	0 02
15	233	do	massive galena vein	w:15	0.0	220.5	0 06	30.70	0.00
16	253	do	stratiform galena-pyrrhotite	w:20	0.1	0.9	0.15	9.24	0 16
17	255	do	do	w.50	0.7	0.6	0 11	26.11	0.02
18	257	Perau Mine	stratiform massive galena	w 30	0.3	459.9	0.07	32.61	11.59
19	260	do	do	w·15	0.0	207.6	0.03	22.55	4.07
20	265	do	do	w·20	0.0	256.5	0 00	31.72	3.49
21	269	Galerita da Azurita	stratiform azulite	w 10	0.3	116.2	29.90	0 04	0.09
22	276	Perau Mine	massive galena-pyrite	w·60	0.1	115.2	0.02	14.84	3.13
23	280	do	massive galena	w:35	0.2	23.3	0.87	27 80	0 30
24	281	do	galena impregnation	w 30	0.0	83.3	0 02	7.35	0.52
25	302	Maximinioro Mine	galena-quartz vein		0.0	32 7	0.05	0.83	0 01
26	306	Perau Mine	coarse galena		0.3	235.2	0.06	33.29	3.64
27	307	do	fine galena		0.3	147.1	2.53	31.40	0.64
28	S–55	Bueno Mine	galena-pyrite vein		0.5	70.2	0.18	23.05	0.01

(2)

No.	Sample No.	Location	Occurrence		Au g/T	Ag g/T	Cu %	Pb %	Zn %
29	S- 57	Paqueiro Mine	massive galena (stockpile)		0 8	57.4	0.25	33.05	0.03
30	58	do	do		2.1	361.6	0.19	30.98	0.04
31	59	do	do		0.4	656.5	0.09	21.83	0 01
32	62	do	galena impregnation	w:100	2.5	110 0	0.03	8 91	0.01
33	63	do	do	w.20	0.1	6 4	0.01	1 61	0.45
34	65	do	galena vein	w 20	0.1	84.5	0.06	5.95	0.01
35	66	Bueno Mine	galena pyrite vein		0.2	1.3	0.16	0 02	0 01
36	67	do	do	w.80	1.0	53.3	0 20	5 99	0.61
37	68	do	massive galena vein	w.50	0.9	424 9	0.07	31.83	0 38
38	70	do	galena impregnation	w·10	0.2	6 1	0.01	0 29	0 01
39	71	do	do	w 40	0.0	18 0	0 07	0 41	0 01
40	72	Barrinha Mine	galena-quartz-calcite	w·50	0.7	199.5	0.26	15 20	0 05
41	75	do	do	w.50	3.9	164 3	0.10	8 30	2 98
42	78	do	oxidized ore		0 0	153 3	0 08	30 61	0.04
43	82	do	stockpile		0.1	187.1	0 09	7.86	0 01
44	85	do	galena-quartz	w 40	0.8	222.9	0.58	17.38	0 06
45	104	Rocha Mine	galena-pyrite vein chip		1 5	140 0	0 23	14.65	0 26
46	113	do	do	w.80	1.8	470 1	0 49	26 95	0.02
47	115	do	do	w 60	0 8	80.8	0 34	5 03	0 04
48	116	do	do	w 40	0 4	63 1	0.35	3.62	0.15
49	117	do	do	w 20	0 2	2126.0	5 07	30.61	0 30
50	118	do	do	w 80	0.7	72 6	0.33	13.43	0.08
51	121	do	do	chip	0 2	123 3	0.45	30.43	0.92
52	123	do	do	chip	0.8	131.4	1.05	18 54	1.73
53	T 52	Furnas Mine	oxidized ore	w 40	0.0	29 8	0.00	13 65	15 91
54	53	do	do	w 40	0 0	19 5	0.00	0.69	27.50
55	56	do	do	w.200	0.0	24.0	0 03	0.28	19 42
56	57	do	do	w 150	0 1	8 2	0.05	0 03	2.30
57	61	do	do	w 10	0 0	8 7	0.15	3.43	2.80
58	71	do	galena-pyrite	w 150	0 4	181.7	0.04	30 37	0.14

(3)

No.	Sample No.	Location	Occurrence		Au g/T	Ag g/T	Cu %	Pb %	Zn %
59	T-72	Furnas Mine	oxidized ore	w.150	0.1	27.0	0.08	1.95	2 52
60	80	do	do	w.50	0.0	36.9	0.00	0.45	20 96
61	81	do	sphalerite-galena vein	w.50	0.0	97.6	0.07	5.06	33 89
62	82	do	do	w:50	0.3	5.9	0.03	9.56	21.01
63	83	do	galena-sphalerite vein	w.40	0 0	311.9	0 07	17.26	27.31
64	84	do	galena vein	w 10	0.0	2.2	0.06	29.51	0 31
65	89	do	oxidized ore vein	w 200	0.0	5.7	0.05	0 96	4 32
66	99	do	do	w.70	0.1	199 5	0 03	3 43	1.89
67	100	do	do	w 40	0 1	26 1	0.08	18.81	2.19
68	102	do	do	w 30	0 0	14.1	0.01	0.31	0.07
69	103	do	galena vein	chip	0.1	1208.0	0.01	31.46	0 06
70	104	do	do	chip	0.0	641 8	0.00	30 98	1.31
71	106	do	oxidizedore vein	w.150	0 4	146 2	0.02	3.33	1.65
72	110	do	do	w.10	0.2	450 8	0.06	30.73	2 15
73	113	do	galena	w 10	0 2	1330 0	0.17	31.10	0.87
74	115	do	oxidized ore	w:10	0.0	9 8	0.00	0.34	0.26
75	118	do	galena	w.10	0.3	233.9	0.05	14.84	7.07
76	K-105	Ribeirão Branco	pyrite-quartze vein		0.0	1.5	0.00	0.03	0.03
77	138	Aracaíba	greenrock with pyrite		0 0	0.5	0.01	0 02	0.03
78	153	do	do		0.0	0.7	0.01	0.03	0.03
79	236	Lageado Mine	altered sandstone		0.0	0.9	0.00	0 02	0.01
80	238	do	limestone with pyrite		0.0	0 1	0.01	0 01	0.02
81	301	do	oxidized ore	chip	1.8	232.4	0.11	19.71	0.30
82	303	do	do	chip	1.7	265.5	0.03	21.71	0.02
83	307	do	galena, vein	w:100	1.2	960.9	0.02	29.15	0.01
84	309	do	do	chip	1.0	798.9	0.04	30.73	0.03
85	315	do	oxidized ore	chip	0.5	4.5	0.01	0.10	0.02
86	316	do	galena-oxidized ore	chip	0.1	1378.0	0.02	30.98	0.01
87	K-319	do	cerussite?	chip	0.0	12.5	0.01	0 87	0.28
88	322	do	do	Max w.150	0.6	630.8	0.13	32.32	0.02

No.	Sample No	Location	Occurrence		Au g/T	Ag g/T	Cu %	Pb %	Zn %
89	K-319	Lageado Mine	oxidized ore vein	w:10	0.0	7.4	0.00	0.21	0 09
90	328	do	pyrite-galena vein	chip	1.4	27.3	1 60	0.46	3 47
91	329	do	pyrite impregnation	chip	0.0	1.9	0 00	0 67	0.01
92	333	do	oxidized ore vein	w·200	1.4	1 4	0.01	0.86	0.03
93	334	do	galena-oxidized ore vein	w 40	0 4	1212.0	0.28	30.21	0 16
94	336	do	galena vein	w.100	0.0	658 8	0.00	29.27	0 17
95	338	do	galena-oxidized ore vein Max	w:200	0.1	1132.0	0 33	29.76	0 12
96	348	do	oxidized ore vein	chip	0 0	595.5	0 00	29.88	0 02
97	350	do	do	chip	0.0	68.0	0 02	4 24	31 82
98	351A	do	galena +pyrite vein	chip	0 0	18.9	0 01	6.34	10.93
99	351B	do	do	chip	0 0	26 1	0 02	8 44	1.67
100	351C	do	do	chip	0.1	1 1	0 00	2.20	0 20
101	351D	do	do	chip	0.0	59.3	0.00	3.57	0 28
102	353	do	galena vein	chip	0 0	690 4	0 05	31 34	1.86
103	358	do	altered sandstone		0 0	3 2	0 00	0 13	0 02
104	403	Rio dos pilões	green rock with chalcopyrite		0.0	1.3	0 10	0 04	0 02

No.	Sample No.	Location	Occurrence	$BaSO_4$ %	S %	Cu ppm	Pb	Zn ppm
105	F- 13	Perau Mine	thin beded barite in schist	87 05	0.76	47	1 92 %	69
106	82	Agua Clara Mine	dolomite	0.34	0.24	29	63 ppm	26
107	113	Pretinhoe Mine	thick beded barite (1~2m) in schist	85 48	0 51	812	54 ppm	61

No	Sample No.	Location	Occurrence	F %
108	F-123	Fluorita de Sete Barras	network of fluorite in limestone	24.64

Rock

(5)

No.	Sample No.	Location	Occurrence	CaO%	MgO%	Al_2O_3%	Fe_2O_3%	C %	CO_2%	Insoluble Residue%
1	F-216	Panelas Mine 150ML	limestone (black)	38.39	3.36	0.21	1.07	–	–	22.58
2	218	do	do (black)	15.39	5.27	0.48	1.76	–	–	58.52
3	225	do	do (grey)	44.40	8.85	0.02	0.14	–	–	1.06
4	228	do	do (grey)	42.92	2.96	0 17	0.61	–	–	15.62
5	230	do	do (black)	52.41	9 66	0 06	0.29	–	–	3 30
6	231	do	do (black)	45 16	1 21	0.08	0.56	0.76	30.20	15 22
7	232	do	do (grey)	31.79	4.34	0.56	2.70	–	–	29 76
8	234	do	do (grey)	52.00	1.15	0 06	0.66	0 01	34.09	3 76
9	256A	Outcrop	banded limestone (black)	45.11	0.96	0.12	1.19	0.02	13.84	14 44
10	256B	do	do (white)	50 67	0 76	0 08	0.94	0.03	21.05	4 84
11	S-126	Rocha Mine 308ML	grey limestone	41.29	2.32	0.09	0.67	–	–	19.84
12	127	do	grey dolomite	25.13	16 72	0.44	1 32	–	–	16.56

Table A–6 Fossils

Formation	Sample No.	Rock	Location	Fossils	Remarks
Açungui III F	S–26	Dolomitic Schist	Rocha Mine	None	
	S–89	Limestone	Diogo Lopes Mine	None	
	S–101	Limestone	Rocha Mine	None	
	S–129	Limestone	Espirito Santo	None	
	T–58	Limestone	Furnas Mine	None	
	T–85	Limestone	Furnas Mine	None	
	T–152	Limestone	Espirito Santo	None	
Açungui I F	F–72	Dolomite	Southeast of Tunas	None	
	F–74	Dolomite	Southeast of Tunas	None	
	F–75	Limestone	Southeast of Tunas (Quarry)	None	
	F–82	Dolomite	Agua Clara Mine	None	

Table A–7. Metal Contents of Geochemical Samples approved for Interpretation

Abbreviation

Sam No.	:	Sample No.
M		Multiple
Area	:	Drainage Area
Lith	:	Lithology

1. Basic Complex
2. Granite
3. Açungui Group – chemical sequence
4. do – upper clastic sequence
5. do – middle clastic sequence
6. do – schist and amphibolite
7. do – metabasite and amphibolite
8. Quartzite
9. Setuva Formation
10. Crystalline Complex

*	:	Mean value of the rank

(1)

No	Sam No	Area	Lith	pH	Cu	Pb	Zn
					[Unit in ppm]		
1	JR0070	3	2	-	10	5	25
2	JR0089	6	4	-	25	10	40
3	JR0090	3	4	-	25	10	40
4	JR0117	4	2	-	15	15	55
5	JR0117	3	2	-	15	15	55
6	JR0118	5	2	-	10	5	25
7	JR0121	3	2	-	5	5	40
8	JR0128	3	2	-	5	15	50
9	JR0129	4	2	-	5	10	60
10	JR0132	3	2	-	5	10	45
11	JR0133	3	2	-	5	10	45
12	JR0135	2	2	-	5	10	35
13	JR0136	4	2	-	7	7	42
14	JR0137	3	2	-	5	5	25
15	JR0138	4	2	-	5	5	30
16	JR0148	4	2	-	5	10	45
17	JR0155	6	2	-	5	5	20
18	JR0156	4	2	-	5	5	15
19	JR0160	3	2	-	5	10	40
20	JR0162	4	2	-	10	10	50
21	JR0167	6	2	-	5	10	25
22	JR0168	4	2	-	5	10	15
23	JR0173	5	2	-	5	5	40
24	JR0174	12	2	-	5	10	20
25	JR0175	4	2	-	5	10	30
26	JR0176	7	2	-	5	5	25
27	JR0183	7	4	-	15	25	40
28	JR0185C	2	5	-	17	7*	75
29	JR0196	13	4	-	20	10	50
30	JR0203	5	3	-	25	5	40
31	JR0216	2	5	-	20	10	30
32	JR0218	4	4	-	55	20	55
33	JR0219	5	4	-	57	45	135
34	JR0223	4	6	-	65	45	170
35	JR0225	4	5	-	92	7	105
36	JR0226	3	4	-	15	10	40
37	JR0227	4	4	-	20	20	95
38	JR0228	6	4	-	50	17	120
39	JR0231	6	4	-	60	17	110
40	JR0232	3	4	-	61	21	88
41	JR0235	10	4	-	30	90	97
42	JR0236	9	4	-	30	20	100
43	JR0237	2	4	-	25	20	90
44	JR0238	2	4	-	35	25	120
45	JR0245	3	4	-	55	20	95
46	JR0246	3	4	-	55	30	110
47	JR0251	5	4	-	57	35	120
48	JR0253	3	4	-	40	25	110
49	JR0256	7	4	-	55	62	160
50	JR0257	10	4	-	35	10	90
51	JR0268	5	5	-	40	5	60
52	JR0269	6	5	-	30	10	45
53	JR0274	3	4	-	30	20	65
54	JR0298	3	4	-	22	22	70
55	JR0306	5	6	-	40	25	90
56	JR0307	2	6	-	40	30	35
57	JR0317	2	4	-	57	30	115
58	JR0318	3	4		25	20	70
59	JR0319	3	4	-	78	28	126
60	JR0320	3	4	-	25	20	95
61	JR0325	7	4	-	20	20	75
62	JR0326	13	4	-	25	20	80
63	JR0329	4	4	-	20	20	85
64	JR0415	8	2	-	82	47	102
65	JR0434	3	4	-	115	10	92
66	JR0435	4	4		100	15	133
67	JR0436	12	2	-	10	15	60
68	JR0439	12	4	-	20	25	80
69	JR0442	11	4	-	62	20	85
70	JR0450	6	4	-	40	90	95
71	JR0453	8	2	-	15	20	55
72	VA0004	5	2	5 3	29	27	120
73	VA0005	9	3	5 7	7	3	20
74	VA0006	10	4	5 5	40	14	100
75	VA0007	9	4	5 5	55	19	140
76	VA0010	9	3	5 7	11	9	45
77	VA0013	13	2	5 7	7	8	30
78	VA0015	6	4	5 5	6	8	30
79	VA0016	4	4	5 7	18	6	35
80	VA0018	10	3	5 7	5	3	22
81	VA0019	7	3	5 7	21	4	30
82	VA0020	7	4	5 5	26	8	50
83	VA0021	7	2	5 5	9	8	40
84	VA0022A	10	2	5 5	9	11	40
85	VA0023	5	2	5 5	15	4	40
86	VA0024	7	2	5 5	26	5	55
87	VA0025	3	2	5 5	45	9	65
88	VA0026	8	3	5 5	30	8	40
89	VA0027	5	3	5 9	9	8	25
90	VA0030	6	3	5 5	6	14	30
91	VA0031	4	4	5 5	35	24	85
92	VA0032	4	4	5 5	60	20	100
93	VA0033	7	3	5 5	6	10	30
94	VA0034	3	2	5 5	6	7	30
95	VA0036	5	2	5 9	17	11	45
96	VA0042	7	2	5 5	9	8	45
97	VA0043	8	4	5 5	7	17	45
98	VA0044	5	4	5 5	8	24	40
99	VA0045	3	4	7 0	7	17	90
100	VA0047A	3	4	5 6	32	11	55
101	VA0050	6	2	5 5	3	5	30
102	VA0052	10	2	5 5	7	9	45
103	VA0053	5	2	5 5	13	12	40
104	VA0054	9	2	5 5	14	17	65
105	VA0055	5	2	5 7	20	8	55
106	VA0056	8	4	5 7	45	10	55
107	VA0057M	7	2	5 7	24	8	55
108	VA0059	4	2	5 7	19	8	60
109	VA0060	8	2	5 7	35	6	75
110	VA0061	10	2	5 7	20	6	70
111	VA0063	5	3	5 9	60	18	90
112	VA0064	10	3	5 9	18	5	120
113	VA0065	4	4	5 9	15	3	30
114	VA0066A	3	3	5 6	24	10	52
115	VA0070M	3	2	5 9	8	8	35
116	VA0071A	2	2	5 5	11	7	47
117	VA0073M	2	2	5 7	12	7	35
118	VA0074M	3	2	5 7	9	22*	50
119	VA0076M	2	2	5 7	24	22*	50
120	VA0079M	2	2	6 5	10	22*	20
121	VA0080M	2	2	5 7	4	7*	40
122	VA0081M	5	2	5 5	6	22*	40
123	VA0082M	4	2	5 5	14	22*	60
124	VA0083M	4	2	5 7	11	22*	50
125	VA0084M	2	2	5 3	15	7*	45
126	VA0085	6	4	7 0	22	7*	35
127	VA0086M	5	2	5 9	14	16*	45
128	VA0086	2	4	6 5	9	7	40
129	VA0087M	5	4	5 7	40	7*	35
130	VA0088M	6	4	5 3	25	22*	50
131	VA0090	6	3	6 5	11	7*	90
132	VA0094A	3	2	5 7	28	7*	55
133	VA0095B	2	2	5 5	12	7*	45
134	VA0095C	2	2	5 5	11	7*	45
135	VA0095D	1	2	5 5	8	7*	35
136	VA0095A	1	2	5 5	13	7*	50
137	VA0101A	8	4	5 7	18	22*	75
138	VA0103	5	4	5 9	14	7*	40
139	VA0105	10	2	5 5	6	7*	40
140	VA0108	10	2	5 5	4	7*	35
141	VA0111A	4	4	5 5	27	22*	62
142	VA0112	4	2	5 5	5	22*	35
143	VA0114	3	2	5 7	12	7*	40
144	VA0115	4	3	6 5	14	7*	25
145	VA0116	18	2	6 5	10	7*	60
146	VA0119A	2	4	5 5	21	22*	60
147	VA0120	4	4	5 5	35	22*	80
148	VA0121	3	4	5 3	30	45*	85
149	VA0122	4	4	5 3	25	22*	95
150	VA0123	3	3	5 7	35	22*	70
151	VA0129	1	4	5 3	27	7*	45
152	VA0130	1	3	5 9	40	1000	710
153	VA0133	2	3	7 0	90	120	110
154	VA0135	6	3	6 2	28	22*	70
155	VA0136	7	3	7 0	40	45*	55
156	VA0138	4	3	7 0	75	45*	95
157	VA0139	2	4	5 3	19	7*	45
158	VA0141	12	4	5 7	70	22*	100
159	VA0142	11	4	5 5	35	22*	70
160	VA0143M	4	4	5 5	24	22*	70
161	VA0144M	6	4	5 7	45	45*	75
162	VA0145M	4	4	5 3	160	1000	390
163	VA0150M	3	4	5 5	75	380	180
164	VA0151M	2	5	5 7	21	50	70
165	VA0152	3	4	5 7	10	7*	40
166	VA0153	5	5	5 3	23	7*	90
167	VA0162	3	3	6 1	40	45*	95
168	VA0165	11	4	5 7	25	22*	75
169	VA0166	7	3	6 2	18	22*	45
170	VA0167	5	3	6 2	24	420	150
171	VA0170	2	5	5 7	40	22*	70
172	VA0171	3	4	5 7	190	7*	65
173	VA0172	7	4	5 5	340	7*	60
174	VA0174	3	4	5 0	23	90	45
175	VA0183	8	5	5 7	22	7*	85
176	VA0185M	3	5	5 3	19	7*	60
177	VA0187	2	6	5 9	35	22*	90
178	VA0188M	2	4	5 9	23	7*	50
179	VA0189M	2	2	7 0	10	22*	30
180	VA0190M	4	4	5 9	45	22*	35
181	VA0191M	2	3	7 0	22	22*	50
182	VA0194A	7	4	5 7	25	7*	54
183	VA0195	3	4	5 5	50	22*	100
184	VA0196	5	2	5 3	5	7*	20
185	VA0200	9	3	5 9	26	22*	45
186	VA0201	7	2	5 3	20	22*	110
187	VA0205	4	2	5 5	5	7*	30
188	VA0206	6	3	5 7	19	22*	50
189	VA0216	7	3	6 5	17	22*	90
190	VA0217	3	3	5 5	80	22*	170
191	VA0219	6	3	6 2	25	22*	80
192	VA0220	6	3	6 2	25	22*	55
193	VA0227	9	3	6 5	30	22*	65
194	VA0228	5	8	6 5	22	22*	90
195	VA0230	5	8	5 7	18	7	100
196	VA0235	4	3	5 7	8	7*	27
197	VA0236	5	4	5 5	75	7*	90
198	VA0250	4	4	5 9	6	7*	30
199	VA0252	6	4	5 3	16	7*	50
200	VA0253	4	3	5 3	26	22*	140

(2)

No	Sam No	Area	Lith	pH	Cu (Unit in ppm)	Pb (Unit in ppm)	Zn (Unit in ppm)
201	VA0257	7	2	5.7	25	7*	80
202	VA0260	9	4	5.9	10	7*	40
203	VA0261	12	4	5.5	20	22*	85
204	VA0262	5	3	6.2	23	22*	90
205	VA0265	3	4	5.9	18	22*	50
206	VA0266	2	3	5.9	30	22*	80
207	VA0268	11	3	6.2	12	22*	50
208	VA0271	6	5	5.5	24	7*	30
209	VA0274	4	10	5.5	13	45*	70
210	VA0275	3	9	5.7	25	22*	80
211	VA0276	5	10	5.9	18	7*	60
212	VA0277M	4	10	5.9	18	7*	55
213	VA0278	4	10	5.7	19	7*	55
214	VA0279	2	4	5.0	40	45*	75
215	VA0280	6	4	5.5	90	22*	65
216	VA0281	5	4	5.0	18	22*	90
217	VA0282	4	4	5.0	21	22	90
218	VA0284	5	4	5.0	40	22*	170
219	VA0285	4	4	5.3	30	22*	130
220	VA0287	7	4	5.3	20	22*	100
221	VA0289	10	4	5.3	15	22*	65
222	TB0003	8	4	5.3	35	16	75
223	TB0004	5	4	5.5	28	65	85
224	TB0008	10	9	5.5	35	40	70
225	TB0008	2	4	5.5	35	40	70
226	TB0009	7	1	5.3	30	35	60
227	TB0010	10	1	5.3	18	24	81
228	TB0011	10	4	5.7	45	20	75
229	TB0012	4	3	5.9	10	7	27
230	TB0013	4	4	5.5	21	13	45
231	TB0015	6	9	5.3	27	18	55
232	TB0016	2	4	5.3	70	23	75
233	TB0017	3	4	5.5	85	21	85
234	TB0018A	3	4	5.7	62	11	75
235	TB0019	5	4	5.5	55	18	70
236	TB0021	4	4	5.3	35	19	85
237	TB0023	5	4	5.5	20	10	45
238	TB0025	7	4	5.3	40	16	75
239	TB0027	6	2	5.3	55	18	75
240	TB0028	6	4	5.3	40	12	75
241	TB0029	3	4	5.3	45	13	85
242	TB0030	4	4	5.5	40	13	80
243	TB0032	4	4	5.3	35	12	95
244	TB0033	5	4	5.3	35	14	80
245	TB0035	7	4	5.5	40	15	120
246	TB0037A	11	4	5.3	20	14	70
247	TB0042	5	3	6.5	45	45	80
248	TB0044	3	4	6.5	11	90	110
249	TB0046	3	3	6.2	29	20	60
250	TB0047A	7	3	6.0	41	30	77
251	TB0049	7	3	5.5	20	20	35
252	TB0050	8	4	5.5	50	17	75
253	TB0052	6	3	5.5	9	15	26
254	TB0053	4	3	5.5	17	30	55
255	TB0054	6	4	5.5	26	18	60
256	TB0055	5	3	5.3	14	13	30
257	TB0056	10	2	5.3	20	21	55
258	TB0059	5	3	7.0	90	1000	140
259	TB0060	6	4	6.2	35	95	85
260	TB0069	6	4	5.5	50	30	65
261	TB0070	3	4	5.3	13	27	85
262	TB0073	2	4	5.5	90	9	80
263	TB0080	10	4	5.5	45	29	65
264	TB0083	3	4	5.7	35	14	50
265	TB0085	3	3	5.5	30	65	85
266	TB0086	9	4	5.5	20	60	75
267	TB0087A	1	3	6.5	17	22	40
268	TB0088	10	4	6.5	35	100	60
269	TB0091A	4	6	5.7	40	14	75
270	TB0092A	3	6	5.6	46	17	90
271	TB0099	3	4	5.5	22	7*	65
272	TB0102	5	4	5.5	23	22*	75
273	TB0103A	9	2	5.5	50	22*	80
274	TB0104	10	4	5.5	11	22*	22
275	TB0105	3	4	5.5	40	22*	90
276	TB0111	7	4	5.3	30	22*	80
277	TB0114	9	4	5.3	20	22*	60
278	TB0116	2	4	5.3	30	22*	95
279	TB0117	2	4	5.3	28	22*	100
280	TB0118	3	4	5.3	29	22*	120
281	TB0124	7	4	5.5	40	22*	95
282	TB0126M	3	3	5.7	35	200	55
283	TB0126	2	4	5.7	35	200	55
284	TB0129M	4	3	6.5	55	14*	50
285	TB0131M	1	4	6.5	17	7*	45
286	TB0133M	2	4	5.9	29	22*	50
287	TB0134	12	5	5.5	26	22*	110
288	TB0137	4	5	5.3	40	7*	60
289	TB0139A	8	5	5.5	45	7*	75
290	TB0140	3	4	5.5	35	22*	140
291	TB0143	11	3	5.7	35	22*	95
292	TB0148	3	4	5.3	35	22*	130
293	TB0149	10	4	5.3	23	8*	40
294	TB0153	3	6	5.5	55	22*	85
295	TB0154	1	4	5.5	75	45*	120
296	TB0155	2	4	5.3	30	22*	40
297	TB0156	9	4	5.5	14	22*	27
298	TB0157	8	4	5.3	11	7*	21
299	TB0160	7	4	5.5	7	7*	13
300	TB0162	7	4	5.3	35	22*	30
301	TB0163	8	2	5.5	10	7*	35
302	TB0164	9	4	5.3	6	7*	18
303	TB0166	9	2	5.3	9	7*	35
304	TB0170	8	4	5.7	21	7*	26
305	TB0171	10	4	5.5	6	7*	19
306	TB0172	7	4	5.5	9	45*	30
307	TB0174	12	2	5.3	8	65	35
308	TB0176	10	2	5.3	6	22*	45
309	TB0179	7	2	5.3	9	22	65
310	TB0180	9	2	5.3	13	22*	30
311	TB0182	10	2	5.3	4	7*	21
312	TB0183	6	2	5.7	11	22*	40
313	TB0184A	4	2	5.6	19	22*	47
314	TB0185	5	2	5.5	11	22*	35
315	TB0191	7	2	5.5	13	7*	26
316	TB0192A	5	2	5.3	18	7*	29
317	TB0194	5	3	5.5	4	7*	19
318	TB0197	8	2	5.3	45	22*	40
319	TB0203	9	2	5.7	8	7*	26
320	TB0204	7	3	5.7	12	7*	26
321	TB0206	7	2	5.5	27	45*	70
322	TB0207	9	2	5.3	9	22*	20
323	TB0215	5	4	5.5	5	7*	15
324	TB0217	4	2	5.3	5	7*	30
325	TB0219	11	2	5.3	9	22*	35
326	TB0248	6	4	5.3	7	22*	15
327	TB0249	6	2	5.9	9	7*	27
328	TB0251	4	2	5.9	10	7*	27
329	TB0274	6	2	5.3	8	22*	23
330	TB0317	10	4	5.5	9	7*	21
331	TB0320	4	4	4.7	30	7*	26
332	TB0321	4	4	4.7	40	22*	29
333	TB0322	3	4	5.0	25	22*	45
334	TB0323	8	5	5.3	30	7*	75
335	TB0325	8	3	6.5	35	45*	85
336	TB0326	11	4	5.3	29	100	95
337	TB0327	10	4	5.3	45	210	170
338	TB0329	3	2	5.5	22	22*	100
339	TB0332A	7	2	5.0	35	45*	90
340	FA0003	3	9	5.5	14	8	40
341	FA0005	1	10	5.5	7	15	50
342	FA0006	2	10	5.5	14	13	60
343	FA0006	3	10	5.5	14	13	60
344	FA0008	4	9	5.5	19	8	60
345	FA0010	7	9	5.5	21	8	60
346	FA0011	12	4	5.5	30	8	85
347	FA0012M	3	5	5.3	40	11	60
348	FA0013M	2	5	5.5	40	14	65
349	FA0014	10	5	5.5	30	15	70
350	FA0016M	2	5	5.7	40	18	60
351	FA0018	6	5	5.5	40	11	60
352	FA0019	3	5	5.5	28	11	60
353	FA0024	9	5	5.5	26	10	70
354	FA0025M	3	5	5.7	19	10	45
355	FA0027	5	5	5.5	30	8	75
356	FA0028	2	5	5.7	45	8	85
357	FA0031	2	10	5.5	17	7	50
358	FA0032	4	5	5.5	28	11	90
359	FA0033	4	5	5.5	28	11	80
360	FA0035	8	5	5.5	28	11	85
361	FA0036	3	5	5.7	35	13	65
362	FA0037	4	5	5.5	21	9	45
363	FA0038	4	5	5.5	30	17	50
364	FA0040	13	5	5.3	45	14	150
365	FA0041	3	5	5.3	23	16	110
366	FA0045M	6	9	5.3	21	11	50
367	FA0046M	4	9	5.5	23	12	55
368	FA0047	9	9	5.5	29	14	55
369	FA0048M	4	9	5.5	18	10	75
370	FA0049M	3	9	5.5	22	10	70
371	FA0052	4	9	5.5	10	12	70
372	FA0053	6	5	5.2	28	13	75
373	FA0055	3	5	5.7	75	13	110
374	FA0056	5	5	5.5	35	14	100
375	FA0057	3	5	5.5	40	9	110
376	FA0058	4	5	5.5	90	10	180
377	FA0059	6	4	5.5	29	12	110
378	FA0060	10	4	5.5	35	10	110
379	FA0063	7	5	5.3	35	14	90
380	FA0064	9	6	5.3	5	8	9
381	FA0065	3	5	5.5	30	13	50
382	FA0068	3	5	5.3	35	60	50
383	FA0069	3	5	5.3	35	8	6
384	FA0075	5	4	5.5	58	16	85
395	FA0076A	3	4	5.5	61	11	85
386	FA0077	5	4	5.5	55	8	120
387	FA0078	7	4	5.5	85	12	95
388	FA0080	4	4	5.5	24	12	60
389	FA0081	8	4	5.3	35	15	120
390	FA0082M	5	5	5.5	14	22*	40
391	FA0083M	3	10	5.3	28	22*	60
392	FA0084	2	5	5.3	19	7*	75
393	FA0085M	4	5	5.3	25	22*	90
394	FA0086M	3	5	5.3	21	7*	55
395	FA0087	4	5	-	40	5	60
396	FA0088M	2	5	5.3	17	8*	70
397	FA0091	3	9	5.3	30	22*	95
398	FA0098	6	4	5.3	35	22*	90
399	FA0100	7	5	5.3	30	22*	90
400	FA0102	4	5	5.3	45	22*	120

(3)

No	San No	Area	Lith	pH	Cu	Pb	Zn
					(Unit in ppm)		
401	FA0106	5	5	5 3	30	22*	80
402	FA0108	4	2	5 3	10	7*	50
403	FA0112	9	2	5 5	14	7*	30
404	FA0113	5	2	5 3	10	20*	45
405	FA0123A	5	2	5 3	13	22*	80
406	FA0126	8	2	5 3	4	22*	40
407	FA0128	7	2	5 3	4	7*	40
408	FA0166	6	9	5 3	8	7	4
409	FA0167	4	9	5 3	25	18	85
410	FA0169	9	9	5 3	12	22*	65
411	FA0171	7	9	5 3	21	22*	110
412	FA0173	11	10	5 5	25	22*	75
413	FA0174	5	10	5 5	20	22*	85
414	FA0176	3	10	5 5	14	22*	70
415	FA0177	4	9	5 3	9	7*	60
416	FA0182	3	5	5 3	19	22*	45
417	FA0247	2	9	5 3	23	22*	95
418	FA0249	7	9	5 3	23	22*	75
419	FA0251	3	9	5 3	15	22*	75
420	FA0252	7	4	5 9	15	22*	70
421	FA0254	4	3	5 3	13	7*	35
422	FA0255A	5	3	5 3	31	7*	90
423	FA0256	7	4	-	37	7*	120
424	AM0019	5	4	5 2	43	20	50
425	AM0024	1	4	5 7	38	46	60
426	AM0030	4	4	6 2	75	1000	63
427	AM0032	4	5	-	29	11	55
428	AM0034	6	4	5 7	45	50	65
429	AM0037	6	3	5 5	20	22*	45
430	AM0039	9	1	5 7	90	22*	55
431	AM0041	5	4	5 5	90	22*	55
432	AM0042A	6	4	5 5	75	7*	55
433	AM0045	7	2	5 3	13	22*	63
434	AM0046	6	2	5 3	7	22*	45
435	AM0047	7	4	5 3	29	7*	130
436	AM0048	6	4	5 3	24	7*	60
437	AM0049	3	2	5 3	9	7*	45
438	AM0050	4	3	6 2	30	7*	50
439	AM0051	1	3	7 0	14	7*	28
440	AM0052	8	2	5 7	13	22*	50
441	AM0054	2	4	5 9	23	10	40
442	AM0055	7	6	5 9	16	8	35
443	AM0058	6	2	5 5	3	7	20
444	AM0069	6	4	5 5	12	7*	17
445	AM0117	8	3	-	5	5	25
446	AM0123	4	3	-	16	5	31
447	AM0124	6	3	-	5	5	25
448	AM0125	5	3	-	5	5	15
449	AM0126	4	3	5 9	35	16	60
450	AM0128	2	3	-	10	5	30

No	San No	Area	Lith	pH	Cu	Pb	Zn
					(Unit in ppm)		
451	AM0133	4	3	-	5	5	25
452	AM0134	18	2	-	10	10	40
453	AM0135	15	2	-	5	5	30
454	AM0136	14	2	-	5	5	45
455	AM0137	3	3	-	10	5	35
456	AM0140	4	3	-	5	10	20
457	AM0150	5	3	-	10	5	30
458	AM0154	2	2	-	5	5	30
459	AM0227	4	10	-	25	20	60
460	AM0228	3	10	-	30	10	65
461	AM0229	2	10	-	25	10	60
462	AM0231	11	10	-	25	10	75
463	AM0234	11	5	-	15	5	50
464	AM0235	5	3	-	20	10	55
465	AM0280	5	10	-	17	7*	50
466	IP0067	3	4	-	5	5	10
467	IP0068	5	2	-	5	5	17
468	IP0070	3	4	-	5	5	15
469	IP0104	5	4	-	10	5	20
470	IP0105	5	4	-	5	5	5
471	IP0129	4	2	-	25	10	35
472	IP0134	6	2	-	5	5	10
473	IP0148	3	2	-	5	5	10
474	IP0155	5	4	-	5	10	30
475	IP0177	6	2	-	5	10	15
476	IP0181	5	2	-	5	7	20
477	IP0198	7	2	-	5	7	20
478	IP0200	3	4	-	5	10	22
479	IP0208	7	4	-	5	10	32
480	IP0210	7	4	-	15	10	30
481	IP0215	8	2	-	5	7	22
482	IP0230	7	2	-	5	10	25
483	IP0303	9	2	-	5	5	25
484	IP0338	4	2		10	10	40
485	IP0339	6	2	-	25	10	65
486	IP0353	7	2	-	5	10	35
487	IP0355	1	2	-	5	35	40
488	IP0357	3	2		10	15	45
489	IP0358	4	2	-	7	7	25
490	IP0359	3	2	-	7	12	42
491	IP0360	2	2	-	15	10	40
492	IP0364	5	2	-	30	10	45
493	IP0367	2	2	-	10	10	75
494	IP0368	2	2	-	5	5	35
495	IP0369	6	2	-	5	10	45
496	IP0371	3	2		5	10	35
497	IP0372	4	2	-	5	15	40
498	IP0376	3	2		10	10	40
499	IP0377	2	2	-	5	5	35
500	IP0380	1	2		5	55	30

No	San No	Area	Lith	pH	Cu	Pb	Zn
					(Unit in ppm)		
501	IP0381	10	1	-	5	55	42
502	IP0384	7	2	-	5	10	45
503	IP0386	2	2	-	5	10	50
504	IP0387	7	2	-	5	10	40
505	IP0388	5	2	-	10	15	70
506	IP0389	2	2	-	5	30	45
507	IP0393	3	3	-	33	26	66
508	IP0394	3	2	-	5	15	45
509	IP0395	2	3	-	10	15	70
510	IP0396	2	2	-	5	10	40
511	IP0400	9	2	-	7	12	37
512	IP0403A	9	4	-	7	15	60
513	IP0403	4	3	-	10	20	65
514	IP0404	2	3	-	10	25	80
515	IP0406	3	2	-	5	10	45
516	IP0407A	2	3	-	7	5	40
517	IP0407	7	2	-	7	5	40
518	IP0408	4	3	-	7	7	52
519	IP0411	4	8	-	10	10	75
520	IP0435	3	1	-	60	5	50
521	IP0438	4	1	-	72	10	107
522	IP0441	2	1	-	50	7	70
523	IP0442	15	2	-	25	52	42
524	IP04 3	7	3	-	126	1000	770
525	IP0474	6	4	-	40	37	50
526	IP0477	5	4	-	27	30	77
527	IP0480	7	3	-	42	7	45
528	IP0481	4	3	-	32	47	70
529	IP0483	2	3	-	55	20	70
530	IP0492	3	3	-	10	10	22
531	IP0493	2	3	-	5	10	20
532	IP0504	1	4	-	30	35	72
533	IP0505	2	4	-	30	42	80
534	IP0508	6	3	-	95	235	230
535	IP0512	6	4	-	20	10	70
536	IP0558	1	2	-	10	20	60
537	IP0559	2	2	-	5	20	60
538	IP0560	3	2	-	10	12	32
539	IP0564	2	4	-	16	15	40
540	IP0566	5	3	-	30	110	100
541	IP0607	2	4	-	30	110	100
542	IP0608	2	4	-	40	55	70
543	IP0611	7	2	-	5	10	50
544	IP0633	7	3	-	20	35	65
545	IP0650	6	2	-	15	30	85
546	IP0659	3	2	-	45	30	65
547	IP0661	2	2	-	25	15	62
548	IP0689	2	3	-	75	7	77
549	IP0695	8	3	-	40	15	60
550	IP0696	2	4	-	60	25	85

No	San No	Area	Lith	pH	Cu	Pb	Zn
					(Unit in ppm)		
551	IP0699	3	4	-	35	20	85
552	IP0700	2	4	-	72	25	130
553	IP0702	2	4	-	55	20	90
554	IP0704	2	4	-	70	42	90
555	IP0705	8	4	-	42	20	87
556	IP0711	8	2	-	12	7	77
557	IP0712	2	2	-	42	12	70
558	IP0713	6	2	-	10	10	75
559	IP0714	4	4	-	57	15	85
560	AG0003	3	4	5 3	5	10	18
561	AG0005	5	4	5 5	13	12	40
562	AG0009	9	9	5 3	19	7	45
563	AG0010	5	6	5 3	30	6	35
564	AG0014	4	9	5 3	8	10	24
565	AG0015	5	9	5 3	7	17	30
566	AG0017	5	9	5 3	35	3	45
567	AG0018	5	9	5 3	28	7	85
568	AG0021	10	9	5 5	18	8	55
569	AG0024	10	9	5 3	9	20	50
570	AG0026	4	9	5 3	15	8	45
571	AG0028	3	4	5 3	3	4	12
572	AG0029	3	4	5 3	19	13	100
573	AG0030	10	9	5 3	9	8	50
574	AG0031	2	9	5 3	6	9	40
575	AG0033	10	4	5 5	45	14	120
576	AG0034	4	4	5 5	40	13	80
577	AG0036	7	3	6 0	19	15	70
578	AG0037	9	9	5 5	78	7	75
579	AG0038	3	4	5 3	14	10	90
580	AG0039	2	4	5 3	26	12	90
581	AG0040A	3	4	5 3	32	27	55
582	AG0041	10	2	5 5	14	40	35
583	AG0042	5	4	5 5	21	30	45
584	AG0043	2	5	5 5	45	10	60
585	AG0044	3	9	5 9	60	9	45
586	AG0046	4	9	5 5	22	40	70
587	AG0047A	9	9	5 5	31	33	55
588	AG0050	5	5	3 9	45	20	70
589	AG0052	4	2	5 5	14	13	40
590	AG0053	9	6	5 3	19	9	40
591	AG0057	9	9	6 5	40	6	30
592	AG0058	5	9	6 5	30	6	45
593	AG0063	3	2	5 9	7	18	30
594	AG0065	6	5	5 5	65	15	70
595	AG0067	5	6	5 7	30	10	50
596	AG0068	4	5	5 3	35	12	60
597	AG0069	3	6	5 5	27	16	45
598	AG0070	2	6	5 5	30	19	60
599	AG0074	3	5	5 3	13	6	24
600	AG0075	8	5	5 3	19	5	35

(4)

No	Sam No	Area	Lith	pH	Cu	Pb	Zn
					(Unit in ppm)		
601	AG0076	3	5	5 3	8	25	20
602	AG0077	4	6	5 3	8	35	20
603	AG0079	5	5	5 5	15	5	47
604	AG0085	3	9	5 5	23	9	55
605	AG0087	10	9	5 5	35	4	28
606	AG0088	3	9	6 5	26	7	24
607	AG0090M	2	4	5 3	35	40	55
608	AG0092	6	9	5 5	40	9	60
609	AG0093A	3	9	5 3	55	4	30
610	AG0095	2	9	5 5	21	16	26
611	AG0097	2	6	5 5	40	10	65
612	AG0098M	1	6	5 5	55	14	60
613	AG0099M	1	6	6 0	27	35	80
614	AG0100M	2	6	5 7	65	4	27
615	AG0102M	2	3	6 5	20	60	25
616	AG0103M	2	6	5 7	75	14	65
617	AG0105M	2	6	5 5	27	19	50
618	AG0107	5	9	5 3	13	6	50
619	AG0109	6	4	5 3	27	20	70
620	AG0112	13	4	5 4	40	15	105
621	AG0114	8	8	5 3	40	6	65
622	AG0116	3	8	5 5	50	8	35
623	AG0121	3	4	5 5	22	4	28
624	AG0122	9	5	5 5	45	14	110
625	AG0124	6	4	5 7	80	18	95
626	AG0126	2	4	5 3	150	7	120
627	AG0129	7	4	5 3	140	22*	110
628	AG0131M	1	2	5 5	13	33*	50
629	AG0132M	2	5	5 3	35	45*	65
630	AG0133	6	5	5 3	23	7*	40
631	AG0138M	11	2	5 4	6	16	26
632	AG0141M	1	4	5 5	28	48*	75
633	AG0142	7	5	5 5	30	22*	120
634	AG0145	8	5	5 5	14	7*	55
635	AG0147	4	3	6 5	18	45*	40
636	AG0148	5	3	5 9	30	7*	60
637	AG0149	6	3	6 2	8	7*	40
638	AG0152	3	3	5 3	8	7*	50
639	AG0154A	9	9	5 3	17	7*	20
640	AG0156	6	9	5 5	75	22*	50
641	AG0157	3	2	5 3	16	7*	70
642	AG0159	12	9	5 3	20	22*	55
643	AG0162	2	8	5 4	23	7*	47
644	AG0163	5	4	5 5	20	22*	62
645	AG0164	8	4	5 5	21	7*	40
646	AG0166	7	4	5 3	95	45*	85
647	AG0170	4	4	6 2	35	22*	40
648	AG0172	8	4	5 5	13	7*	30
649	AG0181	4	4	5 9	28	22*	45
650	AG0183	7	4	5 7	14	22*	56

No	Sam No	Area	Lith	pH	Cu	Pb	Zn
					(Unit in ppm)		
651	AG0185	6	4	5 5	100	22*	55
652	AG0188A	5	4	5 7	45	22*	60
653	AG0191	12	3	5 7	50	7*	75
654	AG0192	4	4	5 7	6	7*	35
655	AG0193	2	4	5 3	26	7*	85
656	AG0196	4	4	5 9	17	7*	40
657	AG0199	10	3	5 5	8	7*	16
658	AG0200	3	4	5 5	8	7*	29
659	AG0205	5	4	5 5	8	7*	35
660	AG0207	5	4	5 7	25	22*	55
661	AG0208	7	4	5 9	5	7*	26
662	AG0236	7	4	5 5	22	7*	50
663	AG0257A	12	4	5 3	5	7*	21
664	AG0261	5	4	5 3	6	7*	22
665	AG0269A	5	3	5 3	15	7*	50
666	AG0271	8	4	5 3	55	7*	85
667	AG0274	7	4	5 5	40	22*	85
668	AG0275	9	4	5 3	35	22*	110
669	AG0276	8	4	5 3	24	22*	95
670	AG5079	5	5	5 5	4	49	50
671	WA0007	10	5	5 7	40	13	106
672	WA0019	2	4	6 5	17	41	50
673	WA0021	2	4	5 8	23	24	44
674	PP0002	10	2	5 0	21	45*	70
675	PP0004	9	4	5 3	15	95	120
676	PP0006	9	2	5 3	6	7*	28
677	PP0008	12	2	5 0	22	45*	90
678	PP0013M	7	2	5 0	4	22*	45
679	PP0014M	3	2	5 3	9	22*	50
680	PP0017M	5	2	5 3	5	22*	50
681	PP0019	4	2	5 9	12	7*	30
682	PP0020	2	3	6 5	65	22*	40
683	PP0021	6	3	6 2	25	60	50
684	PP0022	3	3	6 5	16	50	38
685	PP0023	3	4	6 5	15	22*	26
686	PP0024M	3	2	5 3	19	22*	55
687	PP0025M	4	2	5 3	16	230	380
688	PP0026	6	4	5 3	15	22*	55
689	PP0027M	3	2	5 5	8	22*	45
690	PP0028	5	2	5 3	5	22*	35
691	PP0029	6	3	5 0	7	7*	15
692	PP0031	4	2	5 3	5	22*	50
693	PP0034	3	3	5 5	20	22*	45
694	PP0035	10	2	5 0	11	22*	50
695	PP0036	10	2	5 5	3	7*	14
696	PP0037M	9	2	5 0	5	22*	40
697	PP0038	6	2	4 7	3	7*	13
698	PP0039	5	4	5 0	7	22*	40
699	PP0040	6	2	5 0	9	45*	45
700	PP0042	9	4	5 7	22	22*	50

No	Sam No	Area	Lith	pH	Cu	Pb	Zn
					(Unit in ppm)		
701	PP0044	5	4	5 3	6	22*	45
702	PP0051M	8	2	5 3	7	7*	40
703	PP0052A	9	2	5 3	32	22*	65
704	PP0053	3	2	5 0	6	22*	30
705	PP0054	5	2	5 0	9	7*	30
706	PP0056	5	2	5 5	5	7*	10
707	PP0057	7	2	5 0	28	45*	120
708	PP0058	6	4	5 0	45	22*	60
709	PP0061	12	2	5 0	16	22*	75
710	PP0062	10	2	5 0	9	22*	35
711	PP0064	9	4	5 3	35	22*	70
712	PP0066	4	2	5 3	10	*	30
713	PP0070	10	2	5 3	9	22*	45
714	PP0072	10	2	5 3	18	7*	35
715	PP0073	9	2	5 3	16	7*	40
716	PP0075	7	2	5 3	5	7*	40
717	PP0079	10	2	5 3	15	45*	90
718	PP0080	7	2	5 3	14	22*	75
719	PP0084	9	4	5 7	40	45*	65
720	PP0085	8	2	4 7	11	7*	45
721	PP0086A	3	2	5 5	18	22*	47
722	PP0088	11	4	5 0	40	7*	19
723	PP0090	15	2	5 7	19	22*	95
724	PP0091	9	2	5 0	9	22*	60
725	PP0092	7	2	5 0	8	22*	55
726	PP0093	7	2	5 7	23	22*	45
727	PP0094M	3	2	5 5	8	22*	40
728	FB0098	2	2		5	10	25
729	FB0100	3	2	-	10	10	50
730	FB0102	2	4	-	15	15	50
731	FB0109	9	2	-	5	10	50
732	FB0110	4	2	-	5	7	32
733	FB0111	3	2	-	5	7	25
734	FB0114	3	2		5	10	42
735	FB0115	3	2	-	5	5	25
736	FB0116	8	2	-	10	10	40
737	FB0125	4	2	-	10	10	40
738	FB0127	2	2	-	5	10	40
739	FB0223	8	10	-	20	10	50
740	FB0224	5	10	-	20	10	60
741	FB0230	7	10	-	15	7	42

No	Sam No	Area	Lith	pH	Cu	Pb	Zn
					(Unit in ppm)		

Table A–8. Results of Projeto Geoquimica no Vale do Ribeira (DNPM-CPRM) 1978

1.	TABELA	VIII	Cu–AA–Stream Sediment – Subarea Sudelpa – Summary of Data
2.		X	Matrix of Correlation X Number of Stream Sediment Samples – Subarea Sudelpa (Cu)
3.		XI	Pb–AA–Stream Sediment – Subarea Sudelpa – Summary of Data
4.		XIII	Matrix of Correlation X Number of Stream Sediment Samples – Subarea Sudelpa (Pb)
5.		XIV	Zn–AA–Stream Sediment – Subarea Sudelpa – Summary of Data
6.		XVI	Matrix of Correlation X Number of Stream Sediment Samples – Subarea Sudelpa (Zn)
7.		XXIX	Cu–AA–Stream Sediment – Regional Geschemical Prospection – Summary of Data
8.		XXXI	Matrix of Correlation X Number of Stream Sediment Samples – Regional Geochemical Prospection (Cu)
9.		XXXIII	Pb–AA–Stream Sediment – Regional Geochemical Prospection – Summary of Data
10.		XXXV	Matrix of Correlation X Number of Stream Sediment Samples – Regional Geochemical Prospection (Pb)
11.		XXXVII	Zn–AA–Stream Sediment – Regional Geochemical Prospection – Summary of Data
12.		XXXIX	Matrix of Correlation X Number of Stream Sediment Samples – Regional Geochemical Prospection (Zn)

TABELA VIII – COBRE-AA – SEDIMENTO DE CORRENTE – SUB-ÁREA SUDELPA – SUMÁRIO DOS ESTIMADORES

POPULAÇÕES	NÚMERO DE AMOSTRAS	VALOR MÍNIMO	VALOR MÁXIMO	MÉDIA GEOMÉTRICA (MG)	DESVIO GEOMÉTRICO (DG)	COEFICIENTE DE VARIAÇÃO	GRAU DE DETECÇÃO	MG x DG	$MG \times DG^2$	$MG \times DG^3$
ÁREA TOTAL	256	2,5	120	12	2,787	1,364	235:257	35	96	268
AÇUNGUI GERAL	106	2,5	120	29	2,176	0,911	105:106	64	139	301
AÇUNGUI CLÁSTICO	61	10,0	120	40	1,711	0,578	61:61	68	116	199
AÇUNGUI QUÍMICO	19	5,0	85	28	1,968	0,763	19:19	54	108	211
AÇUNGUI INDIFERENCIADO	26	2,5	90	15	2,432	1,097	25:26	36	87	211
GRANITOS	151	2,5	90	7	2,004	0,788	130:151	14	27	54

OBSERVAÇÕES

1 – Dados expressos em p p m.

2 – MG e DG são geométricos, supondo-se a distribuição log-normal.

3 – Grau de detecção refere-se ao número de valores definidos e transformados em relação ao total de valores analisados.

4 – MG = Background

5 – MG x DG a $MG \times DG^2$ = Alto background.

6 – $MG \times DG^2$ = Limiar.

7 – $MG \times DG^2$ a $MG \times DG^3$ = Anomalia possível.

8 – $\geq MG \times DG^3$ = Anomalia provável.

9 – AA = Absorção atômica, S = Espectrografia.

CPRM

(1)

CPRM

(2)

TABELA X — MATRIZ DE CORRELAÇÃO X NÚMERO DE AMOSTRAS

SEDIMENTO DE CORRENTE-SUBÁREA SUDELPA

COBRE —— ABSORÇÃO ATÔMICA

	ÁREA TOTAL		AÇUNGUI GERAL		AÇUNGUI CLÁSTICO		AÇUNGUI QUÍMICO		AÇUNGUI INDIFERENCIADO		GRANITOS	
	N	Cu-AA	N	Cu-AA	N	Cu-AA	N	Cu-AA	N	Cu-AA	N	Cu-AA
Fe-S	231	O	104	◐	60	O	19	◐	25	●	127	•
Mn-S	229	O	99	•	55	◐	19	•	25	•	130	O
Co-S	222	◐	101	◐	58	◐	18	◐	25	●	121	O
Cu-S	212	●	102	●	59	●	19	◐	24	●	110	◐
Ni-S	233	◐	104	◐	60	O	19	O	25	◐	129	O
Pb-S	207	(•)	81	•	51	O	13	(•)	17	•	126	(•)
Cu-AA		●		●		●		●		●		●
Pb-AA	231	O	101	O	61	•	18	O	22	O	130	O
Zn-AA	235	◐	105	●	61	◐	19	◐	25	●	130	O

OBSERVAÇÕES :

N - nº de amostras que entraram no cálculo
S - espectrografia semi-quantitativa p/ 30 elementos
AA- espectrofotometria de absorção atômica
• - < 0,30
O - 0,30 a 0,59
◐ - 0,60 a 0,79
● - ≥ 0,80
( ) - correlação negativa

TABELA XI – CHUMBO-AA – SEDIMENTO DE CORRENTE – SUB-ÁREA SUDELPA – SUMÁRIO DOS ESTIMADORES										
POPULAÇÕES	NÚMERO DE AMOSTRAS	VALOR MÍNIMO	VALOR MÁXIMO	MÉDIA GEOMÉTRICA (MG)	DESVIO GEOMÉTRICO (DG)	COEFICIENTE DE VARIAÇÃO	GRAU DE DETECÇÃO	$MG \times DG$	$MG \times DG^2$	$MG \times DG^3$
ÁREA TOTAL	257	2,5	280	12	2,060	0,828	251:257	26	53	110
AÇUNGUI GERAL	106	2,5	280	17	2,447	1,108	101:106	42	104	254
AÇUNGUI CLÁSTICO	61	5,0	280	24	2,082	0,844	61:61	50	104	217
AÇUNGUI QUÍMICO	19	2,5	110	14	2,260	0,972	18:19	32	72	163
AÇUNGUI INDIFERENCIADO	26	2,5	130	9	2,536	1,173	22:26	23	59	149
GRANITOS	151	2,5	35	10	1,583	0,485	150:151	16	25	40

OBSERVAÇÕES

1- Dados expressos em p p m.

2- MG e DG são geométricos, supondo-se a distribuição log-normal.

3- Grau de detecção refere-se ao número de valores definidos e transformados em relação ao total de valores analisados.

4- MG= Background.

5- $MG \times DG$ a $MG \times DG^2$ = Alto background.

6- $MG \times DG^2$ = Limiar.

7- $MG \times DG^2$ a $MG \times DG^3$ = Anomalia possível.

8- $\geqslant MG \times DG^3$ = Anomalia provável.

9- AA = Absorção atômica; S= Espectrografia.

TABELA XIII — MATRIZ DE CORRELAÇÃO X NÚMERO DE AMOSTRAS

SEDIMENTO DE CORRENTE-SUBÁREA SUDELPA

CHUMBO —— ABSORÇÃO ATÔMICA

	ÁREA TOTAL		AÇUNGUI GERAL		AÇUNGUI CLÁSTICO		AÇUNGUI QUÍMICO		AÇUNGUI INDIFERENCIADO		GRANITOS	
	N	Pb-AA	N	Pb-AA	N	Pb-AA	N	Pb-AA	N	Pb-AA	N	Pb-AA
Fe-S	247	•	100	O	60	•	18	•	22	O	147	•
Mn-S	245	•	95	(•)	55	•	18	(•)	22	(•)	150	•
Co-S	234	O	97	•	58	•	17	•	22	O	137	•
Cu-S	215	O	98	O	59	•	18	•	21	O	117	O
Ni-S	247	O	100	O	60	•	18	O	22	•	147	•
Pb-S	227	O	81	◐	51	•	13	◐	17	◐	146	•
Cu-AA	231	O	101	O	61	•	18	O	22	O	130	O
Pb-AA		●		●		●		●		●		●
Zn-AA	251	◐	101	◐	61	O	18	O	22	O	150	O

OBSERVAÇÕES :

N - nº de amostras que entraram no cálculo
S - espectrografia semi-quantitativa p/ 30 elementos
AA- espectrofotometria de absorção atômica
• - < 0,30
O - 0,30 a 0,59
◐ - 0,60 a 0,79
● - ≥ 0,80
( ) - correlação negativa

TABELA XIV – ZINCO-AA – SEDIMENTO DE CORRENTE – SUB-ÁREA SUDELPA – SUMÁRIO DOS ESTIMADORES

POPULAÇÕES	NÚMERO DE AMOSTRAS	VALOR MÍNIMO	VALOR MÁXIMO	MÉDIA GEOMÉTRICA (MG)	DESVIO GEOMÉTRICO (DG)	COEFICIENTE DE VARIAÇÃO	GRAU DE DETECÇÃO	MG x DG	MG x DG^2	MG x DG^3
ÁREA TOTAL	257	5,0	270	49	1,794	0,638	257:257	87	156	281
AÇUNGUI GERAL	106	5,0	270	67	1,843	0,673	106:106	123	228	420
AÇUNGUI CLÁSTICO	61	30,0	270	88	1,511	0,431	61:61	133	200	301
AÇUNGUI QUÍMICO	19	20,0	130	60	1,668	0,547	19:19	100	166	276
AÇUNGUI INDIFERENCIADO	26	5,0	130	39	1,989	0,777	26:26	78	153	305
GRANITOS	151	10,0	100	39	1,580	0,468	151:151	60	95	147

OBSERVAÇÕES

1 - Dados expressos em p p m.

2 - MG e DG são geométricos, supondo-se a distribuição log-normal

3 - Grau de detecção refere-se ao número de valores definidos e transformados em relação ao total de valores analisados.

4 - MG = Background.

5 - MG x DG a MG x DG^2 = Alto background.

6 - MG x DG^2 = Limiar.

7 - MG x DG^2 a MG x DG^3 = Anomalia possível.

8 - $\geq$ MG x DG^3 = Anomalia provável.

9 - AA = Absorção atômica; S = Espectrografia.

TABELA XVI — MATRIZ DE CORRELAÇÃO X NÚMERO DE AMOSTRAS

SEDIMENTO DE CORRENTE - SUBÁREA SUDELPA

ZINCO —— ABSORÇÃO ATÔMICA

	ÁREA TOTAL		AÇUNGUI GERAL		AÇUNGUI CLÁSTICO		AÇUNGUI QUÍMICO		AÇUNGUI INDIFERENCIADO		GRANITOS	
	N	Zn-AA	N	Zn-AA	N	Zn-AA	N	Zn-AA	N	Zn-AA	N	Zn-AA
Fe-S	253	◐	105	◐	60	○	19	○	26	●	148	○
Mn-S	251	○	100	•	55	○	19	•	26	•	151	○
Co-S	239	○	102	◐	58	○	18	◐	26	○	137	○
Cu-S	219	◐	102	◐	59	○	19	◐	24	●	117	○
Ni-S	252	○	104	◐	60	○	19	◐	25	◐	148	○
Pb-S	228	•	81	○	51	◐	13	○	17	○	147	(•)
Cu-AA	235	◐	105	●	61	◐	19	◐	25	●	130	○
Pb-AA	251	◐	101	◐	61	○	18	○	22	○	150	○
Zn-AA		●		●		●		●		●		●

OBSERVAÇÕES :

N - nº de amostras que entraram no cálculo

S - espectrografia semi-quantitativa p/ 30 elementos

AA - espectrofotometria de absorção atômica

• - < 0,30

○ - 0,30 a 0,59

◐ - 0,60 a 0,79

● - ≥ 0,80

( ) - correlação negativa

TABELA XXIX — COBRE -AA — SEDIMENTO DE CORRENTE — GEOQUÍMICA REGIONAL
SUMÁRIO DOS ESTIMADORES

POPULAÇÕES	NUMERO DE AMOSTRAS	VALOR MÍNIMO	VALOR MÁXIMO	MEDIA GEOMETRICA (MG)	DESVIO GEOMÉTRICO (DG)	COEFICIENTE DE VARIAÇÃO	GRAU DE DETECÇÃO	MG x DG	MG x DG²	MG x DG³
ÁREA TOTAL	1288	1,5	390	18	2,250	0,965	1288.1288	41	92	207
GRUPO AÇUNGUI	868	1,5	340	23	2.134	0,881	868·868	48	103	220
GRUPO AÇUNGUI(AD-20-40)	69	4,0	170	22	2,422	1,090	69:69	53	129	312
GRUPO ACUNGUI (AD > 40)	22	3,0	100	20	2,247	0,962	22:22	45	101	228
AÇUNGUI SETUVA	197	3,0	150	26	1,904	0,717	197:197	49	92	176
AÇUNGUI SETUVA (AD < 5)	80	3,0	95	26	1,876	0,697	80.80	50	93	174
AÇUNGUI SETUVA (AD=5-10)	53	5,0	110	26	1,773	0,623	53·53	46	81	144
AÇUNGUI SETUVA (AD=10-20)	30	5,0	150	24	2,116	0,868	30.30	51	109	231
AÇUNGUI CLÁSTICO	509	3,0	340	23	2,151	0,893	509.509	49	105	225
AÇUNGUI CLÁSTICO(AD < 5)	147	4,0	150	26	2,002	0,787	147:147	52	103	206
ACUNGUI CLÁSTICO(AD=5-10)	129	4,0	340	22	2,234	0,953	129·129	49	108	242
ACUNGUI CLÁSTICO(AD=10-20)	70	3,0	100	19	2,177	0,912	70:70	42	92	200
AÇUNGUI QUÍMICO	176	1,5	190	18	2,395	1,069	176:176	43	104	248
AÇUNGUI QUÍMICO (AD <5)	61	1,5	190	19	2,506	1,151	61:61	48	120	301
AÇUNGUI QUÍMICO (AD=5-10)	48	3,0	130	-20	2,327	1,020	48:48	47	110	255
AÇUNGUI QUÍMICO(AD-10-20)	30	4,0	120	16	2,434	1,098	30.30	38	93	226
GRANITOS	345	1,5	120	11	1,976	0,768	345:345	22	43	85
GRANITOS (AD<5)	47	3,0	55	11	2,029	0,806	47:47	23	46	94
GRANITOS (AD:5-10)	95	1,5	120	12	2,213	0,938	95:95	27	60	133
GRANITOS(AD=10-20)	65	3,0	65	11	1,965	0,761	65:65	21	41	81
GRANITOS (AD > 40)	13	4,0	23	8	1,568	0,474	13:13	12	19	30
COMPLEXO GN-MIGMATÍTICO	26	7,0	390	21	1,952	0,751	26:26	41	80	155
GRUPO TUBARÃO	27	3,0	80	11	2,083	0,844	27:27	23	48	99
FORMAÇÃO FURNAS	12	1,5	27	6	2,126	0,876	12:12	13	27	58

OBSERVAÇÕES

1— Dados expressos em ppm

2— MG e DG são geométricos supondo-se a distribuição log-normal

3— Grau de detecção refere-se ao número de valores definidos e transformados em relação ao total de valores analisados

4— AD = Área de drenagem expressa em km²

5— MG = Background

6— MG x DG a MG x DG² = Alto background

7— MG x DG² = Limiar

8— MG x DG² a MG x DG³ = Anomalia possível.

9— ≥ MG x DG = Anomalia provável

TABELA XXXI — MATRIZ DE CORRELAÇÃO X NÚMERO DE AMOSTRAS SEDIMENTO DE CORRENTE-GEOQUÍMICA REGIONAL

COBRE —— ABSORÇÃO ATÔMICA

		Cu-AA	Pb-AA	Zn-AA	Ag-AA	Co-AA	Ni-AA	Fe-AA	Mn-AA
ÁREA TOTAL	N		1288	1288	1288	1288	1288	1288	1288
	Cu-AA	●	○	◐	•	◐	◐	◐	◐
GRUPO AÇUNGUI	N		868	868	868	868	868	868	868
	Cu-AA	●	○	◐	•	●	●	●	◐
GRUPO AÇUNGUI AD 20-40	N		69	69	69	69	69	69	69
	Cu-AA	●	○	●	(•)	●	●	●	◐
AÇUNGUI SETUVA	N		197	197	197	197	197	197	197
	Cu-AA	●	•	○	•	◐	◐	◐	○
AÇUNGUI SETUVA AD MENOR 5	N		80	80	80	80	80	80	80
	Cu-AA	●	•	○	•	◐	○	◐	○
AÇUNGUI SETUVA AD 5-10	N		53	53	53	53	53	53	53
	Cu-AA	●	•	○	•	◐	◐	◐	○
AÇUNGUI SETUVA AD 10-20	N		30	30	30	30	30	30	30
	Cu-AA	●	(•)	○	○	◐	◐	◐	○
AÇUNGUI CLÁSTICO	N		509	509	509	509	509	509	509
	Cu-AA	●	○	◐	◐	◐	●	●	○
AÇUNGUI CLÁSTICO AD MENOR 5	N		147	147	147	147	147	147	147
	Cu-AA	●	○	◐	•	◐	●	●	○
AÇUNGUI CLÁSTICO AD 5-10	N		129	129	129	129	129	129	129
	Cu-AA	●	○	◐	•	○	●	◐	◐
AÇUNGUI CLÁSTICO AD 10-20	N		70	70	70	70	70	70	70
	Cu-AA	●	○	◐	•	●	●	●	○
AÇUNGUI QUÍMICO	N		176	176	176	176	176	176	176
	Cu-AA	●	○	◐	○	●	●	●	◐
AÇUNGUI QUÍMICO AD MENOR 5	N		61	61	61	61	61	61	61
	Cu-AA	●	○	◐	○	◐	●	●	◐
AÇUNGUI QUÍMICO AD 5-10	N		48	48	48	48	48	48	48
	Cu-AA	●	◐	◐	○	●	●	●	○
AÇUNGUI QUÍMICO AD 10-20	N		30	30	30	30	30	30	30
	Cu-AA	●	○	◐	•	●	●	◐	●
GRANITOS	N		345	345	345	345	345	345	345
	Cu-AA	●	○	◐	•	◐	◐	○	○
GRANITOS AD MENOR 5	N		47	47	47	47	47	47	47
	Cu-AA	●	○	◐	•	○	◐	◐	○
GRANITOS AD 5-10	N		95	95	95	95	95	95	95
	Cu-AA	●	•	◐	•	◐	◐	○	◐
GRANITOS AD 10-20	N		65	65	65	65	65	65	65
	Cu-AA	●	○	◐	○	◐	◐	◐	○
COMPLEXO GNÁISSICO-MIGMATÍTICO	N		26	26	26	26	26	26	26
	Cu-AA	●	(•)	◐	◐	○	◐	○	•
GRUPO TUBARÃO	N		27	27	27	27	27	27	27
	Cu-AA	●	○	◐	•	◐	◐	◐	◐
FORMAÇÃO FURNAS	N		12	12	12	12	12	12	12
	Cu-AA	●	○	●	•	○	◐	◐	○

OBSERVAÇÕES

N - nº de amostras que entraram no cálculo

AA- espectrofotometria de absorção atômica

( ) - correlação negativa

• - < 0,30

○ - 0,30 a 0,59

◐ - 0,60 a 0,79

● - ≥ 0,80

AD- área de drenagem expressa em km^2

TABELA XXXIII — CHUMBO-AA — SEDIMENTO DE CORRENTE — GEOQUÍMICA REGIONAL
SUMÁRIO DOS ESTIMADORES

POPULAÇÕES	NUMERO DE AMOSTRAS	VALOR MINIMO	VALOR MÁXIMO	MEDIA GEOMETRICA (MG)	DESVIO GEOMETRICO (DG)	COEFICIENTE DE VARIAÇÃO	GRAU DE DETECÇÃO	MG x DG	$MG \times DG^2$	$MG \times DG^3$
ÁREA TOTAL	1288	1,5	1300	16	1,904	0,717	1288.1288	30	56	108
GRUPO AÇUNGUI	868	1,5	1300	15	2,010	0,793	868.868	31	61	123
GRUPO AÇUNGUI(AD-20-40)	69	3,0	50	14	1,701	0,571	69.69	24	40	69
GRUPO ACUNGUI (AD > 40)	22	5,0	50	16	1,800	0,642	22:22	29	52	94
AÇUNGUI SETUVA	197	4,0	380	12	1,773	0,623	197:197	19	32	53
AÇUNGUI SETUVA (AD < 5)	80	4,0	40	11	1,620	0,512	80.80	18	29	46
AÇUNGUI SETUVA (AD:5-10)	53	5,0	40	12	1,576	0,480	53:53	20	31	49
AÇUNGUI SETUVA (AD:10-20)	30	4,0	50	13	1,885	0,703	30:30	24	46	87
AÇUNGUI CLÁSTICO	509	3,0	1300	16	1,860	0,686	509:509	30	55	103
AÇUNGUI CLÁSTICO(AD < 5)	147	3,0	170	16	1,764	0,617	147.147	28	50	89
ACUNGUI CLÁSTICO(AD:5-10)	129	4,0	210	15	1,861	0,686	129.129	29	53	99
ACUNGUI CLÁSTICO(AD-10-20)	70	5,0	100	15	1,608	0,503	70:70	24	39	62
AÇUNGUI QUÍMICO	176	1,5	1300	19	2,561	1,192	176 176	49	125	319
AÇUNGUI QUÍMICO (AD <5)	61	4,0	1300	20	2,654	1,262	61:61	53	144	382
AÇUNGUI QUÍMICO (AD:5-10)	48	1,5	1300	19	2,751	1,336	48.48	53	145	399
AÇUNGUI QUÍMICO(AD-10-20)	30	1,5	100	16	2,235	0,954	30·30	35	79	176
GRANITOS	345	4,0	100	17	1,636	0,524	345·345	27	45	73
GRANITOS (AD< 5)	47	4,0	40	16	1,618	0,510	47:47	25	41	67
GRANITOS (AD:5-10)	95	4,0	65	17	1,758	0,612	95:95	29	51	90
GRANITOS(AD: 10-20)	65	7,0	100	18	1,620	0,512	65.65	29	48	77
GRANITOS (AD > 40)	13	8,0	20	14	1,393	0,341	13 13	19	27	38
COMPLEXO GN-MIGMATÍTICO	26	7,0	35	14	1,556	0,465	26 26	21	33	52
GRUPO TUBARÃO	27	6,0	60	13	1,716	0,582	27:27	22	38	66
FORMAÇÃO FURNAS	12	4,0	22	10	1,632	0,520	12 12	16	27	43

OBSERVAÇÕES

1 — Dados expressos em ppm

2 — MG e DG são geometricos supondo-se a distribuição log-normal

3 — Grau de detecção refere-se ao número de valores definidos e transformados em relação ao total de valores analisados

4 — AD = Área de drenagem expressa em km^2

5 — MG = Background

6 — MG x DG a $MG \times DG^2$ = Alto background

7 — $MG \times DG^2$ = Limiar

8 — $MG \times DG^2$ a $MG \times DG^3$ = Anomalia possível

9 — ≥ MG x DG = Anomalia provável

TABELA XXXV — MATRIZ DE CORRELAÇÃO X NÚMERO DE AMOSTRAS SEDIMENTO DE CORRENTE-GEOQUÍMICA REGIONAL

CHUMBO —— ABSORÇÃO ATÔMICA

		Cu-AA	Pb-AA	Zn-AA	Ag-AA	Co-AA	Ni-AA	Fe-AA	Mn-AA
ÁREA TOTAL	N	1288		1288	1288	1288	1288	1288	1288
	Pb-AA	○	●	○	○	○	•	○	○
GRUPO AÇUNGUI	N	868		868	868	868	868	868	868
	Pb-AA	○	●	○	○	○	○	○	○
GRUPO AÇUNGUI AD 20-40	N	69		69	69	69	69	69	69
	Pb-AA	○	●	◐	•	◐	○	◐	●
AÇUNGUI SETUVA	N	197		197	197	197	197	197	197
	Pb-AA	•	●	○	○	○	•	•	•
AÇUNGUI SETUVA AD MENOR 5	N	80		80	80	80	80	80	80
	Pb-AA	•	●	○	○	○	•	○	•
AÇUNGUI SETUVA AD 5-10	N	53		53	53	53	53	53	53
	Pb-AA	•	●	○	◐	○	•	○	•
AÇUNGUI SETUVA AD 10-20	N	30		30	30	30	30	30	30
	Pb-AA	(•)	●	•	•	•	(•)	(•)	•
AÇUNGUI CLÁSTICO	N	509		509	509	509	509	509	509
	Pb-AA	○	●	○	○	○	○	○	○
AÇUNGUI CLÁSTICO AD MENOR 5	N	147		147	147	147	147	147	147
	Pb-AA	○	●	○	○	○	○	○	•
AÇUNGUI CLÁSTICO AD 5-10	N	129		129	129	129	129	129	129
	Pb-AA	○	●	○	○	○	○	○	○
AÇUNGUI CLÁSTICO AD 10-20	N	70		70	70	70	70	70	70
	Pb-AA	○	●	○	○	○	○	◐	•
AÇUNGUI QUÍMICO	N	176		176	176	176	176	176	176
	Pb-AA	○	●	◐	○	○	○	○	○
AÇUNGUI QUÍMICO AD MENOR 5	N	61		61	61	61	61	61	61
	Pb-AA	○	●	○	○	○	○	○	○
AÇUNGUI QUÍMICO AD 5-10	N	48		48	48	48	48	48	48
	Pb-AA	◐	●	◐	◐	○	◐	○	•
AÇUNGUI QUÍMICO AD 10-20	N	30		30	30	30	30	30	30
	Pb-AA	○	●	○	•	○	○	•	○
GRANITOS	N	345		345	345	345	345	345	345
	Pb-AA	○	●	○	◐	○	•	•	○
GRANITOS AD MENOR 5	N	47		47	47	47	47	47	47
	Pb-AA	○	●	○	○	○	•	○	○
GRANITOS AD 5-10	N	95		95	95	95	95	95	95
	Pb-AA	•	●	•	◐	○	•	•	•
GRANITOS AD 10-20	N	65		65	65	65	65	65	65
	Pb-AA	○	●	○	◐	○	○	○	•
COMPLEXO GNAISSICO-MIGMATÍTICO	N	26		26	26	26	26	26	26
	Pb-AA	(•)	●	•	○	•	•	•	○
GRUPO TUBARÃO	N	27		27	27	27	27	27	27
	Pb-AA	○	●	○	•	○	○	○	○
FORMAÇÃO FURNAS	N	12		12	12	12	12	12	12
	Pb-AA	○	●	○	◐	○	◐	●	○

OBSERVAÇÕES

N - nº de amostras que entraram no cálculo

AA- espectrofotometria de absorção atômica

( ) - correlação negativa

• - < 0,30

○ - 0,30 a 0,59

◐ - 0,60 a 0,79

● - ⩾ 0,80

AD- área de drenagem expressa em km^2

TABELA XXXVII — ZINCO - AA — SEDIMENTO DE CORRENTE — GEOQUÍMICA REGIONAL
SUMÁRIO DOS ESTIMADORES

POPULAÇÕES	NÚMERO DE AMOSTRAS	VALOR MÍNIMO	VALOR MÁXIMO	MÉDIA GEOMÉTRICA (MG)	DESVIO GEOMÉTRICO (DG)	COEFICIENTE DE VARIAÇÃO	GRAU DE DETECÇÃO	MG x DG	$MG \times DG^2$	$MG \times DG^3$
ÁREA TOTAL	1288	3,0	710	47	1,847	0,676	1288:1288	88	162	299
GRUPO AÇUNGUI	868	4,0	710	52	1,865	0,689	868:868	98	182	340
GRUPO AÇUNGUI(AD:20-40)	69	7,0	140	46	1,986	0,775	69.69	92	183	364
GRUPO ACUNGUI (AD> 40)	22	5,0	120	50	2,078	0,841	22:22	104	217	451
AÇUNGUI SETUVA	197	9,0	700	58	1,693	0,565	197.197	94	154	253
AÇUNGUI SETUVA (AD < 5)	80	12,0	180	55	1,743	0,601	80:80	96	167	290
AÇUNGUI SETUVA (AD:5-10)	53	9,0	110	61	1,576	0,480	53:53	97	153	241
AÇUNGUI SETUVA (AD:10-20)	30	25,0	120	57	1,570	0,475	30:30	90	141	221
AÇUNGUI CLÁSTICO	509	5,0	390	52	1,869	0,692	509.509	98	182	341
AÇUNGUI CLÁSTICO(AD < 5)	147	13,0	170	58	1,729	0,592	147:147	101	175	302
ACUNGUI CLÁSTICO(AD:5-10)	129	12,0	170	50	1,879	0,699	129:129	94	177	333
ACUNGUI CLÁSTICO(AD:10-20)	70	6,0	150	49	1,910	0,721	70:70	93	178	340
AÇUNGUI QUÍMICO	176	4,0	710	46	2,115	0,868	176:176	96	204	430
AÇUNGUI QUÍMICO (AD <5)	61	4,0	150	43	2,061	0,829	61:61	89	183	377
AÇUNGUI QUÍMICO (AD:5-10)	48	9,0	710	52	2,363	1,046	48:48	124	292	689
AÇUNGUI QUÍMICO(AD:10-20)	30	13,0	120	44	1,852	0,680	30.30	82	152	282
GRANITOS	345	10,0	120	40	1,521	0,439	345:345	61	92	140
GRANITOS (AD< 5)	47	11,0	120	39	1,622	0,513	47:47	64	103	167
GRANITOS (AD:5-10)	95	13,0	110	41	1,505	0,426	95:95	61	92	138
GRANITOS(AD: 10-20)	65	12,0	90	39	1,597	0,495	65:65	62	99	158
GRANITOS (AD > 40)	13	11,0	50	29	1,440	0,377	13:13	42	60	87
COMPLEXO GN-MIGMATÍTICO	26	40,0	240	69	1,526	0,442	26:26	105	160	244
GRUPO TUBARÃO	27	6,0	50	19	1,747	0,604	27:27	33	58	101
FORMAÇÃO FURNAS	12	3,0	90	14	2,577	1,205	12:12	36	93	239

OBSERVAÇÕES

1 - Dados expressos em ppm

2 - MG e DG são geometricos supondo-se a distribuição log-normal

3 - Grau de detecção refere-se ao número de valores definidos e transformados em relação ao total de valores analisados

4 - AD = Área de drenagem expressa em km^2

5 - MG = Background

6 - MG x DG a MG x DG^2 = Alto background

7 - MG x DG^2 = Limiar.

8 - MG x DG^2 a MG x DG^3 = Anomalia possível.

9 - ≥ MG x DG = Anomalia provável.

TABELA XXXIX— MATRIZ DE CORRELAÇÃO X NÚMERO DE AMOSTRAS SEDIMENTO DE CORRENTE-GEOQUÍMICA REGIONAL

ZINCO —— ABSORÇÃO ATÔMICA

		Cu-AA	Pb-AA	Zn-AA	Ag-AA	Co-AA	Ni-AA	Fe-AA	Mn-AA
ÁREA TOTAL	N	1288	1288		1288	1288	1288	1288	1288
	Zn-AA	◐	O	●	•	◐	◐	O	O
GRUPO AÇUNGUI	N	868	868		868	868	868	868	868
	Zn-AA	◐	O	●	•	◐	◐	◐	O
GRUPO AÇUNGUI AD 20-40	N	69	69		69	69	69	69	69
	Zn-AA	●	◐	●	(•)	●	●	●	◐
AÇUNGUI SETUVA	N	197	197		197	197	197	197	197
	Zn-AA	O	O	●	•	◐	◐	◐	O
AÇUNGUI SETUVA AD MENOR 5	N	80	80		80	80	80	80	80
	Zn-AA	O	O	●	•	O	◐	◐	O
AÇUNGUI SETUVA AD 5-10	N	53	53		53	53	53	53	53
	Zn-AA	O	O	●	•	◐	◐	◐	O
AÇUNGUI SETUVA AD 10-20	N	30	30		30	30	30	30	30
	Zn-AA	O	•	●	O	O	O	◐	O
AÇUNGUI CLÁSTICO	N	509	509		509	509	509	509	509
	Zn-AA	◐	O	●	•	◐	●	◐	O
AÇUNGUI CLÁSTICO AD MENOR 5	N	147	147		147	147	147	147	147
	Zn-AA	◐	O	●	•	◐	●	◐	O
AÇUNGUI CLÁSTICO AD 5-10	N	129	129		129	129	129	129	129
	Zn-AA	◐	O	●	•	◐	●	◐	◐
AÇUNGUI CLÁSTICO AD 10-20	N	70	70		70	70	70	70	70
	Zn-AA	◐	O	●	•	◐	●	●	O
AÇUNGUI QUÍMICO	N	176	176		176	176	176	176	176
	Zn-AA	◐	◐	●	O	◐	◐	●	◐
AÇUNGUI QUÍMICO AD MENOR 5	N	61	61		61	61	61	61	61
	Zn-AA	◐	O	●	O	◐	●	●	◐
AÇUNGUI QUÍMICO AD 5-10	N	48	48		48	48	48	48	48
	Zn-AA	◐	◐	●	O	◐	◐	◐	O
AÇUNGUI QUÍMICO AD 10-20	N	30	30		30	30	30	30	30
	Zn-AA	◐	O	●	•	◐	◐	●	◐
GRANITOS	N	345	345		345	345	345	345	345
	Zn-AA	◐	O	●	•	◐	◐	◐	O
GRANITOS AD MENOR 5	N	47	47		47	47	47	47	47
	Zn-AA	◐	O	●	•	◐	◐	◐	◐
GRANITOS AD 5-10	N	95	95		95	95	95	95	95
	Zn-AA	◐	•	●	•	◐	◐	◐	◐
GRANITOS AD 10-20	N	65	65		65	65	65	65	65
	Zn-AA	◐	O	●	•	◐	O	◐	O
COMPLEXO GNÁISSICO-MIGMATÍTICO	N	26	26		26	26	26	26	26
	Zn-AA	◐	•	●	•	O	◐	O	O
GRUPO TUBARÃO	N	27	27		27	27	27	27	27
	Zn-AA	◐	O	●	•	●	●	◐	◐
FORMAÇÃO FURNAS	N	12	12		12	12	12	12	12
	Zn-AA	●	O	●	O	●	◐	◐	◐

OBSERVAÇÕES

N - nº de amostras que entraram no cálculo

AA- espectrofotometria de absorção atômica

( ) - correlação negativa

• - < 0,30

O - 0,30 a 0,59

◐ - 0,60 a 0,79

● - ≥ 0,80

AD- área de drenagem expressa em km^2